WMRC Reports
One E. Hazelwood Drive, Champaign, Illinois

Accelerated Aging of Stabilized Hazardous Wastes

Robert Fuessle,
Max Taylor
Bradley University

RR-E82
July 1999
Electronic Version

About WMRC's Electronic Publications:

This document was originally published in a traditional format.

It has been transferred to an electronic format to allow faster and broader access to important information and data.

While the Center makes every effort to maintain a level of quality during the transfer from print to digital format, it is possible that minor formatting and typographical inconsistencies will still exist in this document.

Additionally, due to the constraints of the electronic format chosen, page numbering will vary slightly from the original document.

The original, printed version of this document may still be available.

Please contact WMRC for more information:

WMRC
One E. Hazelwood Drive
Champaign, IL 61820
217-333-8940 (phone)

www.wmrc.uiuc.edu

WMRC is a division of the Illinois Department of Natural Resources

This report is part of WMRC's Research Report Series. Mention of trade names or commercial products does not constitute endorsement or recommendation for use.

RR-82

Accelerated Aging of Stabilized Hazardous Wastes

Dr. Robert Fuessle
Department of Civil Engineering & Construction

Dr. Max Taylor
Department of Chemistry

Bradley University
Peoria, IL 61625

Published in Conjunction with the Portland Cement Association

April 1999

Submitted to the
Illinois Waste Management and Research Center
One E. Hazelwood Drive
Champaign, IL 61820
www.wmrc.uiuc.edu
Printed by the Authority of the State of Illinois
2000/150

Acknowledgments

The research reported in this paper (PCA R&D Serial No. 2180) was conducted by Bradley University with the sponsorship of the Waste Management and Research Center, Illinois Department of Natural Resources, and the Portland Cement Association (PCA Project Index No. 90-08a). The contents of this paper reflect the views of the authors, who are responsible for the facts and accuracy of the data presented. The contents do not necessarily reflect the views of the sponsors. The investigators are thankful to many people for their help during this project. These people and their contributions are: Ms. Pamela Tazik and Ms. Jaqueline Peden of the Illinois Waste Management and Research Center and Mr. Charles Wilk from the Portland Cement Association for their helpful suggestions, Mr. John LaPayne of PDC Laboratories, Inc for chemical analyses of TCLP extracts and digestates, Drs. Amir Al-Khafaji and Don Glover, our chairmen at Bradley University for release time; Kamud Archarya, Mahesh Bhatterai, and Shailendra Ganna, our students, for all the hours in the laboratory.

CONTENTS

CHAPTER THREE: Experimental Measurements and Materials

CHAPTER FOUR: Experimental Design

CHAPTER FIVE: Discussion of Results and Conclusions

TABLES

FIGURES

ABBREVIATIONS

Stabilization:

S/S	Stabilization/Solidification
BDAT	Best demonstrated available technology
B/W	Binder to hazardous waste mass ratio
TCLP	Toxicity Characteristic Leaching Procedure
SITE	Superfund Innovative Technology Evaluation Program

Cement Chemistry

C_3S	Tricalcium silicate (Alite)	C_2S	Dicalcium silicate (Belite)
C_3A	Tricalcium Aluminate	NC_8A_3	Tricalcium (sodium aluminate)
C_4AF	Tetracalcium Aluminoferrite	$C\bar{S}H_2$	Calcium sulfate dihydrate (gypsum)
C-S-H	Calcium Silicate hydrate gel	CH	Calcium Hydroxide (Portlandite)
$C_6A\bar{S}_3H_{32}$	Ettringite	$C_4A\bar{S}H_{12}$	AFm phase (Al-Fe-mono–$C\bar{S}$)

Instrumentation

XRD	X-Ray Diffraction	EDX	Energy Dispersive X-ray analysis
^{29}Si NMR	Silicon Nuclear Magnetic Resonance	DTA	Differential Thermal Analysis
MSDS	Material Safety Data Sheet	FTIR	Fourier Transform InfraRed spectroscopy
XPS	X-ray Photoelectron Spectroscopy	SEM	Scanning Electron Microscopy

General Chemistry

Element	**Abbrev.**	**Element**	**Abbrev.**	**Element**	**Abbrev.**
Aluminum	Al	Copper	Cu	Mercury	Hg
Arsenic	As	Iron	Fe	Nickel	Ni
Barium	Ba	Lead	Pb	Silicon	Si
Cadmium	Cd	Magnesium	Mg	Silver	Ag
Calcium	Ca	Manganese	Mn	Zinc	Zn
Chromium	Cr				

ABSTRACT

In Illinois, about 40 million gallons of hazardous waste are treated before land disposal every year. Stabilization is a well-known, accepted, and economical treatment for certain hazardous wastes. It is likely that stabilization before landfilling will continue to be accepted by EPA as BDAT (best demonstrated available technology) for a significant fraction of hazardous wastes.

Stabilization consists of adding cement to waste with pozzolans and various proprietary additives to capture or immobilize contaminants within a solid matrix by physical and/or chemical means. The treatment effectiveness of stabilization is specified in terms of the toxicity characteristic leaching procedure (TCLP). Shortly after stabilization, TCLP tests are performed periodically until treatment standards are satisfied. The implicit assumption is that S/S forms do not degrade upon long-term curing. Issues such as volume efficiency and treatment versus dilution are also important.

Some designs improve stabilization with curing age since wastes frequently retard cement hydration reactions. In other designs, the continuing chemical changes taking place may render stabilization ineffective in the long term. As the cement-based stabilization matrix cures, physiochemical and morphological changes occur rapidly at first and continue more slowly for years. Alkali- aggregate reactions and sulfate damage are long-term degradative processes in concrete. The hazardous components of the wastes involved may also interfere with long-term quality stabilization.

The focus of this research is the development and understanding of an accelerated method that will provide a testing procedure for early detection of stabilizations subject to long-term failure, allowing a landfill operator to predict the long-term treatment efficacy of the stabilized waste. The reliability of an accelerated test is based on its ability to predict the TCLP of naturally-cured mature stabilized forms. The physical and chemical microstructure of the accelerated and natural forms should also be comparable.

This research has characterized a range of mix designs and their long-term treatment effectiveness for K061 waste. The range of mix designs selected for research falls between the extremes of stabilizations that are effective for up to two years and totally inadequate S/S that exceeds TCLP standards at any age. Comparisons of TCLP of short-term accelerated samples with naturally cured samples over the long-term did not yield consistent results. Heat curing by itself will not provide a cure method that yield results predicting future treatment performance.

For many stabilized samples, a lower rate of metal release during column leaching indicated a more effective stabilization according to TCLP results on older samples. The metal release rate during column leaching can be used as a qualitative indicator to compare how two different mix designs may perform in TCLP tests at later ages.

CHAPTER ONE
Long-Term Treatment Effectiveness of Stabilization
Statement of Problem

1.1 Background

In the USA, 265 million tons of hazardous waste are generated every year. In Illinois, about 40 million gallons of hazardous waste are treated before land disposal every year (IEPA, 1990). In response to a growing need for more stringent regulations regarding landfilled hazardous waste, the Hazardous and Solid Waste Amendments of November, 1984 required the U.S. EPA to promulgate regulations prohibiting the land disposal of untreated hazardous wastes except those land disposal units that satisfy the no migration standard. The U. S. EPA responded in November, 1986, by proposing: 1) procedures for setting treatment standards; 2) the toxicity characteristic leaching procedure (TCLP) as a test procedure to verify the acceptability of treatment; 3) treatment standards based on the best available demonstrated technology (BDAT).

Stabilization is a well-known, accepted and economical treatment for certain hazardous wastes; Conner (1990) presents a 3.5 page table of waste types successfully treated with stabilization. The SITE program (USEPA (1989)) has selected demonstration projects using cementitious or pozzolanic stabilization. The many standard references on stabilization include books on specific aspects of stabilization (Conner (1990), Spence (1992)). It is likely that stabilization before landfilling will continue to be accepted by EPA as BDAT (best demonstrated available technology) for a significant fraction of hazardous wastes.

Stabilization consists of adding cement to waste with pozzolans and various proprietary additives to capture or immobilize contaminants within a solid matrix by physical and/or chemical means. The treatment effectiveness of stabilization is specified in terms of the TCLP. Shortly after stabilization, TCLP tests are performed periodically until treatment standards are satisfied. The curing time of the stabilized waste before land disposal may range from days to weeks depending on when TCLP results satisfy standards. Current legislation specifies that once a treated waste passes TCLP, it may be disposed to the landfill. The implicit assumption is that S/S forms do not degrade upon long-term curing.

Long-term chemical reactions within portland cement have been investigated by several researchers. Lenz (1966) demonstrated a measurement of silicate chain polymerization that correlated with curing age up to 14 years. Stanton (1940) observed that the reaction between alkalis in cement with aggregates containing silicates has a half-life ranging from 1 to 20 years, depending on conditions. This alkali-silicate reaction has been studied intensively because the resulting expansion causes detrimental microcracking of the sample. Some slow reactions in cement may be beneficial in certain compositions, while others may not. These slow reactions may be important for the long-term treatment effectiveness of cement-based S/S.

1.2 Long-Term Curing and Stabilization

Some stabilization designs may improve with longer cure times since wastes frequently retard cement hydration reactions. On the other hand, some stabilization mixtures are deceptive because they may pass TCLP after a brief curing but become ineffective in the long term as a result of the deleterious effects of additives and wastes on the continuing chemical reactions in the waste form. Frequently, these deleterious effects may not show up for several weeks or more. For metal waste samples, Cartledge and Tittlebaum (1993) present data showing increased leachability for samples cured one year compared with those cured only 28 days. On the other hand, some stabilization designs exceed TCLP standards after brief curing but slowly mature to solids that satisfy standards (Taylor and Fuessle, 1994).

The critical relationship between cure time and TCLP concentrations from stabilized wastes has important and serious implications for hazardous waste disposal. Stabilized wastes may fail later in the landfill despite the fact that they satisfied TCLP standards after brief curing. Given reports of unreliability of liners, safeguards such as stabilization become even more important. Long-term failure of stabilization could also result in financial burdens for operating companies required to pump and treat leachates. Potential aquifer damage could be a risk. In other cases, slowly-maturing economical designs may be discarded because adequate curing time has not been allowed before testing.

A deeper understanding of the physical and chemical mechanisms involved in stabilization has been an intense area of research in recent years. Various leaching procedures and modeling studies have characterized the rate of contaminant release from the stabilized mass. A large variety of surface analytical techniques (e.g. SEM, X-ray photoelectron spectroscopy and Auger electron spectroscopy), bulk characterization methods (e.g. XRD), and spectroscopies (FTIR, NMR) have been used to investigate the mechanisms of stabilization and leaching. In most cases, synthetic wastes were used. These researchers realize the importance of curing time on stabilized forms so many have selected at least 28 days of curing, the traditional length of time used to test structural concrete for its ultimate strength. Shively, et. al., (1984) selected six months of curing time because their research had indicated that most changes in stabilized forms are negligible after 45 days of curing. Heimann, et. al., (1992) tested stabilized synthetic wastes after 7, 36, and 60 days and concluded that curing time is a significant factor in the rate of metal leaching.

Few investigators have used actual wastes to compare TCLP results as a function of cure time. Perry, et. al., (1992) recognized the lack of published long-term leaching data for the stabilization of actual wastes. They conducted a long-term study of four industrial waste samples stabilized by six commercial vendors. The TCLP test was performed several times over nearly a two-year period. The wastes were representative of a variety of industrial operations; a filter cake containing chromium, a process waste sludge containing cadmium which was also hazardous due to reactivity, an electroplating sludge containing nickel, and a corrosive process waste filter cake containing inorganic arsenic.

Six commercial vendors were selected to represent a variety of stabilization processes using fly ash, portland cement, and siliceous materials. Vendors expressed a willingness to treat the samples. Vendors were supplied with a waste profile listing the composition, contaminants, safety precautions, and MSDS information for the wastes. Vendors were also notified of the requirements for the treated wastes; the stabilized wastes were to be as homogeneous as possible. Treated wastes along with the date of stabilization were returned to Monsanto Labs for TCLP and chemical analyses according to USEPA (1987). Extraction took place after 28 days (in duplicate), 90, 200, 470, and 650 days. The duplication after 28 days for each waste indicated that the stabilized waste was reasonably homogeneous. In three of the wastes, TCLP results indicated at least one sample set that followed a deceptive pattern. As indicated in Figure 1.1, analyses of chromium from TCLP extracts showed stabilization improvement with time (vendor 2) and degradation of the treatment with time (vendor 1). Other data indicated a variety of TCLP profiles over time: satisfactory for all time, improving, or unsatisfactory for all time. These results provide independent analyses of commercial stabilization indicating that the issue of long-term treatment effectiveness is timely and important.

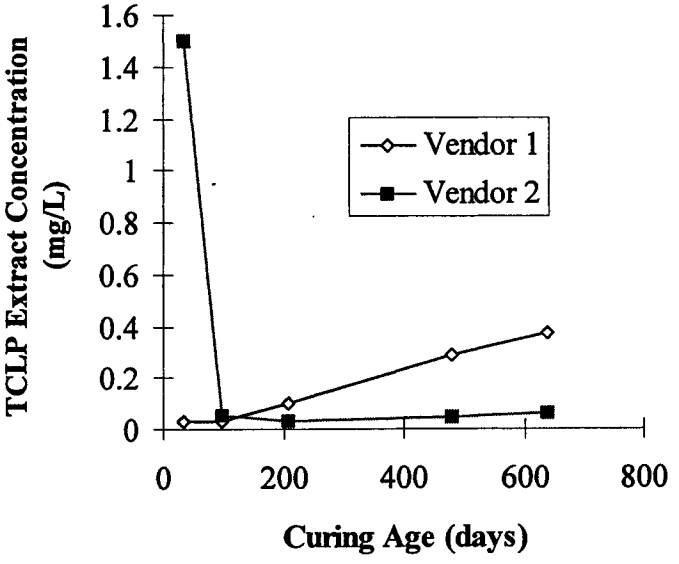

Figure 1.1 TCLP Performance with Cure Age (after Perry, et. al., (1992))

In Tables 1.1 and 1.2, selected TCLP results obtained by the investigators for stabilized actual wastes are shown (Bayasi, et. al., 1992). As can be seen in many cases, stabilizations improve with curing, but occasionally stabilizations may be deceptive and deteriorate with curing. Frequently, curing may improve the stabilization of a waste with respect to one metal, but curing may deteriorate the stabilization with respect to another

metal. A correlation between deceptive stabilization and mix design is difficult to ascertain.

Table 1.1 Portland Cement/Fly Ash Stabilization of K061 Waste Using One and Twenty-One Day Curing TCLP Results For Regulated Metals: Cadmium, Chromium, Lead, and Nickel as a percent of TCLP Standards[1] (Binder/Hazardous Weight = 0.12)

	Water/Binder Ratio								Metal
Fly Ash/Binder Mass Ratio	0.75		1.0		1.25		1.50		
	1 Day	21 Day	1 Day	21 Day	1 Day	21 Day	1 Day	21 Day	
0.0	15	<8	<8	<8	<8	<8	<8	<8	Cd
	206	91	193	133	181	163	181	181	Cr
	<34	<34	38	<34	108	<34	38	<34	Pb
	<0.7	<0.7	0.8	<0.7	0.8	<0.7	<0.7	<0.7	Ni
0.2	15	118	15	<8	<8	<8	3270	788	Cd
	206	48	193	133	169	133	1650	24	Cr
	<34	173	43	<34	<34	<34	2260	155	Pb
	<0.7	<0.7	<0.7	<0.7	<0.7	<0.7	4.5	<0.7	Ni
0.3	1130	<8	<8	<8	<8	917	23	66	Cd
	42	127	193	139	169	24	157	67	Cr
	217	<34	<34	<34	<34	207	330	<34	Pb
	1.9	<0.7	<0.7	<0.7	0.8	<0.7	<0.7	<0.7	Ni
0.4	<8	17	<8	<8	<8	869	<8	394	Cd
	175	91	175	163	175	18	157	36	Cr
	<34	<34	<34	<34	25	239	<34	80	Pb
	<0.7	<0.7	<0.7	1	0.8	0.9	<0.7	1.7	Ni

1.TCLP standards current in 1990 used as a basis.

Table 1.2 Portland Cement/Fly Ash Stabilization of K061 Waste Using One and Twenty-One Day Curing TCLP Results For Regulated Metals: Cadmium, Chromium, Lead, and Nickel as a percent of TCLP Standards[1] (Binder/Hazardous Weight = 0.20)

	Water/Binder Ratio								Metal
Fly Ash/ Binder Mass Ratio	0.75		1.0		1.25		1.50		
	1 Day	21 Day	1 Day	21 Day	1 Day	21 Day	1 Day	21 Day	
0.0	10	13	<8	<8	<8	<8	<8	<8	Cd
	200	157	187	193	212	200	169	163	Cr
	934	1970	281	<34	76	<34	<34	<34	Pb
	<0.7	<0.7	1	<0.7	<0.7	<0.7	0.9	<0.7	Ni
0.2	<8	<8	12	<8	<8	<8	<8	29	Cd
	193	169	187	200	151	163	187	157	Cr
	128	<34	82	<34	<34	<34	55	<34	Pb
	<0.7	<0.7	<0.7	<0.7	<0.7	<0.7	<0.7	<0.7	Ni
0.3	10	162	<8	<8	<8	<8	<8	<8	Cd
	206	48	236	139	193	127	157	139	Cr
	<34	<34	140	<34	<34	<34	<34	<34	Pb
	<0.7	<0.7	<0.7	<0.7	<0.7	<0.7	<0.7	<0.7	Ni
0.4	<8	<8	<8	<8	<8	<8	<8	<8	Cd
	163	121	206	169	175	151	169	157	Cr
	88	<34	57	239	<34	<34	<34	<34	Pb
	<0.7	<0.7	1	0.9	0.9	<0.7	<0.7	<0.7	Ni

1. TCLP standards current in 1990 used as a basis.

Additional results indicating deceptive and improving stabilizations with time are indicated in Figure 1.2 below (Taylor and Fuessle, 1994). TCLP results for mix designs 3 and 4 cured in the short-term exceed standards, however, additional curing improves these stabilizations so they satisfy standards. On the other hand, mix designs 1 and 2 provide satisfactory results in the near term, but fail in the long term.

There are four basic outcomes of the chemical analyses of TCLP extractions from stabilized wastes that have cured either for short or long terms. These possibilities are indicated in Figure 1.3 below. It is most important to detect unsatisfactory and deceptive mix designs early enough to take corrective action. These mix designs will be designated by open symbols. In contrast, improving designs and satisfactory designs will be designated by shaded symbols in this report. In summary, the goal of the project is to develop and test an accelerated curing procedure that could be used to predict long-term effectiveness of stabilized wastes as measured by the TCLP procedure.

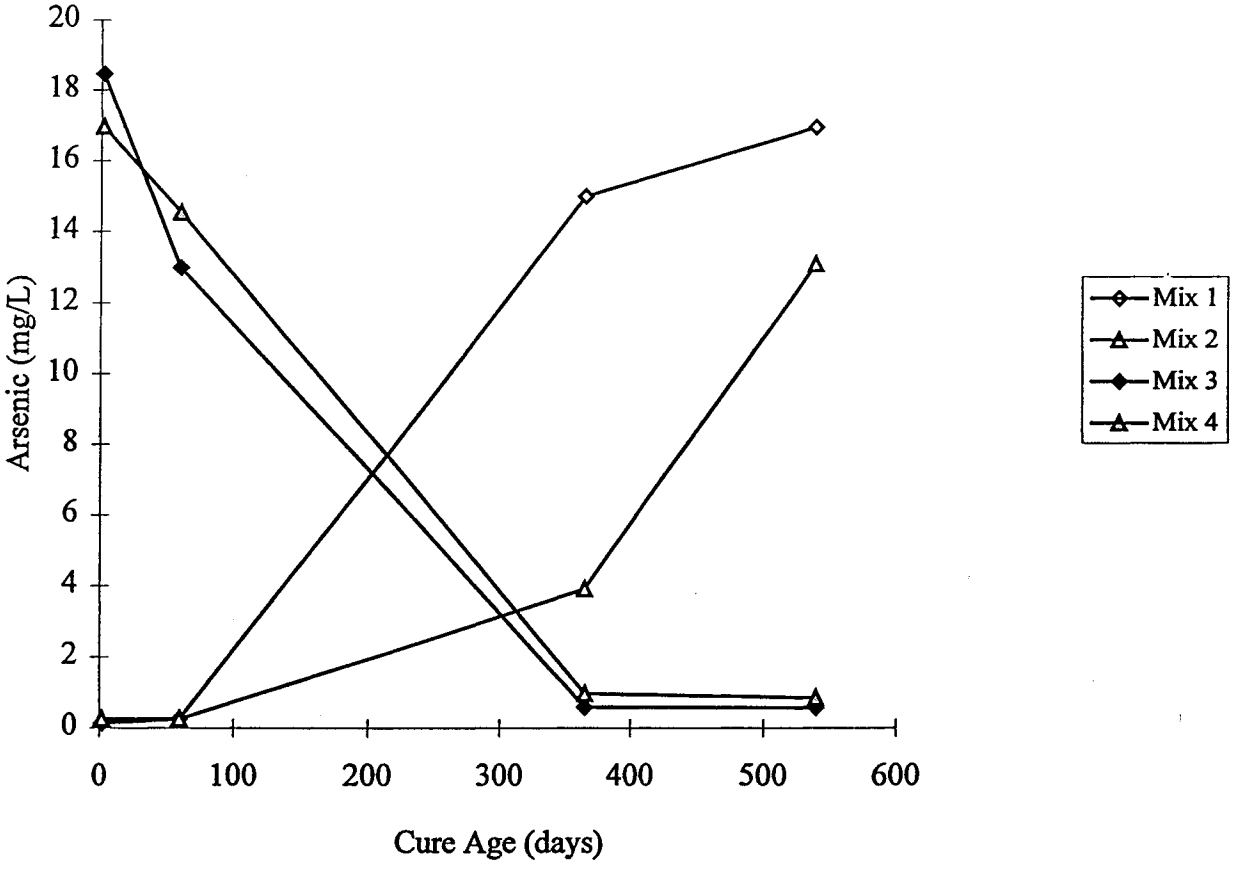

Figure 1.2 Arsenic S/S with Ferric Sulfate

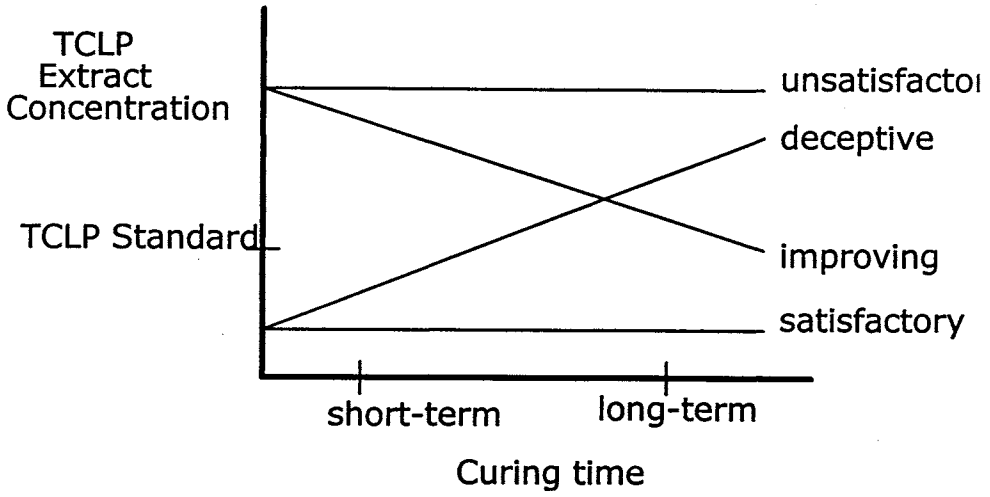

Figure 1.3 Some Potential Outcomes of Stabilization Treatments

1.3 Research Objectives

A procedure is needed that predicts and characterizes the long-term treatment effectiveness of stabilized hazardous waste. Cote, et. al., (1987) and the EPA (1982) have used more harsh leaching procedures to estimate the long-term durability of a stabilized waste. The hypothesis is that a more durable stabilized waste will withstand the harsher leaching processes. This approach does not account for the changes in stabilized wastes with additional curing time. Furthermore, a leaching procedure can be conceived which is harsh enough to tear down any material, so it is questionable whether the actual durability of stabilization is being measured. Another approach is to cure stabilized wastes for extended periods of time before evaluating stabilization effectiveness. This approach is being used in research laboratories, but it is impractical for treatment facilities to wait extended periods of time before obtaining test results indicating if their treatment is viable over the long term.

A different way of attacking the problem is to develop a testing method for stabilized wastes that permits an identification of those stabilization designs that will be effective in the long term. The investigation and understanding of accelerated curing methods is critical for development of a testing procedure that enhances early detection of deceptive stabilizations.

The method should be practical in that it is cost-efficient, reliable, and effective. Cost efficiency implies that testing equipment and person-hours required to perform the test should be small relative to treatment costs. It will allow a landfill operator to predict the long-term treatment efficacy of the stabilized waste using a sample that is closer to its ultimate physical and chemical state. The operator will be able to predict whether additional curing before land disposal is likely to produce a treatment that is satisfactory over the long term. The operator will also have more confidence in the long-term treatment viability of the disposed wastes. The potential for developing an acceleration

method is promising based on acceleration studies of concrete to predict ultimate strength and performance(Kasai, (1990)).

The acceleration method must provide reliable predictions of stabilization performance in the long term. For a given mix design, the TCLP of the accelerated forms (cured for a short term) must reliably indicate if naturally-cured mature stabilized forms (cured over a long term) will satisfy standards. The physical and chemical microstructure of the accelerated and natural forms should also be comparable. The TCLP measure is important as a regulatory tool, and physical/chemical measurements are important for understanding and developing an acceleration method.

An effective acceleration method must apply to a wide range of waste and stabilization designs. Effectiveness also implies that the test must be easy to perform yielding estimates of long- term results in the short term as well as ensuring detection of deceptive mix designs which ultimately fail.

Physical/chemical measurements of stabilized forms during curing will be performed to understand the reliability of the acceleration method. Correlations of these measurements with TCLP results will be used to develop a model for estimation of stabilization effectiveness into longer time frames.

1.4 Report Organization

Characterizations of curing effects on cement and stabilized wastes are summarized in Chapter 2. In addition, various methods for accelerated curing are outlined. Investigations using severe leaching and models to estimate the long-term effectiveness of stabilized wastes are reviewed. In Chapter 3, experimental methods and procedures are described. Where appropriate, the development of the method is also provided. Chapter 4 contains a description of the experimental design, and results and summary are discussed in Chapter 5. Sections in Chapters 4 and 5 are written in parallel so the reader may follow the design and results of any part of the project without any loss of continuity.

CHAPTER TWO
Accelerated Curing and Prediction Methods

2.1 Introduction

The long-term treatment effectiveness of stabilized wastes requires a knowledge of how physical and chemical characteristics of the cement change with curing time. Section 2.2 provides a short summary of the aging process of cements and their constituents. With the project's focus on accelerated curing, sections 2.3 through 2.5 review various methods and results of accelerated curing for cement. The long-term treatment effectiveness of stabilized waste has been estimated by mathematical models which are reviewed in section 2.6.

Short-hand chemical notations are commonly used in the literature and in this chapter. Table 2.1 presents these conventions.

2.2 Aging Process

2.2.1 Hydration of Individual Cement Compounds

The major phases of portland cement are tricalcium silicate ($3CaO{\cdot}SiO_2$), dicalcium silicate ($2CaO{\cdot}SiO_2$), tricalcium aluminate ($3CaO{\cdot}Al_2O_3$) and a ferrite phase of average composition $4CaO{\cdot}Al_2O_3{\cdot}Fe_2O_3$. In commercial clinkers they do not exist in a pure form. The $3CaO{\cdot}SiO_2$ phase is called alite and is a solid solution containing Mg and Al as primary substitutes for Ca. . In clinker, alite consists of monoclinic or trigonal forms whereas synthesized $3CaO{\cdot}SiO_2$ is triclinic. The $2CaO{\cdot}SiO_2$ phase, termed belite, occurs in the β form and contains some K_2O in addition to Al and Mg. Four forms, α,α',β, and γ, of C_2S are known although only the β form with a monoclinic unit cell exists in clinker. The ferrite phase designated C_4AF is a solid solution of variable composition from C_2F to C_6A_2F. The potential components of this compound are C_2F, C_6AF_2, C_4AF, and C_6A_2F. In some clinkers, small amounts of calcium aluminate of formula NC_8A_3 may also form.

The chemical reactions describing the hydration of cement compounds have been worked out through the study of the hydration of the pure cement compounds. If results of these studies are used to model the hydration of cement, it is assumed that the hydration of each compound takes place independently of the others that are present in portland cement. This assumption is not completely valid, since interactions between hydrating compounds can have important consequences, but in most cases it is reasonable. Hydration reactions of calcium silicates are most important.
Their reactions are reviewed here along with tricalcium aluminate, tricalcium ferrite, and ferrite-phase constituents.

Despite large amounts of research, the hydration mechanism of C_3S, the major phase of cement, is not clear. Any mechanism proposed to explain the hydrating

Table 2.1 Composition of Ordinary Portland Cement (OPC) and Common Terms for Hydration Products

Chemical Name	Chemical Formula	Short-hand Notation	Comments
Composition of OPC			
Tricalcium silicate (Alite)	Ca_3SiO_5 or $3CaO{\cdot}SiO_2$ with Fe,Al,Mg,Cr, and Zn substitutions	C_3S	50 % by weight
Dicalcium silicate (Belite)	$2CaO{\cdot}SiO_2$ Ca may be substituted by Mg,Na,K,Cr,Mn; SiO_4 by PO_4 or SO_4	C_2S	25 % by weight
Tricalcium Aluminate	$3CaO{\cdot}Al_2O_3$	C_3A	12 % by weight
Tricalcium (sodium aluminate)	$NaCa_4Al_3O_9$	NC_8A_3	in trace amounts in some clinkers
Tetracalcium Aluminoferrite	$4CaO{\cdot}Al_2O_3{\cdot}Fe_2O_3$	C_4AF	8 % by weight
Calcium sulfate dihydrate (gypsum)	$CaSO_4{\cdot}2H_2O$	$C\bar{S}H_2$	3.5 % by weight
Hydration Products			
Calcium Silicate hydrate gel	$XCaO{\cdot}SiO_2{\cdot}YH_2O$	C-S-H	in substituted form, X and Y vary depending on degree of hydration
Calcium Hydroxide (Portlandite)	$Ca(OH)_2$ (some is amorphous)	CH	product of cement, C_3S, and C_2S
Ettringite	$[Ca_6\{Al(OH)_6\}_2{\cdot}24H_2O](SO_4)_3{\cdot}2H_2O$	$C_6A\bar{S}_3H_{32}$	initial product of C_3A and gypsum
AFt phaste (Al-Fe-tri–$C\bar{S}$)	ettringite phase		forms from C_3A and C_4AF, mostly disappears after few days of hydration
AFm phase (Al-Fe-mono–$C\bar{S}$)	$C_4A\bar{S}H_{12}$		occurs after AFt phase, about 10% of solid phase in mature cement
Miscellaneous Terms			
Lime, calcium oxide	CaO	C	in clinker in small amounts
Silicate	SiO_2	S	
Water	H_2O	H	

behavior of C_3S should take into account the steps through which the hydration proceeds. Five steps can be discerned from isothermal conduction calorimetric studies shown in Figure 2.1.

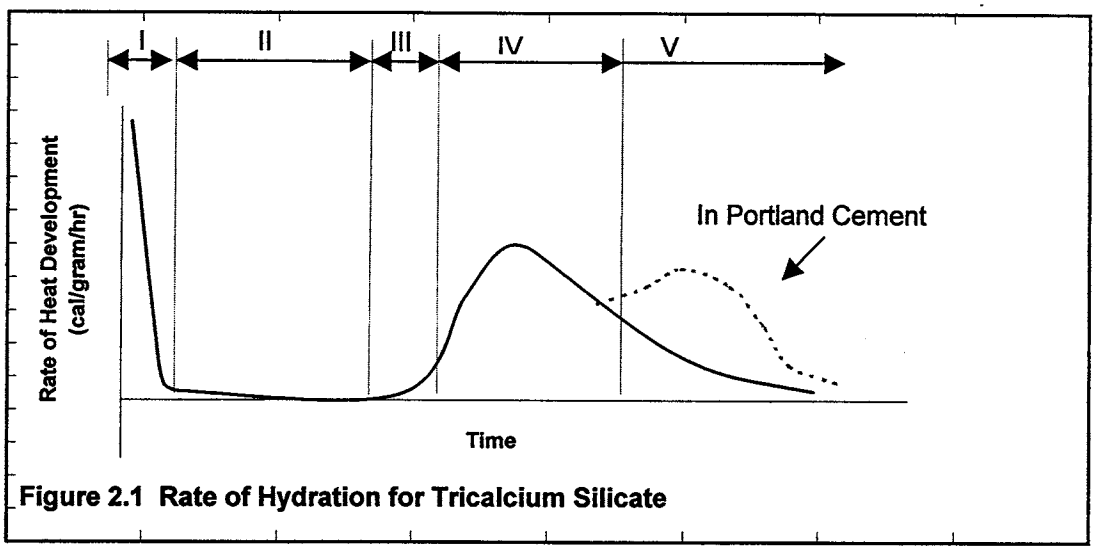

Figure 2.1 Rate of Hydration for Tricalcium Silicate

In the first stage, as soon as C_3S comes into contact with water, there is a rapid evolution of heat which ceases within 15-20 minutes. During this initial stage, C_3S releases calcium and hydroxyl ions into the solution. This stage is called the pre-induction period. In the second stage, the reaction rate is very slow and is known as the dormant or induction period which may extend for a few hours. During this stage, the cement remains plastic and is workable. Calcium dissolution continues and the pH reaches a high value of 12.5. In the third stage, the reaction occurs actively and accelerates with time reaching a maximum rate near the end of this acceleratory period. During this stage, a certain critical value of calcium and hydroxide ions is reached resulting in a rapid crystallization of CH and C-S-H followed by rapid reactions. Initial set occurs at about this time when the rate of reaction becomes vigorous with continuous formation of the hydration products CH and C-S-H. The final set occurs before the end of third stage. In the fourth stage, there is slow deceleration. In the final stage, there is only a slow formation of products and the reaction is diffusion-controlled. As shown in Figure 2.2, initially the hydration products are mostly CH with little C-S-H. Slowly over time, more C-S-H is formed. In mature cements, C-S-H and CH occupy volumes of approximately 50-60% and 20-25%, respectively. An understanding of the first two stages of the reaction has a very important bearing on the subsequent hydration behavior of the sample. Comparatively more attention has been directed to stages I and II than with stages III–V.

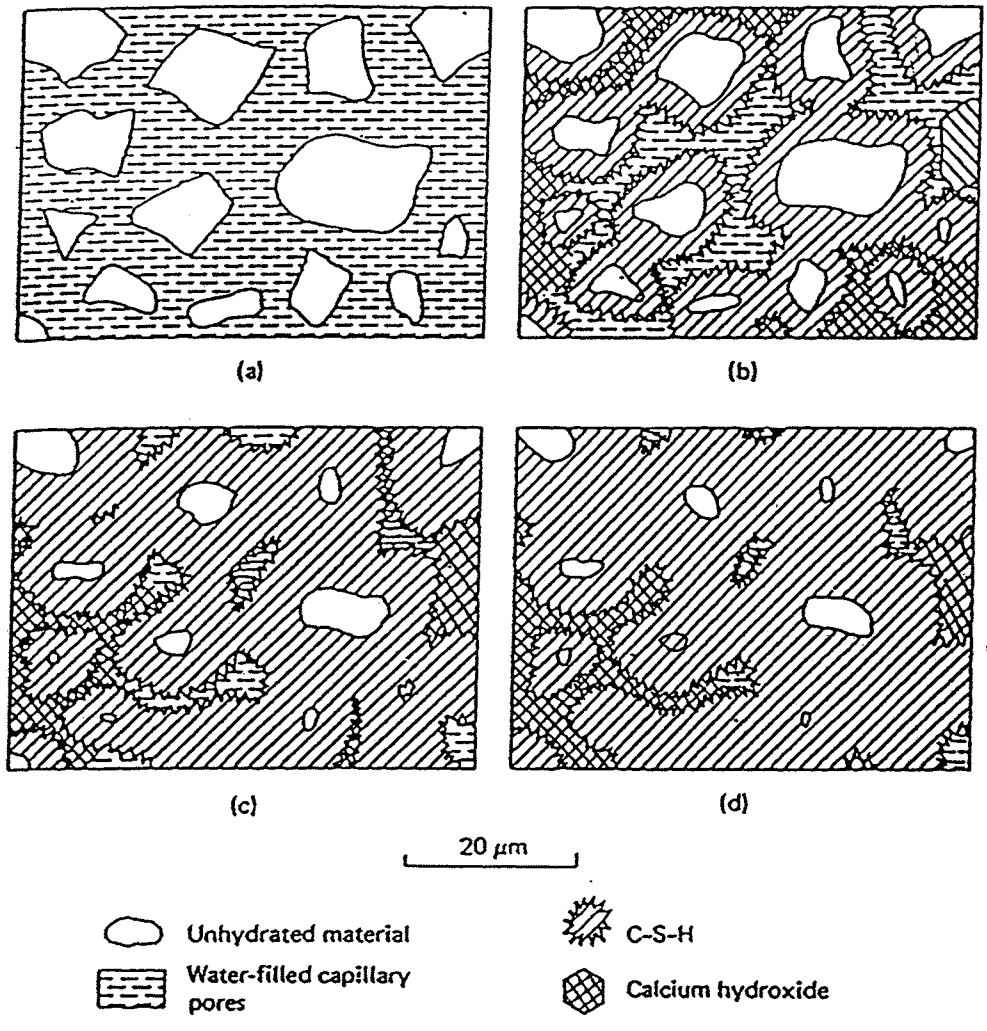

Figure 2.2 Schematic Outline of Microstructural Development of Portland Cement Paste (Calcium Sulfoaluminates are included as part of C-S-H although they are separate phases.) (a) Initial (b) 7 days (c) 28 days (d) 90 days (Mindess and Young (1981))

2.2.1.1 Tricalcium Silicate

Tricalcium silicate and dicalcium silicate together make up 75–80% of non-hydrated portland cement. According to Ramachandran (1984), the early reaction of C_3S with water in the presence of limited amounts of water is represented as follows:

$$3CaO \cdot SiO_2 + xH_2O \rightarrow yCaO \cdot SiO_2 \cdot (x + y - 3)H_2O + (3 - y)Ca(OH)_2$$

or typically

$$2[3CaO \cdot SiO_2] + 7H_2O \rightarrow 3CaO \cdot 2SiO_2 \cdot 4H_2O + 3Ca(OH)_2$$

The above chemical equation is somewhat approximate because it is not easy to determine the composition of C-S-H (the C/S and S/H ratio). In a fully hydrated cement or C_3S paste about 60–70% of the solid comprises C-S-H. The amorphous C-S-H phase contains particles of colloidal size and exhibits only two very broad peaks in XRD. The degree of hydration of C_3S can be measured by determining C_3S or $Ca(OH)_2$ by XRD, the nonevaporable water by ignition, or $Ca(OH)_2$ by thermal or chemical methods.

2.2.1.2 Dicalcium Silicate

Just as in the hydration process of C_3S, there are also uncertainties involved in determining the stoichiometry of C_2S development in the C-S-H phase. The hydration of dicalcium silicate phase can be represented by the equation

$$2(2CaO \cdot SiO_2) + 5H_2O \rightarrow 3CaO \cdot 2SiO_2 \cdot 4H_2O + Ca(OH)_2$$

The amount of $Ca(OH)_2$ formed in this reaction is less than that produced in the hydration of C_3S. The dicalcium silicate phase hydrates much more slowly than the tricalcium silicate phase. Figure 2.3 compares the rates of hydration of C_3S and C_2S. The absolute rates differ from one sample to another; it is apparent that C_3S is much more reactive than C_2S (Ramachandran (1984)).

2.2.1.3 Tricalcium Aluminate

In portland cement, although the average C_3A content is only about 4–11%, it significantly influences the early reactions. The phenomenon of "flash set", the formation of various calcium aluminate hydrates and calcium sulfoaluminates involves the reactions of C_3A. Higher amounts of C_3A in portland cement may pose durability problems. Pure tricalcium aluminate reacts with water to form C_2AH_8 and C_4AH_{13} (hexagonal phase).

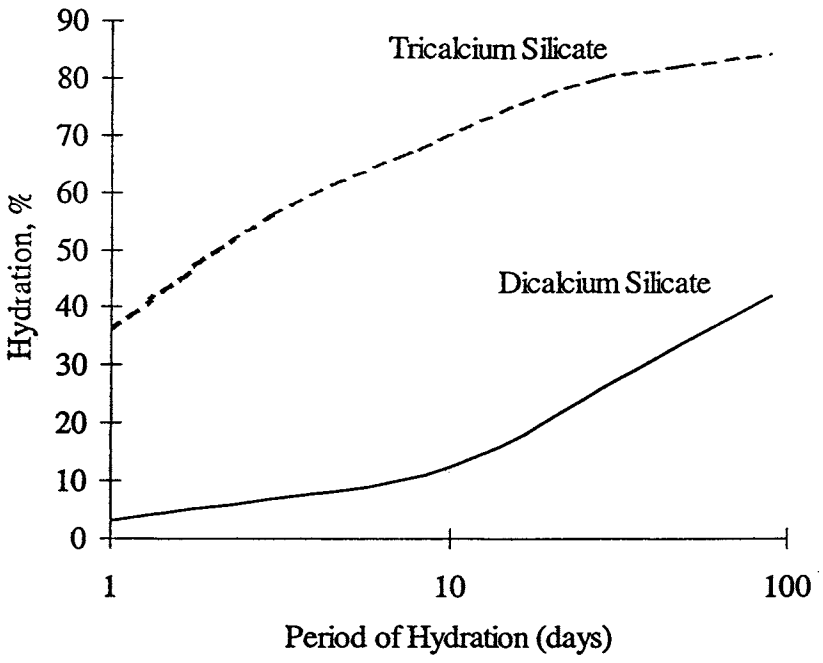

Figure 2.3 Rates of Hydration (Ramachandran (1984))

$$2C_3A + 21H \rightarrow C_4AH_{13} + C_2AH_8$$
$$C_4AH_{13} + C_2AH_8 \rightarrow 2C_3AH_6 + 9H$$

Ramachandran (1984) suggests that these products are thermodynamically unstable so that without stabilizers or admixtures they convert to C_3AH_6 phase (cubic phase). The C_3A pastes exhibit lower strengths than do the silicate phases under normal conditions of hydration. This lack of strength is attributed to the formation of the cubic phase. Under certain conditions of hydration of C_3A, i.e. at lower water/solid ratios and high temperatures, the direct formation of C_3AH_6 can improve the strength of the body substantially by forming direct bonds between particles. In portland cement, the hydration of C_3A phase, controlled by the addition of gypsum, is more important.

2.2.1.4 Ferrite Phase

The ferrite phase constitutes about 8–13% of an average portland cement. The ferrite phase may have a variable composition that can be expressed as $C_2(A_nF_{1-n})$ where $0<n<0.7$. Of the cement minerals, the ferrite phase has received much less attention than

others with regard to its hydration and mechanical characteristics. This may partly be ascribed to the assumption that the ferrite phase and the C_3A phase behave in a similar manner.

The C_4AF phase is known to yield the same sequence of products as C_3A. The reactions are slower however. In the presence of water pure C_4AF reacts as follows:

$$C_4AF + 16H \rightarrow 2C_2(A,F)H_8$$
$$C_4AF + 16H \rightarrow C_4(A,F)H_{13} + (A,F)H_3$$

Hydration of C_4AF at low water/solid ratios and high temperatures may enhance the direct formation of the cubic phase. According to Ramachandran (1984), microhardness measurements show that higher strengths at higher temperatures may be attributed to the direct formation of the cubic phase on the original sites of C_4AF. This results in a closely welded, continuous network with enhanced mechanical strength. In cements, C_4AF reacts much slower than C_3A in the presence of gypsum. In other words, gypsum retards the hydration of C_4AF more efficiently than that of C_3A. The rate of hydration depends on the composition of the ferrite phase; those containing higher amounts of Fe exhibit lower rates of hydration.

2.2.2 Hydration of Cement

Although hydration studies of the pure cement compounds are very useful in following the hydration processes of portland cement itself, they cannot be directly applied to cements because of complex interactions. In portland cement the compounds do not exist in pure form but are solid solutions containing impurities such as Al, Mg, and Na. The rate of hydration of alites containing different amounts of Al, Mg, or Fe has shown that, at the same degree of hydration, iron-alites show the greatest strength. There is evidence that C-S-H formed in different alites is not the same. Significant amount of Al and Fe are incorporated into the C-S-H structure. The presence of alkalis in portland cement also has an influence on the hydration of individual phases. The hydration of C_3A, C_4AF and C_2S in cement are affected because of changes in the amounts of Ca^{2+} and OH^- in the hydrating solution. The reactivity of C_4AF can be influenced by the amount of SO_4^{2-} ions consumed by C_3A. Some SO_4^{2-} ions may be depleted by being absorbed by the C-S-H phase. Gypsum is also known to affect the rate of hydration of calcium silicates.

During the first few days, the rate of hydration in cements proceeds in the order: $C_3A > C_3S > C_4AF > C_2S$. The rate of hydration of the compounds depends on the crystal size, imperfections, particle size, particle size distribution, the rate of cooling, surface area, the presence of admixtures, and the temperature. Similar to observations in pure compounds, there is a significant difference between the rate of hydration of C_3S and βC_2S. Ramachandran (1984) reports on a comparison of hydration rates of C_3S and C_2S having the same surface area (4500 cm^2/g) and same W/S ratio (0.45). The estimated amount of C-S-H in C_2S hydrated for 1,3,7, and 28 days is 4.9, 9.2, 15.2, and 51.6%,

respectively. The corresponding values for C_3S were 34.4, 36.6, 45.5, and 62.0%, respectively. This data indicates that the strength development in hydrating C_2S proceeds at a slower rate than that in C_3S. The C/S ratio of the C-S-H product in the hydrated C_2S is slightly higher than that in the hydrated C_3S.

In a mature hydrated portland cement, the products formed are C-S-H gel, $Ca(OH)_2$, ettringite (AFt phases with the formula $C_6A\overline{S}_3H_{32}$), monosulfate (AFm phases), hydrogarnet phases, and possibly amorphous phases high in Al^{3+} and SO_4^{2-} ions. The C-S-H phase does not necessarily consist of 1:1 molar $CaO:SiO_2$. The X-ray diffraction analysis of C-S-H in cement pastes gives powder patterns very similar to that of C_3S pastes. The composition of C-S-H in terms of C/S ratio is variable depending on the time of hydration. At 1 day, the C/S ratio is about 2.0 and becomes 1.4-1.6 after several years. The C-S-H can take up substantial amounts of Al^{3+}, Fe^{3+}, and SO_4^{2-} ions. This reaction may be important for the long-term effectiveness of stabilization.

Atkins, et. al., (1991) state that cement hydration is at least 95% complete after a year of wet cure at 20° C. The hydration products consist of crystalline and amorphous phases. Crystalline phases include calcium hydroxide, C_4AH_x (where x = 13 to 19), ettringite, and related solid solutions where sulfates may substitute for the hydroxyl ion. Atkins, et. al., (1991) shared data on a synthetic C-S-H gel whose pH was measured after 160 days of curing at 25° C. With aging, the pH decreased as the calcium/silicon ratio decreased from 1.7 to about 0.9. C-S-H may sorb sulfate ions and limited substitutions of Na and K for Ca also occur.

Lenz (1966) and Tamas, et. al., (1976) have shown that both in C_3S and portland cement pastes, the monomer that is present in the C_3S and C_2S compounds (SiO_4^{4-} tetrahedra) polymerizes to form dimers and larger silicate ions as hydration progresses. The gas-liquid chromatographic analysis of the trimethyl silylation derivatives has shown that anions with 3 or 4 Si atoms are absent in immature cements. The polymer content with 5 or more Si atoms increases as the hydration proceeds and the amount of dimer decreases. In C_3S pastes the disappearance of monomer results in the formation of polymers. In cement pastes even after the disappearance of all C_3S and C_2S some monomer remains possibly because of the modification of the anion structure of C-S-H through replacement of Si atoms by Al, Fe, or S. Admixtures can influence the rate at which the polymerization proceeds in portland cement and C_3S pastes.

In fully hydrated portland cement, $Ca(OH)_2$ contributes about 20-25% of the solid content. The crystals are platy or prismatic and cleave readily. They may be intimately intergrown with C-S-H. The crystalline $Ca(OH)_2$ gives sharp XRD patterns, shows endothermal peaks and weight losses in TGA. The morphology of $Ca(OH)_2$ may vary being found as equidimensional crystals, large flat platy crystals, large thin elongated crystals or combinations of them. Some admixtures and hydration temperatures can modify the morphology of $Ca(OH)_2$. According to Ramachadran (1981, 1984) both crystalline and amorphous $Ca(OH)_2$ are formed in portland cement pastes.

2.3 Accelerated Curing-Physical Heat

The temperature and relative humidity during curing influence the strength development, microstructure, and long-term durability of concrete. The effect of

temperature has been studied by many researchers using microwave and conventional ovens at regulated relative humidity. According to Sabir (1995), in most of the results, high-temperature curing (above 50°C) accelerates the strength development at early ages, but long-term strength does not appear to be influenced by temperature. According to Patel, et. al., (1995), a network of microcracks was evident within the matrix of all the concretes cured at 85°C. Samples cured at 16°C, 42°C, and 46°C have shown no differences in spatial distribution, morphology, and volume of hydrates. Concretes cured between 50°C and 70°C have been reported to exhibit a coarser C-S-H morphology and pore structure than that characteristic of pastes cured under ambient conditions (Patel, et. al., (1995)). Recent works indicate a growing concern that, after a long-term exposure, concrete cured at elevated temperatures may show abnormal expansion and associated micrcracking, which may lead to failure. According to Cao and Detwiler (1995), elevated curing results in a coarser, more continuous pore structure and nonuniform distribution of hydration product. They suggested that the use of slag, silica fume and/or fly ash might mitigate the effects of high temperature curing. The durability of stabilized waste depends largely on the permeability, which in turn depends on the continuity of pore structure.

Masse and Zanni (1993) used ^{29}Si solid state NMR with high resolution to observe the hydration kinetics of class G cement and C_3S at temperatures ranging from 60° C to 120°C. The hydration was stopped at times ranging from 30 minutes to 14 days using an "acetone-ether method of removing water". C_3S and cement were similar; spectral results for cement were less sharp than that for C_3S because of other impurities in the cement. After 6 hours of hydration, Q_o monomeric species decrease with temperature, Q_2 chain middle groups increase, and dimeric species Q_1 remain constant. Q_3 and Q_4 were never observed after 510 days at 60° C or after 4 days at 120° C. Spectra for 120°C at 3 hours were very similar to spectra at 100°C after 14 days. After 3 hours, it appears $Q_1 > Q_2$ whereas Q_2 becomes most significant at 120°C. After 14 days, $Q_2 < Q_1$ up to 80°C whereas above 80°C, $Q_2 > Q_1$. At 80°C, very little changes were shown in the first hour of hydration. With hydration at room temperature, Q_o exists after 2 months, and $Q_2 < Q_1$ after 2 months.

Since S/S of radioactive waste will involve significant heats, Atkins, et. al., (1991) considered the effects of heat on cement curing. They mentioned that autoclaved cements are usually steam-cured 12-24 hr at 160 to 190°C. The required silica is added as a fine sand to achieve a Ca:Si ratio close to 1.0 With these curing conditions, autoclave products are normally mixtures of crystalline tobermorite and low ratio C-S-H gel. Atkins, et. al., (1991) also presented NMR data indicating that the ratio Q_2/Q_1 increases with a decrease in Ca/Si ratio and with increases in temperature and aging. This ratio provides a measure of the mean length of the silicate chains where Q_2 is a Si chain mid-member and Q_1 a Si chain end-member.

Silica chain length analyses have been conducted with heat cured cements, naturally aged cements, and with cements used in waste stabilization. These analyses are important because they provide a chemical description of how heat curing and wastes affect the chemistry of cement. Silica chain length analyses are discussed later in the review.

For cement exposure to intermediate temperatures, 40–100°C, information is sparse. A synthetic system of CaO-SiO_2-H_2O was prepared with Ca/Si ratios of 0.9, 1.3, and 1.7. These samples were cured at 25, 55, and 85°C for up to 200 days. Samples were analyzed with X-ray diffraction and ^{29}Si NMR. X-ray diffraction results indicated that C-S-H gel persists to about 60°C except at low Ca/Si ratios where partial crystallization occurred. At 85°C, crystallization occurred for all mixes; tobermorite for mixes with lower Ca/Si ratios, and jennite with higher Ca/Si ratios. In general, crystalline components have lower surface areas (and probably less sorption capacity) than C-S-H.

The silicate structure of C_3S cured at 20 and 60°C was investigated by Parrot (1981), using the molybdate complexing method. The formation of polysilicates was associated with an increase in the degree of condensation of the polysilicate. Heat accelerated the formation of polysilicates without altering the process. Most of the monomeric silica could be accounted for by tricalcium silicate.

Hirljac, et. al., (1983) prepared two types of monoclinic alites including some with additives: $CaCl_2$, Na_2CO_3, NaF, and $CaSO_4$. Trimethylsilyl derivatives were separated by gel permeation chromotography. Semi-isothermal calorimetry and quantitative X-ray diffraction were used. For the same degree of hydration, admixtures had no effect on the proportion of polymers; i.e. admixtures affect the hydration rate and polymerization equally.

Higher temperature curing causes an initial accelerated consumption of C_3S, but later hydration is not sensitive to temperature. At elevated curing temperatures, the polysilicate fraction in C-S-H increased significantly and became more marked as times progresses. Hirljac, et. al., (1983) provide a summary of the activation energy E_a and degree of hydration α determined by quantitative X-ray diffraction analyses as shown in Table 2.2.

Table 2.2 Summary of Polymerization Data (After Hirljac, et.al. (1983))

Reaction	E_a (kcal /mol)	65 deg C		25 Deg C.		5 Deg C.	
		Time	α	Time	α	Time	α
Monomer→ Dimer	9	<1h	<10%	0-6h	<15%	0-1d	<20%
Dimer→ Pentamer	9±1	0-5d	10-30%	6h-1d	15-30%	1-3d	20-40%
Pentamer→ Octamer	13±1	5h-1d	30-45%	1-7d	30-50%	3-14d	40-60%
Octamer→ Med. MW polymer	13±1	1-14d	<45%	7-90d	<50%	14-90d	<60%
Med. MW →High MW polymer	13±1	<14d	<60%	<90d	<60%	–	–

Shi and Day (1993) examined the relation between curing temperature and initial hardening time, ultimate strength, and rate of strength development for lime-pozzolanic cement pastes. The effects of chemical accelerators 4% Na_2SO_4 and 4% $CaCl_2 2H_2O$ were also studied. A water to cement ratio of 0.5 was used at temperatures of 23, 35, 50, and 65 °C. Strength equations are shown in Table 2.3.

Table 2.3 Effect of Heat on Strength Equations for Cement[1]

Pastes	Equations	Correlation Coefficient
Control, 23°C to 65°C	$S_o = 18.6 - 0.20T$	0.996
Control + 4% Na_2SO_4, 35°C to 65°C	$S_o = 28.4 - 0.29T$	1.000
Control + 4% $CaCl_2$ H_2O, 35°C to 65°C	$S_o = 35.3 - 0.31T$	0.985

1. After Shi and Day (1993)

Shi and Day (1993) also employed the Arrhenuis equation to relate "the effect of curing temperature on cement hydration or the strength development of cement pastes." They provide evidence demonstrating that there is a correlation between cement hydration and strength development. The form of the equation:

$$K_T = A\exp\left(\frac{-E_a}{RT}\right)$$

where:
K_T= strength development rate constant as described by the following equation:

$$S = S_o \frac{K_T(t - t_o)}{1 + K_T(t - t_o)}$$

S = compressive strength [Mpa];
S_o = ultimate compressive strength at infinite age [Mpa];
t = actual curing age at temperature T [days];
t_o = theoretical initial hardening time [days];
A = frequency factor [1/days];
E_a = apparent activation energy [kJ/mol];
R = universal gas constant [kJ/mol-deg].

Shi and Day (1993) concluded: 1) Elevated curing temperatures can shorten the initial hardening of lime-pozzolanic pastes. The addition of Na_2SO_4 does not influence the initial hardening time, but $CaCl_2$ prolongs it; 2) Strength-development rate constants

increase with curing temperatures; 3) Lime-pozzolanic pastes are more sensitive to elevated curing temperatures compared to plain OPC.

Table 2.4 Activation Energies for Heat Curing of Cement[1]

Pastes	A(day^{-1})	correlation coefficients	activation energy (kJ/mol)
control	8.71×10^{9}	0.999	66
control+4% Na_2SO_4	5.74×10^{11}	1.000	75
control+4%$CaCl_2$	1.62×10^{15}	0.999	99

1. After Shi and Day (1993).

Using ^{29}Si NMR spectroscopy, XRD, and thermal analyses, Cong and Kirkpatrick (1995) considered the effects of temperature (from 25 to 200 °C), and/or relative humidity, (from 9% to 100%) on synthetic C-S-H with Ca/Si ratios ranging from 1.13 to 1.56. Polymerization of the C-S-H did not change with relative humidity, but local structural disorder increased according to the full-widths at half-heights of both Q_1 and Q_2 peaks which increased with decreasing relative humidity. Heating drives out OH^- and water with an increase in polymerization and basal spacing. Broader NMR peaks indicate a more disordered structure with a smaller basal spacing.

2.4 Accelerated Curing- Chemical

Chemical accelerators are used in cold weather concreting operations. A significant increase in the rate of early strength development at normal or low temperatures enables reduction in the curing and protection periods necessary to achieve specified strengths in concrete. Accelerators are being used in solidification and stabilization of wastes also. Many substances are known to act as accelerators for concrete. They include alkali hydroxides, silicates, flurosilicates, organic compounds, calcium formate, calcium nitrate, calcium thiosulfate, aluminum chloride, potassium carbonate, sodium chloride, and calcium chloride. Among the various materials which accelerate the development of strength in cements, several chlorides have a significant place, and of those, calcium chloride has proven to be the most widely used accelerator because of its availability, low cost, and predictable performance (Ramachandran, 1984). Calcium chloride is the most widely used because of its ready availability, low cost, predictable performance characteristics, and successful application over several decades. Calcium chloride has been used as an admixture for a longer period than most other

admixtures. The first documented use of calcium chloride in concrete can be traced to the year 1873 and the first patent in 1885.

2.4.1 Hydration Behavior

The silicate phases C_3S and C_2S together constitute the major portion of the components in portland cement, influencing considerably its hydration and strength development. Sloane, et. al., (1931) and Haegermann and Forsen (1938) observed the accelerating influence of $CaCl_2$ on the hydration and hardening behavior of C_3S about 60 years ago. According to Ramachandran (1981), additions of calcium chloride also result in a decrease in the dormant or induction period in the hydration of C_3S (and other constituents of cement). This decrease can be observed by periodic measurements of the residual unhydrated C_3S, the amount of $Ca(OH)_2$, loss on ignition, electrical conductivity, and rate of heat liberation.

As the accelerating effect of $CaCl_2$ on cement is related mainly to the C_3S phase it is important to gain an understanding of the influence of $CaCl_2$ on this phase. Calcium chloride is somewhat unique because the cation-anion Ca^{2+}–Cl^- combination ranks as one of the best accelerators for the hydration of C_3S. According to Ramachandran (1981), the accelerating effect of cations is in the decreasing order $Ca^{2+}>Sr^{2+}>Ba^{2+}>Li^+>K^+$ and that of anions, $SO_4^{2-}>OH^->Cl^->Br^->NO_3^->CH_3COO^-$. There is some evidence that Cl^- is a better accelerator than SO_4^{2-} in the hydration of portland cement. Calcium chloride not only alters the rate of hydration of cement minerals but may also combine with them. It also influences such properties as strength, chemical composition, surface area, morphology, and pore characteristics of the hydration products.

2.4.2 Influence of Calcium Chloride on the Hydration of Cement Minerals: Tricalcium Silicate

Many researchers have used differential thermal analysis (DTA) to follow the hydration of C_3S and portland cement in the presence of calcium chloride. Typical results given by Kawada, et. al., (1967) and Ramachandran (1981) are illustrated in Figures 2.4 and 2.5. Thermograms of C_3S hydrated to different times in the presence of 0, 1 and 4% $CaCl_2$ enable a study of the progress of hydration, identification, and estimation of some of the products. Unhydrated C_3S exhibits endothermal effects at about 680°C, 930°C, and 970°C–980°C representing crystalline transitions. The onset of hydration is indicated by endothermal effects below 300°C. Endothermal effects are caused by the expulsion of water from the C-S-H gel. This effect intensifies with time indicating the formation of larger amounts of C-S-H.

In the presence of 1% $CaCl_2$, the thermograms of hydrating C_3S show significant differences from those without $CaCl_2$. 25% of all $Ca(OH)_2$ that is formed in 30 days is

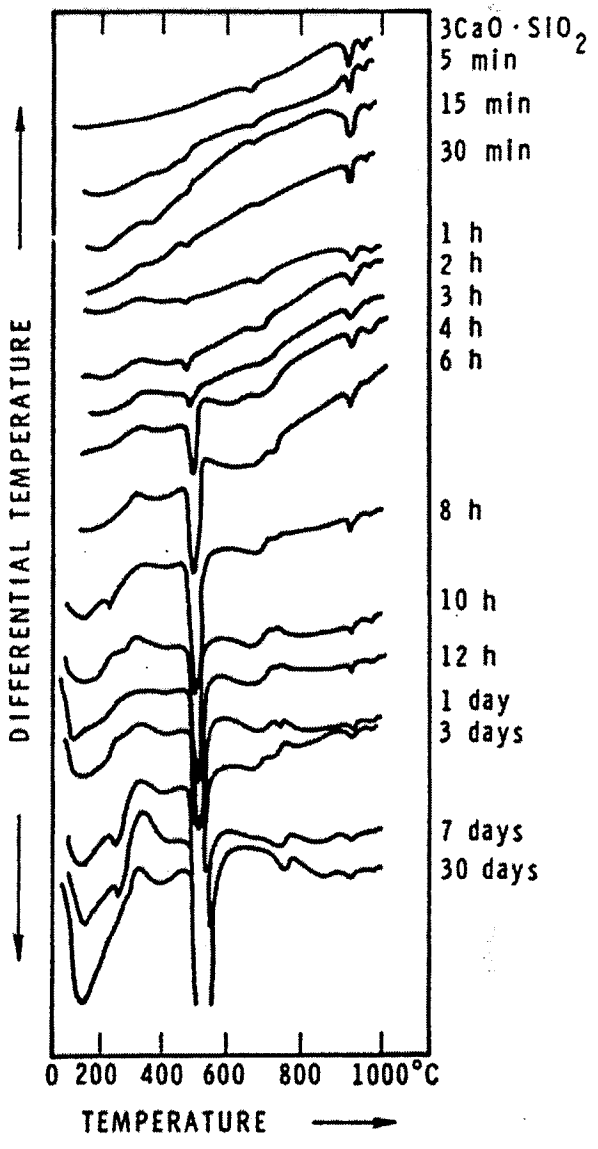

Figure 2.4 Hydration of C_3S by DTA by DTA (Ramachandran (1981))

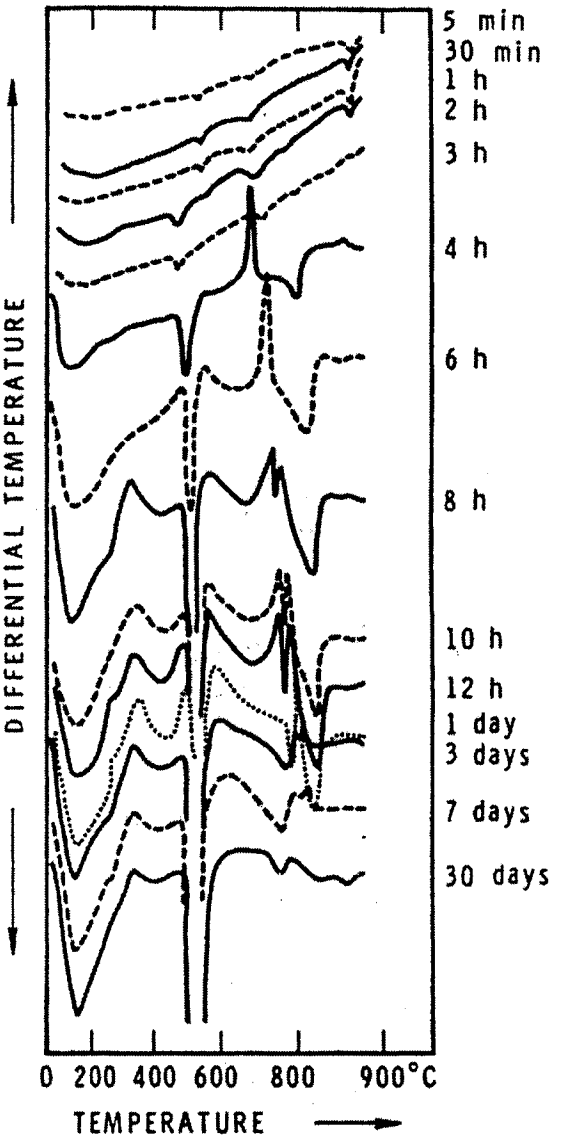

Figure 2.5 Hydration of C_3S with 1% $CaCl_2$ by DTA (Ramachandran (1981)

produced in the first 8 hours without $CaCl_2$, whereas 33% of estimated total $Ca(OH)_2$ is formed within 5 hours in the presence of 1% $CaCl_2$. In the presence of 4% $CaCl_2$, some of the thermal effects become more intense at earlier times than the corresponding ones hydrated in the presence of 1% $CaCl_2$.

The amount of $Ca(OH)_2$ formed at different periods may be determined by measuring the endothermal areas of $Ca(OH)_2$ decomposition. Rio, et. al., (1970) and Ramachandran (1981) suggested that if the amount of $Ca(OH)_2$ formed at different periods represent the degree of hydration, then at 30 days, C_3S+1%$CaCl_2$ > C_3S+0%$CaCl_2$ > C_3S+4%$CaCl_2$. If the rate of hydration is determined by the disappearance of C_3S, then at 30 days it would be C_3S + 4%$CaCl_2$ > C_3S + 1% $CaCl_2$ > C_3S + 0% $CaCl_2$. This apparent anomaly can be explained by the formation of a higher C/S product in the presence of 4% $CaCl_2$. The rate of hydration of C_3S (determined by estimating unhydrated C_3S) with 2% $CaCl_2$ shows increasing amounts of C-S-H at all times up to 1 month.

Calcium chloride accelerates the hydration of C_3S even at higher temperatures. The effect is particularly greater at earlier periods of hydration. After 24 hours with no added $CaCl_2$, C_3S hydrates approximately to the extent of 30% and 60% at 22°C and 80°C, respectively. With the addition of 2% $CaCl_2$, the corresponding degree of hydration at 22°C and 80°C is 60% and 70%, respectively. According to Skalny and Maycock (1974), at temperatures of 25°C, 35°C, and 45°C, additions of 2% $CaCl_2$ not only intensifies the total heat developed at early periods but also reduces the time at which the maximum rate of heat evolution occurs. Because of the accelerated hydration, the silicate phases show rapid setting characteristics in the presence of $CaCl_2$. In a C_3S:C_2S mixture containing 0%, 1%, and 2% $CaCl_2$, the setting times have been reported to occur at 790, 525, and 105 minutes, respectively.

2.4.3 Influence of Calcium Chloride on the Hydration of Cement Minerals: Dicalcium Silicate

Compared to the extensive investigations of the hydration of C_3S in the presence of $CaCl_2$, only meager work has been done on the action of $CaCl_2$ in the hydration of C_2S. Calcium chloride accelerates the hydration of C_2S but the actual values reported in the literature on the relative accelerating action vary because of the differences in the nature of the sample, experimental conditions, and method adopted for determining the degree of hydration. According to Teoreanu, et. al., (1974), at early times the accelerating action of $CaCl_2$ in C_2S is less dramatic than that observed in the hydration of C_3S. Addition of $CaCl_2$ also influences the C/S ratio of the C-S-H product. For example, the ratio increased from 1.7 to 1.82 with 2% $CaCl_2$.

According to Ramachandran (1981), the porosity of a C_2S paste containing $CaCl_2$ is slightly higher than that without it, being 0.183 and 0.168 mL/g (of hydrated C_2S), respectively. The surface area in C_2S pastes containing $CaCl_2$ is only slightly higher than the surface area in pastes without it. Calcium chloride does not seem to influence the morphology of hydrated C_2S as it does hydrated C_3S.

2.4.4 Influence of Calcium Chloride on the Hydration of Cement Minerals: Tricalcium Aluminate

A study of C_3A hydration in the presence of $CaCl_2$ is important because of the formation of calcium chloroaluminate hydrate in portland cement. Two calcium chloroaluminate hydrates are known; $C_3A{\cdot}CaCl_2{\cdot}xH_2O$ and $C_3A{\cdot}3CaCl_2{\cdot}yH_2O$. It is generally believed that the low calcium form is the main reaction product during normal hydration.

2.4.5 Rate and Mechanism of Hydration for $3CaO{\cdot}SiO_2$

In the earlier literature, Candolt, et. al., (1886) ascribed the accelerating action of $CaCl_2$ to the formation of a calcium oxychloride hydrate. In the system $CaO–CaCl_2–H_2O$, two oxychlorides, $3CaO{\cdot}CaCl_2{\cdot}16H_2O$ and $CaO{\cdot}CaCl_2{\cdot}2H_2O$ are formed, the former being stable at a $CaCl_2$ concentration of 18% or more. Ramachandran (1981) discounted this mechanism because the concentrations of $CaCl_2$ normally used to accelerate the hydration of C_2S do not attain such a high value.

In the absence of evidence for the existence of a complex, it is suggested that $CaCl_2$ acts catalytically. The exact mechanism by which this occurs in the $C_3S–CaCl_2–H_2O$ system is not clear. This mechanism is based on the premise that $CaCl_2$ does not combine chemically. There is however, some evidence that $CaCl_2$ may in fact be rigidly bound in the hydrating C_3S. Ramacharndran (1981) speculated about the possible states of chloride in the hydrating C_3S. The chloride may be in the free state, as a complex on the surface of C_3S during the dormant period, as a chemisorbed layer on the C-S-H surface, in the interlayer surfaces of C-S-H, or in the lattice of C-S-H. In the acceleratory period, adsorption of Cl^- ions may lead to an autocatalytic effect so that hydration proceeds at a fast rate. The increase in the surface area and modifications in the morphological features of hydrated C_3S in the presence of $CaCl_2$ may perhaps be due to Cl^- being chemisorbed or in the interlayer positions. The inhibition of formation of afwillite in the presence of $CaCl_2$ during C_3S hydration may be related to the existence of Cl^- in the C-S-H lattice.

According to Collepardi, et. al., (1972), the accelerating action of $CaCl_2$ is due to its ability to promote the instability of the primary hydrosilicates, thus enhancing the formation of nuclei of a lower lime content and more porous hydrosilicates. This explanation is based on the observation that the addition of $CaCl_2$ to a prehydrated C_3S does not accelerate further hydration.

According to Skalny and Odler (1967), the addition of $CaCl_2$ reduces the alkalinity of the aqueous phase in the hydrating C_3S. For example, without the addition of $CaCl_2$ the pH values at 1,2,4, and 24 hours are respectively 12.31, 12.28, 12.41, and 12.43; with $CaCl_2$, corresponding values are 11.67, 11.77, 11.85, and 11.91. Thus a reduced pH might be compensated by the liberation of more lime through an increased rate of C_3S hydration. Acceleration can also be achieved in an environment of higher pH, and hence it is doubtful whether acceleration can be explained by pH effects only.

The condensation characteristics of silicate ions in the hydration of silicates with or without $CaCl_2$, may have a role in the mechanism of hydration and strength development. Skalny and Odler (1967) stated that calcium chloride seems to promote higher condensation initially in the hydration of C_3S, thus possibly enabling a high level of water diffusion through gel. Some evidence suggests that cations with smaller ionic radii are more effective accelerators of C_3S hydration. This would indicate that solid state diffusion plays a role in the accelerating mechanism.

Skalny and Odler (1967) suggested that the formation of calcium aluminate chloride hydrates is responsible for the growth of cement strength. The formation of calcium aluminate hydrates is possible only in the absence of calcium sulfate and therefore they cannot form until the gypsum has been fully exhausted in the hydration process. Kurczyk and Schwiete (1960) account for the favorable influence of calcium chloride upon the strength of hydrated C_3A as the consequence of increased formation of C_4AH_{13}, to the detriment of the C_3AH_6 phase.

No single mechanism can explain the effect of $CaCl_2$ on the hydration kinetics of C_3S, the morphological features, changes in pore volume and surface area, and strength development. Probably a combination of mechanisms may be operating depending on the experimental conditions and the period of hydration.

2.4.6. Effects of Chemical Accelerators on Physical Properties of C_3S

With curing time, changes in matrix constituents, physical strength, specific surface area, porosity, and pore size distribution will affect the long-term stability and leachability of S/S wastes. Researchers have investigated the effects of calcium chloride on physical properties of C_3S and the more complex portland cement paste. A summary of these investigations are reviewed for C_3S paste and cement in sections 2.4.6 and 2.4.7, respectively.

2.4.6.1 Porosity

Porosity and pore size distribution characteristics in a cementitious system can be helpful in predicting shrinkage, durability, strength, and leaching characteristics. After one day of hydration, total porosity is higher in samples containing $CaCl_2$ than in those without it. Increased porosity of $CaCl_2$-treated samples is attributed to the greater number of small pores of size 10-50 A°. After approximately 6 months of curing, samples of C_3S hydrated at a W/S of 0.3 and 0.5 with 2 and 5% $CaCl_2$, respectively, show lower porosity than samples hydrated without $CaCl_2$. For a particular W/S ratio, strength increases as the average pore radius decreases. Compressive strength can be expressed as a function of microhardness. Traetteberg (1974) suggested that an approximate linear relationship exists between log microhardness and porosity for samples with or without $CaCl_2$.

2.4.6.2 Surface Area

The surface area of C_3S hydrated in the presence of $CaCl_2$ is much higher than that hydrated without $CaCl_2$ provided N_2 is the adsorbate used for surface area measurement (Collepardi, et. al., (1972)). The extent of this increase may differ, depending on the particle size, purity of C_3S, W/S ratio, amount of calcium chloride added, temperature of hydration, extent of hydration, and drying conditions. If water is used as the adsorbate, surface area values are much higher than those with N_2.

Figure 2.6 presents Collepardi's values for N_2 surface area as a function of time of hydration for C_3S hydrated with or without 2% $CaCl_2$. In the first 4 hours of hydration, C_3S+0% $CaCl_2$ shows a rapid increase in surface area, reaching a value of about 130 m^2/g. Subsequently the value decreases at a rate of 4 $m^2/g/hr$ in the first day, 0.1 $m^2/g/hr$ during the following week, and 0.01 $m^2/g/hr$ between 7 days and 3 months. In the presence of $CaCl_2$, the surface area is about 220 m^2/g during the first day and falls to a value of about 80 m^2/g in 3 months. This latter value is still about three times that determined for C_3S+0%$CaCl_2$. Nitrogen surface area for C_3S +5% $CaCl_2$ is higher than that for C_3S+0%$CaCl_2$ or C_3S+2%$CaCl_2$. Though surface area decreases as the temperature of hydration is increased, samples containing $CaCl_2$ show higher surface areas than those without it at any temperature. Figure 2.6 indicates that all samples show a decease in the surface area as the hydration progresses. This phenomenon is called aging (thickening) of the porous structure due to physical and/or chemical interlayer bonds.

2.4.6.3 Morphology

Distinct differences in morphology are observed in samples of C_3S hydrated with $CaCl_2$ compared to those without $CaCl_2$. Depending on drying techniques, actual descriptions of the morphology may vary (Ramachandran (1981)). According to Odler and Skalny(1971), in the absence of $CaCl_2$, hydrated C_3S forms sheets rolled into cigar–shaped fibers 0.25 to 1 μm long. In pastes with 2% $CaCl_2$, the products assume a spherulitic morphology. Kurczyk and Schwiete (1960) observed that needle-shaped hydration products initally obtained in the absence of $CaCl_2$ were also transformed to spherulites with additional curing. Ramachandran (1981) reported that C_3S hydrated without $CaCl_2$ showed needles whereas that hydrated with 1 or 4% $CaCl_2$ exhibited a platy or crumpled foil-like morphology.

This morphological difference was attributed to chemisorption of chloride on the C-S-H surface. Collepardi and Marchese (1972) obtained similar results. Young (1974) has described the morphological difference between hydrated C_3S without $CaCl_2$ and hydrated C_3S+2% $CaCl_2$ as needle-like versus a lace-like structure. In contrast, Murakami and Tanaka (1968) propose a fibrous cross-linked structure in C_3S pastes treated with $CaCl_2$. Hydrated C_3S prepared at a W/S ratio of 0.3 and containing 2 or 5% $CaCl_2$ showed higher strengths than that obtained without $CaCl_2$, and this result is attributed to the denser morphology.

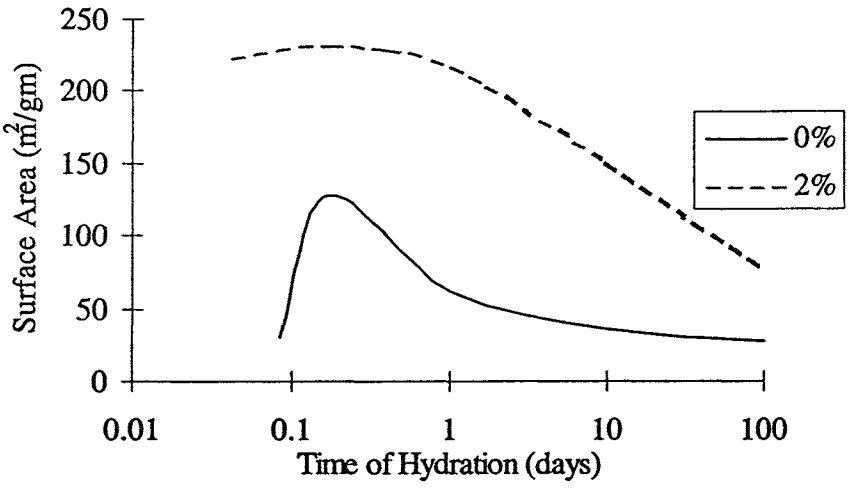

Figure 2.6 Surface Area of C_3S Paste containing Calcium Chloride (after Ramachandran, (1984)).

2.4.6.4 Strength Development

A small addition of $CaCl_2$ to portland cement accelerates the setting and hardening characteristics of the cement. Haegermann and Forsen (1938) observed that $CaCl_2$ accelerated the hardening process in C_3S which has been confirmed by many researchers. The setting time of a 1:1 mixture of C_3S to C_2S decreases from 790 minutes to 525 minutes with 1% $CaCl_2$. Similar results have been reported by Tsivilis, et. al., (1995). Figure 2.7 compares the rate of strength devleopment in C_3S pastes hydrated with and without $CaCl_2$ (Rio, et. al., 1970). Up to 28 days, the strength in the paste containing 2% $CaCl_2$ is higher than the specimen hydrated without the chloride. The percentage increase of strength, however, decreases as the hydration proceeds. The increase in strength at earlier periods (with $CaCl_2$ addition) may be explained by the increased amount of hydration product formed. Increased rate of hydration by itself does not assure increased strengths. Although the amount of hydration with >2% $CaCl_2$ is at least as great as that with 1.5–2% $CaCl_2$, higher concentrations of $CaCl_2$ generally lower the strength.

The hardening behavior of a C_3S+$CaCl_2$+H_2O system not only depends on the percentage of $CaCl_2$ but also on the W/S ratio. The enhancement of strengths in C_3S pastes with 1–2% $CaCl_2$ cannot be explained only in terms of the degree of hydration. It may be related in a complex way with porosity, morphology, chemical composition, surface area, and density. According to Rio, et. al., (1970), a higher condensation degree of the hydrated products will result in strength increase.

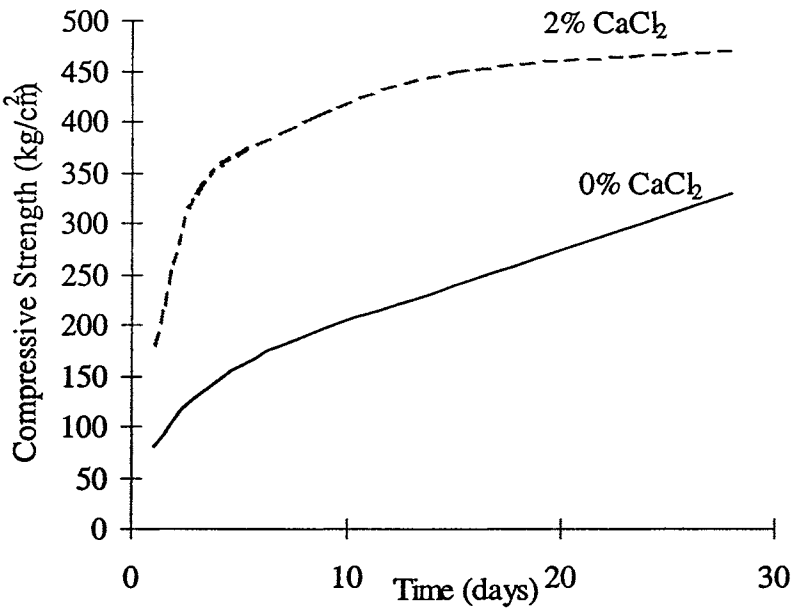

Figure 2.7 Compressive Strength of Tricalcium Silicate Paste Containing $CaCl_2$ (Ramachandran (1984))

2.4.7 Effects of Chemical Accelerators on Physical Properties of Cement

Ramachandran (1984) reviewed the effects of accelerators on cement pastes. The hydration and hardening of C_3S with $CaCl_2$ is measured in several ways: a decrease in the dormant or induction period, the amount of $Ca(OH)_2$, loss on ignition, electrical conductivity, heat of liberation, and DTA. Using DTA, unhydrated C_3S displays endothermal effects at about 680, 930, and 970° C representing crystalline transitions. Hydration is indicated by endothermal effects below 300° C caused by the release of water from the C-S-H gel. During hydration, it was once thought that a calcium oxychloride hydrate complex was involved in the hydration reactions, but in the absence of discovering this complex, most researchers believe that $CaCl_2$ acts as a catalyst. Diffusion seems to play a role in some way. Some suggest that $CaCl_2$ enhances the condensation of calcium silicates with a higher diffusive rate of water through the gel. Chloride diffusion into the gel may enhance OH^- diffusion outward. Also, $CaCl_2$ seems to promote condensation of the silicates, thus enabling a higher level of water diffusion through the gel. Several other suggestions for a hydration mechanism have been made.

The microstructural change with accelerated curing has also been investigated. With acceleration, the morphological change is more pronounced at higher water/solid ratios where the lattice has more space to expand. Descriptions of the change vary among researchers but generally accelerators yield a more condensed structure. With accelerators, "needle-like" products are transformed with curing to a "lace-like" or "crumpled foil" morphology.

The porosity of pastes hydrated with and without accelerators has been compared for equal degrees of hydration. The porosity of accelerated pastes is lower. The surface area of C_3S and C_2S increased in the presence of $CaCl_2$. The increase in surface area depends on particle size, silicate purity, and w/s ratio among other variables. The effects of accelerators on C_2S are similar but less pronounced than that for C_3S. Porosity and surface area increase with an accelerated hydration. The only difference is there does not appear to be an effect of accelerators on C_2S morphology.

Early strength (up to 28 days) of accelerated pastes is greater than that for normally-cured samples. Later hydration indicates that the strength of normally-cured samples surpasses that with chemical accelerators.

Minor components of cement, C_3A and C_4AF, are also affected by $CaCl_2$. The reaction of C_3A and C_4AF with gypsum is accelerated by $CaCl_2$. After the gypsum has reacted, monochloroaluminate is formed. After $CaCl_2$ has been consumed in reaction, ettringite is converted to monosulfoaluminate.

Because of $CaCl_2$ corrosion of steel reinforcements, accelerators without chloride have been proposed. Much less investigation of these accelerators has taken place. Proposed compounds include: aluminates, sulfates, formates, thiosulfates, nitrates, carbonates, halides, urea, glyoxal, triethanolamine, and formaldehyde. Triethalonamine (TE) accelerates the hydration of C_3A. After a brief initial retardation, TE also accelerates C_3S and C_2S. Calcium formate also accelerates the hydration of C_3S but not as effectively as $CaCl_2$.

2.5 Accelerated Curing-Carbonation

Hannawayya (1984) studied accelerated curing by subjecting samples to pressurized CO_2. The two critical parameters for mix design were compaction pressure and water/solids ratio. These parameters were critical because a high pressure decreases porosity and diffusion of the CO_2; while a low pressure or high values of water/solids permit larger pores of water thereby decreasing CO_2 diffusion. Samples with lower water/solids ratios do not allow enough water for the carbonation reaction. Maximum strength for accelerated specimens was obtained by 30 minutes of curing followed by 38 minutes of carbonation. The early strength of accelerated specimens was greater than the early strength of specimens undergoing normal curing. However, the 28-day strength of accelerated specimens was less than those undergoing normal cure. X-ray diffraction revealed a retardation of the reaction involving aluminite and ferrite components with SO_3 to form ettringite. With SEM, the structure of $CaCO_3$ crystals was described as short prismatic rods with cutoff ends.

Lange, et. al., (1996) investigated the curing of a stabilized waste consisting of electroplating and metal finishing wastes. Waste solids were 55%, pH = 8, TDS = 9200 mg/L, and aqueous soluble TOC = 2 mg/L. The stabilization mixes were designed with 35% waste, and water/cement ratios ranging from 2.25 to 1.33. The mixes were cured in either air, nitrogen, or CO_2. The relative humidity was 50% at a temperature of 20-23° C. After 28 days, samples were analyzed for unconfined strength, leachate metals resulting

from a modified leaching procedure, and mineralogy using x-ray diffractometry. Higher strengths were obtained for specimens cured in air or CO_2; the highest strength depended on the cement content of the mix.

X-ray diffractometry indicated that portlandite, calcite, and ettringitte were all present for specimens cured with air. Specimens cured with CO_2 showed larger amounts of calcite and less portlandite. Lange, et. al., (1996) suspect that portlandite reacted with CO_2 to produce more calcite. The volume change associated with this reaction may reduce pore space and improve microstructure. This reaction may also lead to the precipitation of metal carbonates.

In general, metal leaching results followed this pattern: Air < CO_2 < N_2. Although carbonation lowered the pH of S/S forms by approximately 3 units, metal leaching from samples cured with CO_2 was less than that from samples cured with N_2.. Therefore, the combination of C-S-H and CH to maintain a higher pH favorable for metal stabilization does not explain metal leaching results. Apparently, microstructural changes and precipitation of salts containing toxics were also important.

2.6 Estimations of Long-Term Effects on Stabilized Wastes

The long-term retention of waste by cements is determined by many factors. One primary factor is pH which is determined mostly by the solubility of calcium hydroxide and C-S-H, and the soluble alkali content. A second factor is the amount of porosity and its interconnectivity that controls the effective permeability. Other factors include the redox potential, sorption, and solubility considerations. The treatment effectiveness of old stabilized wastes has been estimated by severe leaching tests and by mathematical modeling.

According to Fuhrmann, et. al., (1990), short-term tests cannot yield data to predict long-term service life of the S/S form. They propose an accelerated test that yields data required to make predictions about long-term leachability provided diffusion is the leaching mechanism. A test was provided to determine if diffusion is the leaching mechanism. The reference and accelerated tests are semi-dynamic leach tests with leachants at 20° C. and 50° C. respectively. The leachant is sampled and replaced periodically; twice on the first day and then daily for 11 more days. Data from these tests are compared with models to determine if diffusion is the leaching mechanism. The criterion for goodness-of-fit is a sum of differences between model and test data. If diffusion is the controlling mechanism for metal release, then projections of long-term releases can be made. If diffusion is not the controlling mechanism, Fuhrmann, et. al., (1990) suggest models that cannot be used for long-term projections.

Fuhrmann, et. al., (1990) review two solutions to Fick's diffusion equation: $\frac{\partial C}{\partial t} = -D_e \nabla^2 C$ where C is the concentration of the species, t is time, and D_e is the effective diffusion coefficient. The two solutions are for a semi-infinite media and a finite cylinder with a constant diffusion coefficient. The solution for diffusion from semi-infinite media is:

$$\frac{\sum a_n}{A_o} = \frac{2S}{V}\left[\frac{D_e t}{\pi}\right]^{1/2}$$

where a_n is the total amount of material released in all leaching periods up to time t, A_o is the initial amount of metal, V is the volume of the waste form, S is the surface area of the waste. The solution for leaching from a finite cylinder with constant diffusion is more complex:

$$\frac{\sum a_n}{A_o} = 1 - \frac{32}{\pi^2}\sum_{n=1}^{\infty}\sum_{m=1}^{\infty}\frac{e^{-tD_e\left[\beta_m^2+(2n-1)^2\pi^2/4\ell^2\right]}}{(2n-1)^2\left(\beta_m\right)^2}$$

where ℓ is the half height of the cylinder(cm), β_m is the positive roots of the Bessel function where $J_o(\beta_m) = 0$. This equation converges slowly, so Fuhrmann, et. al., (1990) suggest a complex set of equations that approximate the solution.

Batchelor (1990) describes a variety of leaching models based on different assumptions. The effective diffusivity of a non-reactive contaminant is defined in a similar way to that for molecular diffusion in Fick's Law. The effective diffusivity, D_e, is less than the molecular diffusion, D_m, because of the tortuosity of the porous solid. If all pores are connected and parallel, the following relationship holds: $D_e = \frac{\varepsilon D_m}{\delta}$ where ε is the porosity and δ is the tortuosity.

Various physical-chemical reactions may affect the mobile and immobile fractions of a contaminant. These reactions include: precipitation, sorption, oxidation-reduction, and acid-base reactions. Because at least one of these reactions occurs, Batchelor (1990) distinguishes between D_e which only accounts for the physical matrix of the porous media and D_{obs} which also accounts for any reactions.

The material balance for a rectangular waste form with Fickian diffusion can be written as:

$$\frac{\partial C}{\partial t} = D_e\frac{\partial^2 C}{\partial X^2} - R$$

where R is the net rate of contaminant production. Typical assumptions for leaching models are: 1) The waste has a rectangular geometry; 2) The concentration of the contaminant at the solid-solution interface is zero (infinite bath); 3) The contaminant is distributed homogeneously before leaching begins; 4) The concentration of the contaminant at the solid's center does not change during leaching (infinite solid). The solution is:

$$C(X,t) = C_o\,\mathrm{erf}\left(\frac{X}{(4D_e t)^{0.5}}\right)$$

and

$$\frac{M_t}{M_o} = \left(\frac{4D_e}{\pi L^2}\right)^{0.5} t^{0.5}$$

where C_o is the initial concentration of the waste form, M_t/M_o is the fraction of contaminant leached at time t, and L denotes the distance from the edge of the slab to its center. If precipitation and dissolution are prevalent,

$$\frac{M_t}{M_o} = \left(\frac{4D_{obs}}{\pi L^2}\right)^{0.5} t^{0.5}$$

$$D_{obs} = \frac{\pi\left[F_m(1-F_m)+0.5F_m^2\right]D_e}{2}$$

Although D_{obs} can be estimated from a leaching test, D_e can be determined from leaching data only if the tracer is completely non-reactive and mobile. Batchelor (1990) recommends a conductivity method to estimate D_e with reference to the MacMullen number defined as the solid conductivity divided by the pore-water conductivity.

Assuming that the length variable can be approximated by the particles' volume/area ratio, a modified solution for the TCLP results can be written as follows:

$$C_{TCLP} = C_o' \frac{M_t}{V_b}\frac{A}{V}\left(\frac{4D_{obs}}{\pi}\right)^{0.5} t^{0.5}$$

where C_o' is the initial mass of contaminant per mass of solid. A value for D_{obs} can be determined from TCLP data according to this equation. A qualitative comparison can be made between leaching data from different S/S mix designs by comparing the ratio of the observed diffusion rate divided by the molecular diffusion rate.

Cote, et. al., (1987) evaluated the long term leachability of synthetic waste forms by using a dynamic leaching test with DI water as the leachant which was renewed periodically. Four waste forms were made using arsenic, cadmium, chromium, and lead in four types of binders: lime and fly ash, fly ash and cement, bentonite and cement, and cement and soluble silicates. The leaching was conducted for 665 days. Regressions of cumulative fractions leached were compared with results of semi-empirical mathematical models. Cumulative fractions of the chromium, cadmium, and lead were less than 1% of total metal available, while arsenic leached more readily up to 15%. The leaching of chromium, cadmium, and lead was a function of the square root of time, indicating that the leaching was controlled by diffusion of the soluble fraction through the pores of the matrix. The arsenic leaching was limited by the availability of carbon dioxide which was introduced with the fresh leachant. The reaction of CO_2 with lime and basic calcium arsenite yields a mobile arsenite ion. Four types of mathematical models described by Cote, et. al., (1987) are summarized in Table 2.5.

Groot and Sloot (1992) state that the regulatory emphasis should be on waste release patterns over time and not on concentrations to be satisfied at one point in time. For monolithic solids (> 40 mm), tank leaching with its similarities to ANS 16.1 is superior to other leaching methods because leaching mechanisms (dissolution, surface runoff, and matrix diffusion) can be identified. According to Groot and Sloot, (1992), values for leach parameters, availability, tortuosity, and chemical retention, can be determined to permit the estimation of contaminant release over long periods of time.

Availability is a measure of the contaminant fraction that is mobile. The availability test requires finely ground particles where 95% are less than 125 μm. The leachant to solid ratio is 100 with leachant pH maintained at 4. Results of the tank test yield a characterization of the leaching mechanism. Surface wash-off is described by an initial cumulative release that levels out over time. Diffusion of the contaminant through the solid matrix yields a slope of approximately 0.5 on a log-log plot of cumulative release versus time. Dissolution is indicated by a rapid release of contaminant with slopes of about 1 on the log-log plot.

Groot and Sloot (1992) use Crank's solution to the diffusion equation for a solid of semi-infinite dimensions:

$$\frac{C-C_1}{C_o-C_1} = \text{erf}\frac{x}{2\sqrt{Dt}}$$

where:

- C = concentration at location x at time t;
- C_1 = constant concentration at the surface, x = 0;
- C_o = initial uniform concentration in the solid at t = 0;
- D = diffusion coefficient;
- x = distance from surface;
- t = time;
- erf = error function.

If $C_1 = 1/2C_o$, then $D_e = \frac{\pi B_t^2}{t(U_{max}d)^2}$ where D_e = effective diffusion coefficient in m^2/sec, B_t = cumulative release in mg/m^2; U_{max} = the maximum leachable quantity in mg/kg; and d = bulk density of the product in kg/m^3. Rearrangement and taking logs yields:

$$\log(B_t) = \frac{1}{2}\log(t) + \log\left[U_{max}d\sqrt{\frac{D_e}{\pi}}\right]$$

According to this equation, a log-log plot of cumulative release gathered from experimentation versus time will yield a value for D_e. This value is valid only if the slope is approximately 1/2 indicating that diffusion controls.

Assuming that sodium does not interact with the solid matrix, then the tortuosity can be calculated according to: $\tau = \frac{D_{Na}}{D_{e,Na}}$ where D_{Na} is the diffusion coefficient of sodium in water in m^2/s, and $D_{e,Na}$ is the effective diffusion coefficient of sodium in the solid in m^2/sec. The chemical retention factor is also calculated according to: $R = \frac{D}{D_e\tau}$.

Long-term predictions of leachability are complicated by assumed constant boundary conditions for the mathematical model and by finite dimensions of the solid. Groot and Sloot (1992) have developed a 3-D model and preliminary results were presented. Their 1-D model overestimates the long-term leaching since projections

Table 2.5 Mathematical Models for Leaching from Stabilized Wastes

Type	Equation	Solution	Assumptions
I	$\frac{\partial C}{\partial t} = D_e \frac{\partial^2 C}{\partial z^2}$	$L(t) = C_T\left[\frac{D_e}{\pi t}\right]^{1/2}$ $F(t) = 2\frac{A}{V}\left[\frac{D_e t}{\pi}\right]^{1/2}$	bulk diffusion of contaminant in its mobile form with concentration, C
II	$\frac{\partial C_{mo}}{\partial t} = \frac{D_e}{(1+K_d)} \frac{\partial^2 C_{mo}}{\partial z^2}$	$L(t) = (C_{mo} + C_{im})\left[\frac{D_e'}{\pi t}\right]^{1/2}$ $F(t) = 2\frac{A}{V}\left[\frac{D_e' t}{\pi}\right]^{1/2}$	linear adsorption isotherm: $K_d = C_{im}/C_{mo}$ $D_e' = \frac{D_e}{(1+K_d)}$ chemical reaction slows down leaching
III	$\frac{\partial C}{\partial t} = D_e \frac{\partial^2 C}{\partial z^2} + k(C_e - C)$	$L(t) = C_T(D_e'' k)^{1/2}\left[erf(kt)^{1/2} + \frac{e^{-kt}}{(\pi k t)^{1/2}}\right]$ where: $D_e'' = \frac{D_e}{\left(\frac{C_T}{C_e}\right)}$	C represents the mobile concentration at (t,z) and C_e is the mobile concentration at time = 0 for all z; first-order production of mobile species
IV	$\text{contaminant}_{\text{solid phase}} \underset{k_d}{\overset{k_t}{\leftrightarrow}} \text{contaminant}_{\text{aq. phase}}$	$L(t) = f\left[e^{-(k_t + \beta k_d)t}\right]$	β is the solid surface area to leachant volume; for short times where surface processes dominate
	$L(t) = K[C_{sat}^{(w)} - C^{(w)}(t)$ $u(t) = L(t)/C_T$; $u_o = L_o/C_T$	$F(t) = \frac{A}{V} u_o t$	surface leach rate as mass transfer coefficient: network dissolution velocity u; $C_{sat}^{(w)} >> C^{(w)}(t)$; $u(t) = u_o$
	Cote et al. combined solutions from above	$CAL(t) = k_1(1 - e^{-k_2 t}) + k_3 t^{1/2} + k_4 t$	

exceed the total amount available for leaching. The 3-D model appears more valid since projections approach the total amount available asymptotically.

Hung (1982) reviewed briefly long-term leaching for solidified wastes. The finite solid diffusion model results in a solution composed of infinite series and tedious numerical summations. Solutions of an infinite solid-diffusion model are of simpler algebraic form. Accounting for the effects of desorption, diffusion, and radioactive decay, a mass balance yields:

$$\frac{\partial C}{\partial t} = \left(\frac{D}{\varepsilon R}\right)\left(\frac{\partial^2 C}{\partial x^2}\right) - \lambda_d C \quad \text{where}$$

R is the retardation factor and λ_d is the first-order decay rate. Defining dimensionless groups as: $c' = C/C_o$; $x' = x/L$; and $t' = Dt/\varepsilon RL^2$; $\xi = \lambda_d \varepsilon RL^2/D$; and $\ell' = \frac{\varepsilon RaC_o L}{A_o}\left.\frac{\partial C'}{\partial x'}\right|_{x'=0}$, the solution to the mass balance in dimensionless terms leads to:

$$\ell' = F(\xi, t')$$

or

$$\frac{\ell}{A_o \eta} = F(\xi, t') = F\left(\frac{\lambda_d}{\eta}, \eta t\right)$$

where

$$\eta = \frac{D}{\varepsilon RL^2}$$

Hung (1982) estimates long-term leaching with the following procedure:

1. Find η and ξ from test data.
2. Find η_p (p for prototype) by: $\eta_p = \eta(L_m/L_p)^2$.
   Scale effect is based on the assumption that leaching is characterized by waste volume/leaching surface area, thus, length. The author shows that the ratio of leaching numbers is equals to a ratio of squared lengths.
3. Calculate $\frac{\ell}{A_o}$ to forecast long-term leaching.

The assumptions are: homogeneous solidified waste; one-dimensional transport, negligible thermal effects, physiochemical properties (e.g. porosity, tortuosity, retardation factor) remain constant during leaching; concentration of the radionuclide is zero at the solid-liquid interface.

Mathematical models require significant simplifying assumption and values for empirical parameters. Considering all the complexities of modeling, Medici, et. al., (1992) and others suggest a very simple model: $y = at^b$ where y = cumulative amount of contaminant released, and a,b are empirical constants. An alternative approach is a short-term leaching procedure whose results indicate long-term treatment performances.

CHAPTER THREE
Experimental Measurements and Materials

3.1 Sample Collection and Composition of Wastes, Binders, and Reagents

Approximately 70 pounds of K061 arc furnace dust were collected at one time which was sufficient for the project duration. Chemical analyses of nitric digestates and TCLP extracts of the waste are provided in Tables 3.1 and 3.2, respectively.

Sufficient amounts of binders were stocked and homogenized before beginning this project. Two bags of Type I portland cement and class C fly ash were used. Tables 3.3 and 3.4 provide information on the binder chemical compositions.

Table 3.1 Chemical Analyses of Nitric Digestates of K061 Waste, ppm

Element	Sample 1	Sample 2	Average
Cadmium	16.6	16.0	16.3
Chromium	73.5	67.8	70.6
Copper	0.78	0.78	0.78
Iron	65.0	60.9	62.9
Lead	22	22	22
Manganese	7.78	6.95	7.37
Nickel	4.07	4.07	4.07

Table 3.2 Chemical Analyses of TCLP Extracts of K061 Waste, ppm

Element	Sample 1	Sample 2	Sample 3	Sample 4	Average
Cadmium	7.02	5.32	7.655	7.975	6.99
Chromium	≤2.04	≤2.04	≤2.04	≤2.04	≤2.04
Copper	≤0.34	≤0.34	≤0.34	≤0.34	≤0.34
Iron	4.71	4.71	4.71	4.71	4.71
Lead	5.08	4.52	6.82	8.64	6.26
Manganese	4.22	3.94	5.86	7.37	5.35
Nickel	≤2.03	≤2.03	≤2.03	≤2.03	≤2.03

Table 3.3 Manufacturers' Composition of Binders: Fraction of Total Mass(%)

Compound	Portland Cement[1]	Class C Fly Ash[2]
SiO_2	20.80	33.55
Al_2O_3	4.10	18.95
Fe_2O_3	2.78	6.35
SO_3	2.60	1.87
CaO	63.90	27.25
MgO	4.50	3.88
Na_2O		1.73
K_2O		0.35
C		0.20

1. Loss in ignition 1.80%. Insoluble residue 0.15%.
2. Particles greater than No. 325 sieve (45 microns = 0.018 in.) = 18%. Specific gravity = 2.72.

Table 3.4 Chemical Composition of Binders

Metal	Cement[1] Total (mg/kg)	Cement[2] TCLP (mg/L)	Fly Ash[1] Total (mg/kg)	Fly Ash[2] TCLP (mg/L)
Arsenic	1.	0.13	24.	0.14
Barium	170	0.30	5742	0.32
Cadmium	3.4	0.02	8.3	0.02
Chromium	170	1.2	57.	0.26
Lead	8.5	0.13	19.	0.14
Nickel	40.	0.05	53.	0.05
Calcium	381,000	3120	180,000	1490
Iron	14,600	0.10	34,100	0.10
Copper	24.	0.021	140	0.14
Potassium	2820	53	1560	1.7
Magnesium	22,700	0.16	30,300	52.
Manganese	910	0.015	202	0.02
Sodium	815	8.4	9560	36.
Sulfur	10,200	204	11,300	160
Zinc	207	0.33	237	0.21

1. Nitric acid digestion followed by chemical analysis with an inductively-coupled plasma emission spectrometer. (USEPA, 1986, Method 6010).
2. TCLP (USEPA, 1986, Method 1311)

3.2 Stabilization Procedures

Mixing is the most important part of the stabilization process because of the homogeneity requirement. Maximum care was taken to prepare a uniformly homogeneous sample throughout all experimental mixes. Mixing was performed in a Kitchen-Aid Mixer Model K45 with an acid-rinsed stainless-steel bowl and stainless-steel wire impeller. Dry waste was mixed alone for 5 minutes to make it homogeneous. Three grams of waste from different positions in the mixing bowl were collected for nitric digestion of the raw waste. A maximum of 500 grams of waste was stabilized in one batch. Cement and fly ash were added to the bowl and mixed dry with the waste for 5 more minutes. Water was then added and mixing continued for 15 minutes. In the case of mix designs with chemical accelerators, the required amount of accelerator was so small that it was not possible to obtain a homogeneous mix by adding directly to the waste and binder mixture. Therefore, the required amount of accelerator was measured and added to the water.

The purpose of this mixing procedure is to ensure a consistent application of water and additive to dry materials from one experiment to another. Speed of rotation and duration of mixing were two key parameters that characterize mix intensity. Consistent results with mix durations of at least one minute at an impeller speed of 140 rpm were obtained by Bayasi, et. al., (1992) in an investigation of mixing intensity and stabilization results. Andres and Irabien (1994) studied the influence of the processing variables mixing time, waste/binder ratio, and water/solid ratio on the S/S of steel foundry dust. Their results indicated that mixing time and water/solid ratio had a negligible effect on solidified products whereas, the waste/binder ratio showed an influence on the amount of leached metals. They used a contact time varying from 1/2 hour to 1.5 hours with a water/solid ratio from 0.33 to 0.5.

A mixture was partitioned into approximately 110-gram samples and cured in acid-rinsed plastic cups. The 10 grams in addition to the 100-gram TCLP requirement allows for moisture loss during curing. If more than ten grams were lost, then like samples were combined to satisfy the 100-grams TCLP requirement.

Samples were loosely covered with laboratory plastic film and air cured within the protection of a lab cabinet to reduce any air-borne dust deposition on the sample. Cure times of 2 days were selected to model common industrial practice. Longer cure times were studied to assess S/S durability.

3.3 Leaching Procedures

3.3.1 TCLP

The TCLP (USEPA, 1986, Method 1311) is recognized by the U.S. EPA as a standard method for measuring treatment effectiveness of S/S. The TCLP is a batch procedure with a leaching duration of 18 hours ± 2 hours. Information pertaining to the time and sequence of metals leached cannot be obtained by the TCLP so a dynamic

leaching procedure was also used. Equipment and procedures for both leaching tests are described below.

Standard equipment for TCLP testing were used (Code of Federal Regulations, 1987). These include: a) Model DC-18 rotary agitator from Analytical Testing and Consulting Services, Inc.; b) Type 316, stainless steel, 142 mm (5.6 in) filter holder from Fisher Scientific; c) Borosilicate glass fiber filters (GF/F Whatman Grade) with a 0.7 micrometer effective pore size; d) High- density polyethylene bottles for agitation and for sample storage which were obtained from Crown Glass Corporation; and e) pH meter with a relative accuracy and repeatability of 0.01 pH.

Standard TCLP procedures were used. Pertinent to the inorganic hazardous waste used in this research, a brief, nontechnical summary of the TCLP procedure follows (Code of Federal Regulations, 1987): One hundred grams of stabilized waste were ground with mortar and pestle to pass a 9.5 mm standard sieve. The waste was put into a 2000-mL bottle containing 2.000 kg of an extraction fluid consisting of diluted glacial acetic acid. Although the bottle size is designated as 2000-mL, sufficient headspace was available for fluid agitation. Extraction fluid Type 2 (pH = 2.88 $\pm$ 0.05) was selected on the basis of EPA-specified test procedures. The mixture of S/S form and extraction fluid was agitated end-over-end for 18 $\pm$ 2 hours. The fluid was extracted from the solids by means of positive pressure filtration through a 0.7 micron borosilicate fiber filter. The pH and alkalinity of the extract were measured. Alkalinity was measured by the amount of 1.00N sulfuric acid necessary to decrease the pH to 4.5. Extract samples were preserved by acidification to pH < 2 with nitric acid, sealed, and stored at 4 degrees C prior to chemical analysis.

In addition to standard procedures, the following precautions were taken in order to achieve consistent high-quality data. First, nitrogen was the pressurizing gas. Second, approximately 2000-mL of extract were obtained during the extraction which takes 5-20 minutes. The 2000-mL of extract were well- mixed to obtain a representative sample for preservation and chemical analysis. Third, new acid-rinsed bottles were used for agitation and for storage of the TCLP extract.

3.3.2 Column Leaching

For dynamic leaching experiments, a vertical glass column 47 cm long and 1.6 cm in diameter, was used. Perpendicular tapered glass connections at the bottom and top allow the introduction and exit of extraction fluid. A 3.0 mL/min flow of fresh leachant was continuously fed to the bottom of the column by a peristaltic pump using 0.8 mm (inner diameter) Norprene tubing. Openings at the top and bottom of the glass column allowed easy filling and removal of waste samples from the column. During the leaching process, the open ends were plugged with stoppers covered with Parafilm.

In preparation for column leaching, stabilized waste was first crushed with a mortar and pestle and passed through a series of sieves. Fines were excluded because they would tend to escape with the eluant. Based on results from section 3.7.4, various particle sizes were permitted because metal leachate concentrations were not related to

particle size. Initial compaction of 50 grams of stabilized material in the tube was kept constant from one experiment to another by using a spring-loaded penetrometer to compact material. Glass wool fiber was placed on top of the waste to restrain any suspended particles from escaping with the eluant.

During the column leaching experiment, effluent samples were collected at time intervals given by the empty bed detention time which equals the column volume divided by the leachant flowrate. Fluid was collected from the top of the glass tube into 50 mL plastic beakers for 3 minutes. For each test, the starting time for collection, sampling time, and ending time were recorded. At the rate of 3 mL/min, about 5.5 hours are required to pump 1000 mL, the amount of eluant necessary to maintain the same liquid/solid ratio as that used in the TCLP test. After the pH was measured, samples were passed through a 0.45 μm Acrodisc filter to remove any suspended fine particles and stored in acid-rinsed test tubes. Samples were preserved by adjusting the pH to below 2 with nitric acid. To avoid any contamination, test tubes were covered with Parafilm and stored at 4°C. The analyses of samples collected over time allows the determination of leaching rates for various metals.

3.4 Chemical Analyses

Initial screening of samples were performed at the Environmental Engineering Laboratory at Bradley University using a Buck Scientific Model 200A/210 atomic absorption spectrophotometer. Wavelengths and slit widths were set according to the library data installed in the instrument. Air and acetylene gas flow rates were set according to the operation manual. A set of four standard solutions were freshly prepared for each metal prior to sample analysis. Standard solutions were prepared by diluting 500 mg/L reference solutions with 0.1 N nitric acid. A serial dilution process was used to prepare solution concentrations spanning the linear range. The concentration of the standard solutions, linear range, wave length, and slit for each metal are shown in Table 3.5. The concentrations of standard solutions listed are nominal values. Samples with higher concentrations than the calibrated linear range were diluted with DI water immediately before analysis to bring measurements within the linear range.

The sensitivity of an AA spectrophotometer varies with time so standard solutions were tested after every 30 samples. Whenever a concentration difference of more than 15% was found, standard solutions were prepared again and a new calibration curve prepared for sample testing.

For independent experimental verification of laboratory procedures, selected extracts and solid digestates were analyzed at PDC Laboratories, Inc. with an inductively coupled argon plasma (ICAP) emission spectrophotometer, Model ICAP 61 made by Thermo Jarrel Ash Corporation. This is a simultaneous vacuum spectrophotometer with a 23-element configuration. A standard cross-flow nebulizer is used to atomize the extract or digestate into a plasma emission source. The intensity and wavelength of the photon emissions resulting from orbital transitions of excited electrons are determined. A number of orbital transitions are possible for a given element leading to a number of

Table 3.5 Calibration of Atomic Absorption Spectrophotometer

Element	Concentrations of Standard Solutions (mg/L)	Linear Range (mg/L)	Wavelength (nm)	Slit	Detection Limit (mg/L)
Ag		3.0	328	7	0.01
As		20.0	193	7	0.08
Ba		25.0	554	7	0.17
Ca	0.5,1.0,1.5,2.0	2.0	422	7	0.04
Cd	0.5,1.0,1.5,2.0	2.0	228	7	0.01
Cr	2,4,6,8,10	10	357	7	0.005
Cu	1.0,2.0,3.0,5.0	5.0	324	7	0.01
Fe		5.0	248	2	0.02
Mg		0.5	285	7	0.002
Mn		2.0	279	2	0.01
Mo		25	313	7	0.25
Na		0.5	589	7/2	0.001
Ni	0.5,1.0,2.0,3.0	3.5	232	2	0.02
Pb	5,10,15,20	20.0	283	7	0.08
Se		100	196	2	0.15
Sn		200	286	7	2.5
V		200	318	7	0.32
Zn	0.2,0.4,0.6,1.0	1.0	214	7	0.005

possible emission lines for the element. The excitation energy is provided by the high temperature of the inductively coupled plasma, a largely ionized gas in an oscillating magnetic field.

After the temperature of the plasma has equilibrated after startup, a mercury vapor lamp is used to precisely align the optics of the instrument. Instrumental calibration follows by using three points plus a blank for each element. This calibration is confirmed by verification measurements that must be within ± 10% of their known concentration value for the initial calibration to be considered valid. These calibration and verification procedures are repeated after the analysis of every ten samples. If an element could not be calibrated properly, that data were flagged and samples were rerun at a later date. Samples with questionably extreme values were typically rerun.

For each element, the calibration and verification standards, detection limits for TCLP and solid measurements, and analytical ranges are provided in Taylor and Fuessle (1994). The acid-preserved TCLP extracts were routinely diluted ten-fold to avoid emission interference by the high levels of calcium present in the extracts.

3.5 Digestion Studies

Nitric digestion of raw waste samples were performed frequently to correct for the nonhomogeneity of the raw waste. Nitric digestion is a much stronger extraction process than TCLP, and it is assumed that virtually all metals present in the waste are detected in the digestate. A 100 mL centrifuge glass tube containing 3 ± 0.1 grams of raw waste was filled with 8 ± 0.1 mL of concentrated nitric acid using a pipette. Measuring by mass, the acid-waste mixture was diluted up to 25 mL with DI water. The tube and mixture were heated in a water bath at 70° C for three hours. After heating, 25 mL more DI water was added to the tube which was closed with a rubber stopper. The tube was placed in a centrifuge for 15 minutes at 60 rpm. The mixture was filtered and stored at 4° C prior to analysis.

For screening purposes, TCLP extracts analyzed in the Bradley University Environmental Engineering Laboratory were not routinely digested because there is no significant difference observed in the chemical analyses of digested and undigested TCLP extracts. This conclusion has been verified by independent testing performed by PDC Laboratories, Inc. and by studies conducted during earlier research in this laboratory (Bayasi (1992), Taylor and Fuessle (1994)). Chemical analyses of the TCLP extracts and digestates of the same extracts were highly correlated. This high degree of correlation is reasonable because the extracts have been filtered through a 0.7 micron filter and stored at a $pH < 2$.

3.6 Methods for Monitoring Curing: Introduction

Three methods were considered for monitoring the "age" of a stabilized waste. As discussed in section 3.6.1, the degree of hydration can be measured directly by XRD or indirectly by various methods which are reviewed and compared. Section 3.6.2 presents methods used by researchers to investigate polymerization as cements age. Polymerization has been measured by procedures such as gas chromatography, ^{29}Si NMR, FTIR, and wet chemistry methods including molybdate complexing and trimethysilylation. Results of research investigations using the FTIR and NMR have been summarized in chapter two. Without access to the NMR, the authors relied on wet chemistry methods which are reviewed in more detail. Finally, section 3.6.3 presents an electrokinetic test to measure ion movements through stabilized forms.

3.6.1 Degree of hydration

The degree of hydration is the weight fraction of material reacted. QXRD can be used to make a direct measurement of the degree of hydration. Indirect methods include: a) non-evaporable water measured on loss on ignition using TGA; b) conduction calorimetry, c) chemical shrinkage determinations. Measurements were made by the

British Cement Association and the Technical University of Denmark on samples with curing periods ranging from 2 hours to 90 days. Parrott, et.al., (1990) show close correlations between the results of the hydration measured directly by QXRD and results from the indirect methods, e.g. non-evaporable water, chemical shrinkage and heat of hydration. The correlations were not always linear and they were affected by the kind of cement, but in general, the indirect methods indicated the same trends as the direct method, QXRD.

3.6.2 Silica Chain Length

Barnes, et. al., (1985) used solid-state ^{29}Si nuclear magnetic resonance with magic angle spinning on Blue Circle Portland cement and Aalborg white Portland cement. The spectra of anhydrous cements, C_3S, and βC_2S were compared with spectra after 1 week of hydration. With this comparison, Barnes, et. al., (1985) deduced that the silicate chain length increases during C_3S hydration. C_3S is more than 50% hydrated after 1 week compared to <20% hydration for βC_2S. The degree of hydration was calculated by areas under the NMR spectra. After 1 week, the βC_2S shows only Q_1 resonance whereas the C_3S and the cements show Q_2 resonances of significant intensity. Clayden, et. al., (1984) arrived at the same conclusions as Barnes, et. al., (1985).

According to Butler, et. al., (1993), orthosilicates Q_0 present in the clinker during cement hydration are polymerized mostly to Q_1 with much smaller contributions to Q_2 and little or no contributions to Q_3 (chain branching) or Q_4 (crosslinking). The loss of Q_0 with time is a measure of the overall degree of hydration. Butler, et. al., (1993) compared Portland cement (OPC) with OPC doped with: $NaAsO_2$, $Na_2HAsO_4 \cdot 7H_2O$, $Cr(NO_3)_3 \cdot 9H_2O$, $Na_2CrO_4 \cdot 4H_2O$, or $Pb(NO_3)_2$. After curing for 28 days, OPC showed resonances at -70, -79, and -84 ppm corresponding to Q_0, Q_1, and Q_2 respectively. Older samples with Pb showed more polymerization with greater Q_2 resonance intensities. Both forms of arsenic inhibited polymerization as indicated by less Q_2. Both forms of Cr inhibited polymerization by retarding the hydration of Q_0 units.

Cd samples showed a slightly higher proportion of CSH and a slightly higher degree of polymerization. Butler, et. al., (1993) proposed that Cd had little impact on cement hydration because the $Cd(OH)_2$ formed provided nucleation sites for CSH and $Ca(OH)_2$ development. Lead retarded cement hydration by forming an impervious layer around the clinker grains. The fluctuating pH of pore water during hydration causes a solubilization and reprecipitation of Pb. Hence, the leaching of Pb and Cd is quite different even though they have comparable low solubilities. NMR spectra of samples before and after TCLP at pH=5 yielded an increase in Q_3 and Q_4 intensities after TCLP.

Ortego, et. al., (1991) used FTIR and ^{29}Si NMR to study OPC clinker, OPC, and OPC laden with either zinc or lead. In OPC clinker, OPC, and C_3S, the predominant silicon species is SiO_4^{4-}. With the hydration of OPC, SiO_4^{4-} reacts with water to form dimers and short and cyclic polymers. The highly basic condition in cement ensure that this polymerization is a slow process. The main products of the hydration are detected by FTIR from the $\nu 3$ (asymmetric Si-O stretching) bands at 1000–980 cm^{-1}, $\nu 4$ (out of plane

Si-O bending) at 525-546 cm^{-1}, and v2 (in-plane bending) at 457-464 cm^{-1}. According to data from NMR and FTIR, lead caused a slight increase in polymerization (v3) while zinc caused a slight decrease in v3. Acid leaching caused even more polymerization. Ortego, et. al., (1991) explain that metal is lost to the silicate matrix and replaced by H^+ according to:

$$SiOX + nH^+ (aq) \rightarrow Si(OH)_n + X^{n+}$$

The branching and cross-linking reactions of the silicates destroy the cement matrix.

Mohan and Taylor (1982) analyzed by trimethylsilylation C_3S and alite pastes cured up to 30 years. The resulting derivatives were examined by gas-liquid chromatography and gel permeation chromatography. For curing up to 6 months, silicate anion polymerization occurs mostly in the formation of CSH and not within existing CSH. Fractions of silicon in dimer and polymer increase during the first 6 months. After 6 months, another process becomes predominant and slowly proceeds for many years. A decrease of dimer silicon is accompanied by an increase in polymer silicon fraction. This reaction probably occurs within the existing CSH and slowly changes it. The exact form of the polymer is unknown although some researchers believe it to be a pentamer.

According to Parrott and Taylor (1979), the molybdate complexing method can yield quantitative data regarding the proportions of mono, di and polysilicates in silicate mixtures together with the reaction rate of the polysilicate. This characterization is important for correlating the age of accelerated samples with naturally cured samples. In the development of improvements for the molybdate complexing method, Parrott and Taylor (1979) compared advantages and disadvantages of two methods of silicate structure analyses: the molybdate complexing method and the trimethysilylation method. The former method did not yield quantitative estimates of proportions of silicates present, while the latter method did not always yield reliable quantitative estimates of silicate proportions in the original samples. Parrott and Taylor (1979) chose to improve the molybdate complexing method for several reasons: 1) rapidity of silicic acid preparation should limit the production of unrepresentative silicic acids; 2) suitability for the study of the polysilicate phase; and 3) repeat analysis of results to obtain additional information about the cement paste. The molybdate method consists of a reaction between ammonium paramolybdate with monomeric silicic acid to form β-molybdosilicic acid. All Si-O-Si bonds must be broken before the formation of the blue molybdosilicic acid complex. The rate of the complex formation is slower for silicicic acids with greater degrees of condensation.

For this project, experimental procedures were adapted from Parrott and Taylor (1979). Four reagents were required. Molybdate reagent was prepared by dissolving 10 grams of ammonium heptamolybdate tetrahydrate $[(NH_4)_6Mo_7O_{24} \cdot 4H_2O]$ in 100 mL of DI water with gentle heating. Silica free aqueous NaOH was used to keep the pH between 7 and 8. Reaction vessel water was made by diluting 0.52 mL concentrated HCl with 250 mL of DI water resulting in a pH of 1.6. Methanolic HCl is a mixture of 3.1 mL of concentrated HCl with 250 mL of methanol.

One-tenth gram samples were added to 100 mL methanolic HCl at 25° $\pm$ 0.1C and mixed vigorously for 60 seconds. In this project, samples were either cement paste, prepared with a water to cement ratio of 1:2, or stabilized waste. Three reagents: 5 mL

of sample solution, 43 mL of reaction vessel water, and 2.5 mL of molybdate reagent were mixed in a spectrophotometer cuvette. Using a Hach DR/3000 spectrophotometer set at a 410 nm wavelength, adsorption readings were taken at frequent intervals up to 600 seconds. A final reading was taken after 3 hours.

Reaction rate constants and time shifts for mono, di and polysilicates are required for data analysis. Reaction rate constants for mono, di and polysilicate were calculated by regression analysis of 55 sample data points. Time shifts were directly adapted from Parrot and Taylor (1979). Using the relations given in their article, the proportion of silica, a_n, with degree of condensation, n, was calculated as follows.

$$Y = a_1 f_1(t) + a_2 f_2(t) + a_p f_p(t)$$

$$f_n(t) = 1 - \exp\left[-b_n\left(t - t_n\right)\right]$$

$$Y = a_1\left[1 - \exp\left[-b_1\left(t - t_1\right)\right]\right] + a_2\left[1 - \exp\left[-b_2\left(t - t_2\right)\right]\right] + a_p\left[1 - \exp\left[-b_p\left(t - t_p\right)\right]\right]$$

where Y = total proportion of silica complexed;
a_n = proportion of silica complexed with degree of condensation n;
a_1 = proportion of monosilicate;
a_2 = proportion of disilicate;
a_p = proportion of polysilicate;
b_n = rate constant;
t_n = time shifts.

Parrott and Taylor (1979) evaluated rate constants and time shifts by preparing monomeric, dimeric, and polysilicic acid to undergo complexing reactions with ammonium molybdate. The β-molybdate acid was monitored continuously using a spectrophotometer set at 400 nm. Using an iterative least-squares computation, Parrott and Taylor (1979) evaluated b_n, t_n and the relative standard deviation (RSD) as shown in Table 3.6.

Table 3.6 Empirical Parameters for the Molybdate Method (Parrott and Taylor (1979))

	b_n (sec^{-1})	t_n (sec)	RSD
Monosilicic acid	0.0890	3.0	0.005
Disilicic acid	0.0152	5.5	0.008
Polysilicic acid	0.00189	12.0	0.004

Analyses of known mixtures of monomeric, dimeric, and polymeric silicicic acids yielded favorable results

3.6.3 Electrical Conductivity and Permeability

If leaching is diffusion controlled, then permeability of a stabilized waste is another parameter of interest. Concrete permeability can be measured by the rapid chloride permeability test. Permeability of stabilized wastes can be measured by modifications of the rapid chloride permeability test that permit the use of smaller amounts of hazardous waste by using a smaller sample. The diameter to length ratio of the cylindrical sample was as required in the ASTM rapid chloride permeability test for concrete. A 2.5 inch length of 1.5 inch diameter polyethylene pipe was used to cast the stabilized waste sample. The sample was allowed to cure in the pipe at room temperature. After curing for the required period, 1 inch at each end of the pipe was cut off with 0.5 inch remaining for the test. The purpose for removing 1 inch of sample on each end was to remove surfaces exposed to the air. The sample was placed in a vacuum for 3 hours to remove air and water from the voids. Subsequently, the sample was totally immersed in de-aerated water without letting air enter the sample. After 12 hours of immersion, the sample was placed between two electrolytic cells as shown in the Figure 3.1. The electrolytic cells were fabricated from polymethylmethacrylate blocks that were outfitted with a copper electrode in the form of an annulus. The cathodic electrolyte was 0.3% NaCl and the anodic electrolyte was 0.3 N NaOH. A constant potential of 11 volts was applied to the specimen for 6 hours. Current flow was recorded every 20 seconds for 6 hours with computerized data acquisition.

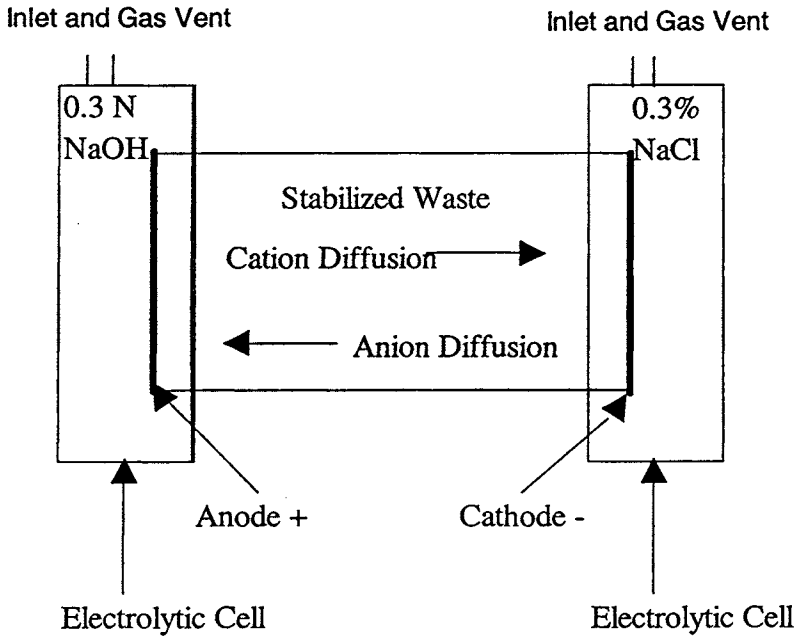

Figure 3.1 Electrolytic Cell Diagram

3.7 Quality Assurance/Quality Control- Error Analysis

3.7.1 Instrumental Analysis

The analysis of TCLP extracts by AA in the Bradley University Environmental Engineering Laboratory and by ICAP at PDC Laboratories, Inc. were carried out following the standard quality control procedures of the US EPA.. Samples were diluted as necessary to fall within the linear range while maintaining sufficient sensitivity to meet TCLP standards. Before and after samples were analyzed, the instrument was standardized with three to four standard solutions with concentrations shown in Table 3.5. For data to be considered valid, standards are required to agree with instrumental specifications before and after samples are analyzed.

For ICAP analyses performed at PDC Laboratories, Inc, samples were analyzed three times with blanks aspirated between to prevent sample cross-talk in the ICAP torch. A percent relative standard deviation was calculated for the three sample determinations and reported along with the mean of the values. Because the sources of instrumental noise are varied, the precision of determinations often is best understood as a function of the concentrations being determined. In this project the detection limit for such a determination is defined as the concentration where the noise is 100% of the analytical signal. Table 3.7 lists instrumental detection limits for ICAP-based analyses for elements of interest in this research.

Table 3.7 ICAP Detection Limits (Bayasi (1992))

Element	Instrumental Detection Limit, mg/L	TCLP Detection Limit, mg/L	TCLP Standard, mg/L
Ca	0.01	0.05	-
Cd	0.003	0.015	0.19
Pb	0.025	0.125	0.37

3.7.2 TCLP Procedures

Reproducibility of the TCLP has been studied by several researchers. Williams, et. al., (1986) consider the TCLP method precise for single laboratory analyses if the relative standard deviation (RSD) of replicate sample analyses is less than 25%. Data for TCLP metals was considered to be "quite good" provided that concentrations did not approach detection limits. Taylor (1986) found RSDs of 10 to 20% for TCLP metal analyses. A study of various factors that affect TCLP results of S/S wastes has also been included in previous projects from the investigators (Bayasi, et. al. (1992) and Taylor and Fuessle (1994)). Bayasi, et. al., (1992) determined the average and coefficient of variation for 12 TCLP samples for each of four mix designs. Of the 13 metals reported, most were consistent except for the sporadic results for lead and zinc. The study also

concluded there was no correlation between mixing speed and mixing duration given that wastes were mixed at least a couple of minutes.

Taylor and Fuessle (1994) also considered an error analysis of the TCLP process in a previous report. A propagation of errors approach was used to provide a very pessimistic view of the overall error associated with an experimental result. The TCLP concentration is written as a function of the independent variables:

$$\text{TCLP}(\text{mix composition, mix parameters, extract analysis})$$

and the derivative is taken. Assuming linear behavior for the independent variables and stochastic independence, the maximal estimated relative error in the final TCLP extracts can be written as:

$$\frac{\text{TCLP error}}{\text{TCLP}} = \frac{\text{composition error}}{\text{composition}} + \frac{\text{mix error}}{\text{mix}} + \frac{\text{analytical error}}{\text{analysis}}$$

In this case, following the discussion above, the relative error in the composition of the stabilized mixtures is 1% for lead and cadmium. The uncertainties found in the mixing study in Bayasi, et. al., (1992) were 10% or less for elements of interest and probably are insignificant compared to the variability of raw waste composition because waste variability is folded into the mixing experimental design. A conservative estimate for analytical precision is 5%, so that the expected overall uncertainty in the TCLP results is about 15%. This is within expected uncertainties estimated by Williams, et. al., (1986) and Taylor (1986).

3.7.3 Repetitive Studies

Preliminary TCLP results in this project were quite variable so error analyses were carried out on each phase of the experimental process: 1) homogeneity of water, cement, waste, fly ash; 2) mixing process; 3) TCLP bottle preparation and agitation; 4) chemical analyses. The investigators concluded that the primary reason for variability in TCLP results was because of waste non-homogeneity. This conclusion is supported by a study of twelve samples taken from different locations in the overall project sample. Nitric digestions and AA analyses were performed for lead and cadmium according to procedures described in section 3.4. . In Table 3.8, average concentrations and standard deviations are reported for waste, cement, fly ash, and accelerators.

Despite laboratory procedures to homogenize the waste, the variability of the waste far exceeds the variability of the binders, mixing process, or analytical error. The non-homogeneity of the waste is the major source of variability in the final TCLP results. This variability persisted despite the strong efforts by the research team to mix the original waste in a variety of ways. One way to eliminate this source of variability would be to use a synthetic artificial waste. Although this approach is meaningful and is used in some investigations, it has drawbacks. For example, the complex chemical nature of an

Table 3.8 Repetitive Analyses of Waste, Binders, and Accelerators

	Lead		Cadmium	
Constituent	Avg. Conc. (mg/L)	Standard Deviation	Avg. Conc. (mg/L)	Standard Deviation
Waste	728	95.1	17.7	3.2
Cement	2.99	0.02	0.181	0.00802
Fly Ash	2.23	0.335	0.133	0.0185
Darraccel	6.33		0.205	
Polarset	8.14		0.184	

actual industrial waste may change the experimental results observed with synthetic artificial waste. In order to account for the variability of the waste and its impact on the final TCLP result, the authors compared ratios of C/C_o among samples where C is the TCLP concentrations representing leachable metal and C_o represents the available metals in the raw waste as determined by nitric digestion and AA.

3.7.4 Particle Size and Distribution

Waste variability was further characterized by first partitioning the waste by particle size with sieves ranging from #4 to fines. Ten grams of each particle fraction was leached in 200 mL of TCLP fluid in a shaker set at 100 rpm for 18 hours. Lead and cadmium concentrations in the leachates are reported in Table 3.9. Mass percentage leached represents the mass of metal that leached out with the TCLP fluid as a percent of metal originally present according to the nitric digestion results.

The results shown in Table 3.9 indicate that lead and cadmium are well distributed among all particle fractions. Based on these results, it is justifiable to perform leaching studies on various particle sizes. The investigation took all precautions to exclude any fines from leachates before analyses. Random inclusions of fines in leachates could lead to significant random variations in results. For dynamic leaching in a column, glass fiber wool at the top and Acrodisc filtration of leachates were used to exclude fines.

Analytical data comparing TCLP concentrations to nitric acid digestions on untreated raw waste indicates that much of the variability in the TCLP values is due to variations in the TCLP-extractable fraction of metal in the waste. This could be due to metals appearing in the waste in different chemical forms. This data is shown in Table 3.10 for a few metals of interest.

Table 3.9 Variation of Leachability with Particle Size

Particle Size (mm)	Pb (mg/L)	Cd(mg/L)	Mass % Leached, Pb	Mass % Leached, Cd
4.75	57.25	8.29	8.66	50.37
2	63.1	10.67	6.60	28.19
0.85	60.3	13.24	14.27	64.15
0.425	70	9.81	13.51	44.66
0.25	72.1	11.02	8.47	53.02
0.106	71.1	9.64	10.19	47.49
0.075	79.4	10.53	13.90	61.03
<0.075	51.9	9.64	6.95	43.55

Table 3.10 Analyses of Raw K061 Waste

Element	Nitric Digestion, ppm	Digestion Standard Deviation, %	TCLP, ppm	TCLP Standard Deviation, %	Analytical Precision, ppm
Cd	9.2	2.7	4.6	4.4	0.15
Cr	71.	4.3	4.7	110.	5.1
Mn	8.5	28.	6.5	39.	2.1
Pb	24	3.7	5.4	61.	0.61

CHAPTER FOUR
Experimental Design

4.1 Introduction

Results of preliminary experiments helped the investigators identify the most important empirical parameters, refine experimental procedures, and finalize the experimental design for the project. For mix designs, the mass ratios binder/waste and water/solids were most important. Appropriate ranges for these parameters were determined through preliminary experiments. Initial tests with heat curing identified the duration and level of heat with the most potential for success. Finally, the nonhomogeneity of an actual industrial waste was characterized and identified as the major source of variability for TCLP results. For the sake of comparisons, this variability was accounted for by the use of the ratio C/C_o, where C is the metal concentration in the leachant and C_o is the concentration in the nitric digestate of a 3-gram waste sampled directly and randomly from the waste mass used in the stabilization mix.

Section 4.2 presents a matrix of mix designs used in this project. The background and preliminary tests used to determine this mix design matrix are described. Early tests with heat curing are discussed in section 4.3. These tests were necessary to determine which empirical variables (e.g. heat temperature, humidity, duration of heat, lag time after stabilized mixing and before heat curing) are most important and the appropriate range of values for these variables. An experimental design for heat curing is presented. Section 4.4 provides an experimental design for accelerated curing using chemicals.

4.2 Mix Design Matrix

Numerous samples were prepared over a wide range of values for each mix parameter: binder/waste and waste/solids. Based on previous work (Bayasi, et. al., (1992); Taylor and Fuessle (1994)) and that of others (Williams, et. al., (1986)), the binder/waste is the most important mix parameter. Water/solids is also important because sufficient water is necessary for proper hydration, but on the other hand, excessive water may increase porosity and has been found to be detrimental for concrete performance. With the curing of each sample, periodic observations were made for excess standing water and structural hardness as determined by touch or mortar and pestle. A range of sample designs were selected for study according to the following considerations: 1) the mix design matrix should exhibit a range of physical hardness in the range from a loose hard crusty soil to a hard monolithic solid; 2) standing excess water or excessive dryness and cracking should be avoided in the mix design.

In Table 4.1, a matrix of mix designs show a water/solid mass ratio ranging from 20% to 30% and a binder/waste ratio ranging from 0.08 (8%) to 0.26 (26%). As shown by the first entry in each cell of the Table 4.1, mix designs are referred to by these two

Table 4.1 Mix Designs[1] Without Chemical Accelerators Conduct of Experiments After Corresponding Cure Periods[2]

Water/Solid[3] Ratio (%)	Binder/Waste Ratio[3] (%)		
	8	14	26
20	[8:20] TCLP: 2,30,60,120,265, 370 Column: 4,20 and 40°C Si Chain: 2,30 and 40°C Permeability: 7,30,55, and 40°C		[26:20] TCLP: 2,30,60,120,370 Column: 4 and 40°C Silica Chain: 2,30
25		[14:25] TCLP: 2,30,60,120,370 Column: 4 and 40°C Silica Chain: 2,30	
30	[8:30] TCLP: 2,30,60,120,370 Column: 4 and 40°C Silica Chain: 2,30		[26:30] TCLP: 2,30,60,120,265, 370 Column: 4,20 and 40°C Silica Chain: 2,30 and 40°C Permeability: 7,30,55 and 40°C

1. Mix designs are designated by: [binder/waste ratio (%): water/solid ratio(%)] where: solid = binder + waste; binder = 70% cement + 30% fly ash (constant mix proportions of cement and fly ash)
2. Sample ages in days for each test are listed after the corresponding test in the table body.
3. Mass ratio

ratios separated by a colon and enclosed in brackets. For example, [8:20] refers to a mix design with 8% binder/waste and 20% water/solids. This mix design is low in water and high in waste. It is volume efficient in the treatment of waste, and its physical nature is characterized as a hard crusty soil. At the other extreme, [26:30] refers to a mix design with 26% binder/waste and 30% water/solids. This mix cures slowly given its more generous amounts of water and binder. Its cured physical state can be described as a monolithic solid.

In the body of the Table 4.1, tests performed on each mix design are listed in the corresponding cell. The cure age of each sample are listed after each test. For examples, TCLP: 2,30 means TCLP was conducted on that mix design after 2 and 30 days of air curing at ambient laboratory temperature. Column: 4 means column leaching was conducted after 4 days of natural curing. Column: 4 and 40°C means that column leaching was conducted on two different samples of the same mix design but with different curing methods. First, column leaching was conducted on samples after 4 days of natural curing. Second, samples with heat curing at 40°C for 3 hours followed by curing at room temperatures for 10 hours also underwent column leaching. Silica Chain: 2,30 indicates that silica chain testing was conducted on samples with 2 and 30 days of natural curing. Some samples for the silica chain test were heat-cured in the same way as that for the column test. Permeability: 7,30,55 means an electrokinetic permeability test was conducted after 7, 30, and 55 days of natural curing. Heat cured samples for the permeability test underwent 40°C heat for 3 hours followed by 30 days of natural curing.

Methods and procedures for these tests have been described in chapter 3. The reason for heat curing at the selected temperature of 40° C is discussed in section 4.3.

4.3 Early Testing with Heat Curing

Accelerated curing of cements and concrete with heat can be performed in a variety of ways (Clifton (1980)). The physiochemical effects of heat curing have been reviewed in Chapter 2. While performing the work described in section 4.2, preliminary tests with oven heat-curing were conducted to determine an experimental design for heat curing. The preliminary results also offer some initial insights on the physical-chemical effects on the cement-waste matrix.

Two batch mixes, PD1 and PD2, were used and closely approximate [8:20] and [26:30] from Table 4.1. The actual mix designs are listed in Table 4.2. Both waste and sand mixes were prepared to observe the effects of waste on curing with and without heat. Sand provides the presence of an inert solid which distinguishes it from waste samples. PD1 and PD2 were used to determine the difference and effect of binder/solid (either waste or sand) ratio. The oven-cured samples underwent 70° C at 100% relative humidity. The naturally cured samples were placed in the laboratory environment.

Table 4.2 Mix Design for Preliminary Experiments with Heat Curing

Mix Design	Preliminary Design 1 (PD1)		Preliminary Design 2 (PD2)	
Mix Materials	Waste-based (grams)	Sand-based (grams)	Waste-based (grams)	Sand-based (grams)
K061 Waste	100	0	100	0
Sand	0	100	0	100
Fly Ash	2.4	2.4	3.6	3.6
Cement	5.6	5.6	8.4	8.4
Water	22.4	22.4	33.6	33.6
Total Weight	130.4	130.4	145.6	145.6

These mix designs were prepared in sufficient quantities so that samples could be withdrawn over time and tested for weight loss, calcium-$Ca(OH)_2$, and total calcium. The mass of samples for weight determinations were made large enough to minimize measurement errors. Weight measurements over cure time are shown in Table 4.3.

In Figure 4.1, a graph of this data is presented in terms of percent weight loss over time. The last four of the six mix designs listed are all sand-based mixes and exhibit the same pattern of weight loss. Within 1-2 days, an initial drastic weight loss is followed by virtually no weight loss from 2-60 days. The equilibrium weight loss percent for these four sand-based mixes are also ranked in a predictable order. Oven-cured samples exhibit about 1 to 1.5% more weight loss than air-cured samples. Also, PD2 samples (both oven and air cured) with more water and binder show more percent weight loss than PD1 samples with less water and binder.

PD1 samples with waste show a different weight loss pattern than the four sand based mixes. A continuous gradual exponential increase in weight loss is shown throughout the 60 day duration. Comparing oven and air curing, oven curing has a far more significant impact (over 6% difference) on this waste-based sample. PD1 samples with waste solidified more rapidly in both oven and air than the sand-based mixes.

The Ca-$Ca(OH)_2$ was estimated by performing a TCLP-like extraction using two liters of de-ionized water as the extraction fluid on 5 grams of ground sample. Total calcium was determined by analyzing nitric acid digestates. Atomic absorption spectrophotometry was used as described in chapter 3. The difference between total calcium and hydroxide calcium represents calcium that is immobilized by curing, primarily in the form of C-S-H. Results of calcium analyses are summarized for selected samples in Table 4.4.

Table 4.3 Weight Loss Over Curing

Mix Design	Preliminary Design 1 (PD1)				Preliminary Design 2 (PD2)	
Base material	K061 waste		sand		sand	
Curing method/ Age(days)	Oven[1] (grams)	Air[2] (grams)	Oven (grams)	Air (grams)	Oven (grams)	Air (grams)
0	1589.3	1574.4	1198.8	1190.3	1261.7	1262.0
1	1554.7	1551.6	1125.2	1169.1	1170.9	1223.6
2	1523.8	1537.8	1104.7	1134.1	1140.4	1190.2
3	1497.4	1530.7	1095.4	1126.2	1123.9	1171.2
4	1465.2	1520.2	1094.3	1118.6	1114.6	1157.9
6	1449.1	1513.9	1094.0	1115.1	1113.9	1149.4
7	1438.4	1509.1	1093.9	1112.4	1113.7	1149.4
8	1427.5	1503.8	1093.8	1109.8	1113.3	1146.8
9	1422.9	1498.8	1093.6	1108.2	1112.9	1143.9
10	1417.8	1492.7	1093.5	1107.0	1112.7	1142.3
13	1396.1	1483.6	1093.4	1104.4	1112.6	1137.4
21	1368.6	1459.2	1093.1	1100.8	1112.3	1130.2
31	1351.0	1440.8	1092.7	1099.4	1112.0	1125.3
37	1349.0	1425.1	1091.7	1099.2	1111.7	1124.1
44	1330.0	1418.2	1090.9	1098.7	1110.6	1123.7
60	1325.2	1414.4	1090.8	1098.3	1110.4	1123.5

1. Oven cured at 70° C, 100% relative humidity.
2. Air cured under ambient laboratory conditions.

These results show a decrease in calcium as $Ca(OH)_2$ with curing. As discussed in Chapter 2, if pozzolans are present, calcium is converted into the calcium silicate form (C-S-H) with age. The oven-cured samples show a slightly more rapid decrease in $Ca(OH)_2$ with time than the air-cured samples.

The last phase of preliminary heat-curing involved mixes [8:20] and [26:30] described in Table 4.1. Samples of these mixes were prepared and cured at temperatures, 40°C, 60°C, 80°C, and 110°C (in an autoclave at about 13 psig steam pressure) for

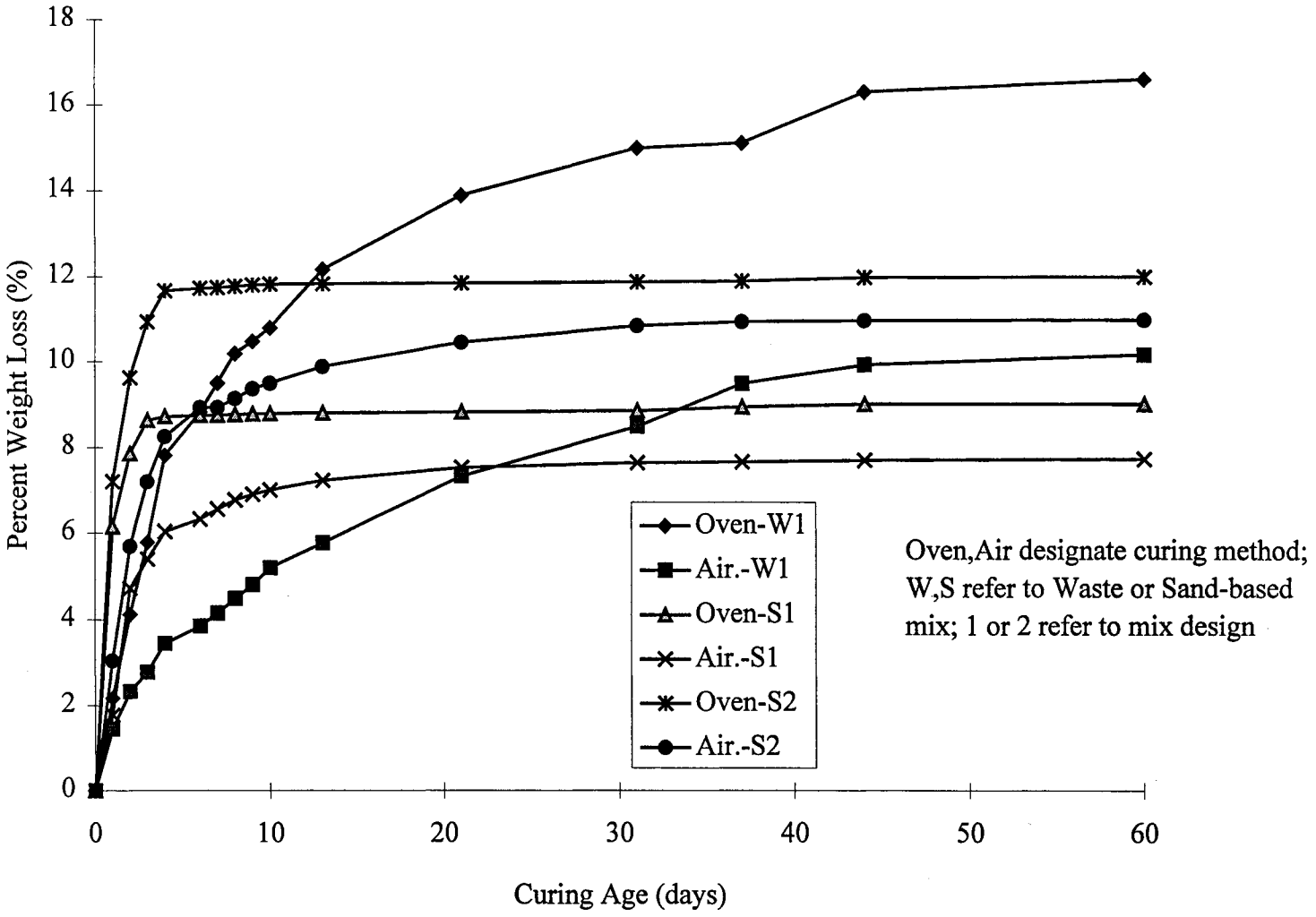

Figure 4.1 Loss of Water from Cement with and without Heat Curing

Table 4.4 Calcium in $Ca(OH)_2$ as a Percent of Total Calcium

	$Ca(OH)_2$ as a Percent of Total Calcium in PD1 Mixes			
	Sand-based		Waste-based	
Age (days)	Oven	Air	Oven	Air
28	49	46	36	34
85	36	33	33	36
153			31	34
166	23	27		

durations ranging from 1-8 hours. Initial results expressed in terms of metal concentrations were inconclusive. The erratic results may be explained by the non-homogeneity of the waste (especially with the use of smaller sample size). Also, temperatures exceeding 50°C may cause significant physio-chemical changes so that TCLP results of these cured samples cannot be anticipated. Expressing results in terms of C/C_o accounts for some of the variability stemming from the nonhomogeneity of the waste. These results showed that the TCLP lead concentrations were stable after 1-4 hours of heat curing, but cadmium TCLP concentrations were affected as the duration of heat progressed.

From Chapter 2, high temperature heat curing causes significant physiochemical changes in cement hydration. Furthermore, the research objective is an accelerated test performed in the short-term that predicts the long-term treatment performance of the stabilized waste. Therefore, longer durations of heat curing were excluded from this study. Samples [8:20] and [26:30] were selected for heat curing because they are significantly different in the matrix of mix designs. Heat curing was performed at 40° C for durations of 3 or 8 hours.

4.4 Accelerated Curing with Chemicals

Another common method for accelerated curing is with the use of chemicals. According to Chapter 2, calcium chloride is the most common accelerator whose effects have been studied extensively. Accelerator A is a commercial $CaCl_2$-based accelerator solution. Using the manufacturer's recommended dosages for concrete, Table 4.5 presents the mix designs and tests performed for each sample. Mix designs [8:20] and [26:30] from Table 4.1 are dosed with .5%, 1%, and 2% mass ratio: accelerator A/binder. These accelerated mix designs are designated by adding a third number inside the brackets indicating the accelerator dosage. For example, [8:20:2A] refers to a mix design with 8% binder/waste, 20% water/solids, and 2% of accelerator A. The sample and its cure age are indicated for each test performed.

Table 4.5 Mix Designs[1] With Accelerator A Conduct of Experiments After Corresponding Cure Periods[2]

Water/Solid[3] Ratio (%)	Accelerator/Binder Ratio[3] (%)		
	0.5	1.0	2.0
20	[8:20:0.5A] TCLP: 6-hr, 1, 2, 15, 30, 90 days Column: 4 and 40°C Si Chain: 2,30,90 and 40°C	[8:20:1A] TCLP: 6-hr, 1, 2, 15, 30, 90 days Silica Chain: 2,30,90	[8:20:2A] TCLP: 6-hr, 1, 2, 15, 30, 90 days Column: 4 and 40°C Silica Chain: 2,30,90 and 40°C
30	[26:30:0.5A] TCLP: 6-hr, 1, 2, 15, 30, 90 days Column: 4 and 40°C Si Chain: 2,30,90 and 40°C	[26:30:1A] TCLP: 6-hr, 1, 2, 15, 30, 90 days Silica Chain: 2,30,90	[26:30:2A] TCLP: 6-hr, 1, 2, 15, 30, 90 days Column: 4 and 40°C Silica Chain: 2,30,90 and 40°C

1. Mix designs are designated by: [binder/waste ratio (%): water/solid ratio(%):percent accelerator] where: solid = binder + waste; binder = 70% cement + 30% fly ash mixture (constant mix proportions of cement and fly ash); and percent accelerator means accelerator dosage as a percent of binder. Percent dosages of 0.5, 1, and 2 mean 0.03 kg, 0.06 kg, and 0.12 kg of accelerator A respectively per 100 kg of binder.
2. In the body of Table 4.5, times (days) of curing before tests are performed; e.g. TCLP: 2,30 means TCLP was conducted on samples after 2 and 30 days of air curing at ambient laboratory temperature; Column: 4 and 40°C means column leaching was conducted on some samples after 4 days of natural air curing and on other samples of the same mix design with heat curing: 40° C heat for 3 hours following by 10 hours of air curing. Silica Chain: 2,30 and 90 means silica chain test was conducted on samples after 2,30, and 90 days of curing. Samples heat-cured for the silica-chain test underwent the same heat treatment as that for the column test.
3. Mass ratio

In addition to the widespread use of $CaCl_2$, many other chemicals are also used for accelerating the cure rate of cement for a variety of reasons. Accelerator B, a calcium-nitrite-based solution, was used in this study at dosages recommended by the manufacturer. The experimental design for samples with accelerator B are shown in Table. 4.6. Mixes are designated in a similar manner, but an index B is used to distinguish them.

Table 4.6 Mix Design[1] With Accelerator B Conduct of Experiments After Corresponding Cure Periods[2]

Water Solid[3] Ratio (%)	Accelerator/Binder Ratio[3] (%)	
	1.0	2.0
20	[8:20:1B] TCLP: 6-hr, 1,2,15,30,90 days Column: 4 Silica Chain: 2,30,90	[8:20:2B] TCLP: 6-hr, 1,2,15,30,90 days Silica Chain: 2,30,90
30	[26:30:1B] TCLP: 6-hr, 1,2,15,30,90 days Column: 4 Silica Chain: 2,30,90	[26:30:2B] TCLP: 6-hr, 1,2,15,30,90 days Silica Chain: 2,30,90

1. Mix designs are designated by: [binder/waste ratio (%): water/solid ratio(%):percent accelerator] where: solid = binder + waste; binder = 70% cement + 30% fly ash mixture (constant mix proportions of cement and fly ash); and percent accelerator means accelerator dosage as a percent of binder. Percent dosages of 0.5, 1, and 2 mean 0.03 kg, 0.06 kg, and 0.12 kg of accelerator B respectively per 100 kg of binder.
2. In the body of Table 4.5, times (days) of curing before tests are performed; e.g. TCLP: 2,30 means TCLP was conducted on samples after 2 and 30 days of air curing at ambient laboratory temperature; Column: 4 and 40°C means column leaching was conducted on some samples after 4 days of natural air curing and on other samples of the same mix design with heat curing: 40° C heat for 3 hours following by 10 hours of air curing. Silica Chain: 2,30 and 90 means silica chain test was conducted on samples after 2,30, and 90 days of curing. Samples heat-cured for the silica-chain test underwent the same heat treatment as that for the column test.
3. Mass ratio

4.5 Data Analysis: Simple Linear Regression

A least-squares procedure is used to fit a straight line through the column extract data plotted against time of leaching in the column. The reasonableness of using simple linear regression may be seen qualitatively by observing a scatter diagram of the data. However, this is a subjective assessment. A quantitative assessment of whether simple linear regression is appropriate and reasonable is presented by Milton and Arnold (1990). The magnitude of the residual or sum of squared errors, SSE, is determined by two factors: a natural variability of the ordinate Y variable (metal eluant concentration, in this case) and/or the lack of data fit to the model (i.e. the degree that linear regression is inappropriate). The independent variable X is time in this case. The statistical method to determine the reasonableness of using simple regression entails partitioning SSE into two components attributable to these two factors. The portion of SSE attributable to the natural variability of Y is designated as SSE_{pe} and is called the pure or experimental error. The remaining portion of SSE attributable to the inappropriateness of using simple regression is called error due to lack of fit, SSE_{lf}. The relative magnitudes of SSE_{lf} and SSE_{pe} can be used to assess the appropriateness of assuming simple linear regression. For example, if SSE_{lf} is relatively small compared to SSEpe, then simple regression is considered appropriate.

Values for SSE_{lf} and SSE_{pe} are estimated from repetitions of the column test. Define n to be the number of column tests performed under identical conditions. Define k to be the number of X values used in each test. Therefore, the experimental design can be presented as in Table 4.7.

Table 4.7 Experimental Design for Repeated Column Testing

	Time from Start of Column Leaching (min)	
Test	X_1	X2...Xk
1	Y_{11}	Y_{12}....Y_{1k}
2	Y_{21}	Y_{22}...Y_{2k}
...	...	...
n	Y_{n1}	Y_{n2}....Y_{nk}

where:

X_j = value of the jth time when a sample was taken from the column eluant for chemical analyses; j=1...k;

Y_{ij} = the metal concentration in the column eluant from the sample taken at the jth time during the ith column test.

Milton and Arnold (1990) present the following tests:

H_o: the linear regression is appropriate;

H_1: the linear regression is not appropriate.

The test statistic is: $\frac{SSE_{lf}/(k-2)}{SSE_{pe}/(n-k)}$ and follow the F distribution with (k–2) and (n–k) degrees of freedom. A poor fit will be reflected in an inflated value for SSE_{lf} and the ratio. We accept the linear regression model with a probability α when:
$P\left(F_{(k-2),(n-k)} \leq \text{test}\right) = \alpha$.

According to Table 4.1, [8:20] and [26:30] were selected for column testing. In each test, fifteen samples were taken for cadmium and lead. These column tests were repeated, so n=2 and k=15 using the above terminology. There are four duplicate sets of data because there are two metals, cadmium and lead. In all four tests, the null hypothesis can be accepted with greater than 99% probability. The data are shown in Table 4.8 below.

Table 4.8 Summary Statistics for 99% Confidence in Describing Column Leaching Results with Linear Regression

Column Test	$\frac{SSE_{lf}/(k-2)}{SSE_{pe}/(n-k)}$	$F_{(k-2),(n-k)}$
[8:20] for lead	2.39	3.612
[8:20] for cadmium	0.187	3.612
[26:30] for lead	0.074	3.612
[26:30] for cadmium	0.748	3.612

The linear regression of metal concentration with leaching time may also be reasonable in view of results of Cote, et. al., (1987) outlined in Chapter 2. Cote, et. al., (1987) propose mechanisms to explain why metal release rates may be proportional with time. These mechanisms may provide rationales for the results of this project. First, metal release may be proportional to time if surface dissolution is the controlling mechanism. A slow chemical rate of mobilization is a second possibility. Finally, chemical reactions may depend on species supplied in the eluant, in which case, the metal release will be proportional to the flow rate of eluant (and thus, also time).

CHAPTER FIVE
Discussion of Results and Conclusions

5.1 Characterization of Naturally-Cured Samples

The careful characterization of naturally-cured samples is essential for this study. As discussed in chapter 1, the research premise is that the treatment effectiveness of aging stabilized waste may be characterized by one of four different prospects: satisfactory for all time, unsatisfactory for all time, deceptive (satisfactory to unsatisfactory over time) and improving (unsatisfactory to satisfactory over time). The authors and other researchers (e.g. Perry, et. al., (1992)) have observed samples exemplifying each of these prospects. The objective of sections 5.2 and 5.4 is to characterize the profile of stabilization effectiveness for five different mix designs described in Table 4.1. These samples were cured naturally in ambient laboratory conditions. Sections 5.5, 5.6, and 5.7 present the results of column leaching for samples cured naturally, for those cured with heat, and for those cured with chemical accelerators, respectively. Silica chain results are discussed in section 5.8, and a summary is provided in section 5.9.

5.2 Average TCLP Concentrations of Naturally-cured Samples

Some of the metal in a waste sample may not be subject to leaching because of its chemical form; for example, reduced forms of metal may not appear in TCLP extracts. Therefore, it is interesting to represent the results in terms of a ratio defined as the metal leached divided by the total amount of metal that is in leachable form, the leaching potential. In Table 5.1, the total metal available (as measured by AA on nitric digestates of untreated waste) and metal available for leaching (as measured by TCLP on the raw waste) are reported respectively in rows 1 and 2. The potential leachable fraction, shown in row 3 is row 2 divided by row 1. Cadmium has a much higher potential leachable fraction at 48% compared to the corresponding fraction of 2.6% for lead. TCLP results reported in row 4 are averages of tests taken on samples after 2, 30, 60, 120, 265, and 370 days of sample curing. In row 5, the average mass of metal leached from treated waste (row 4) is divided by the total leachable metal (row 2). The result in row 5 represents the mass of metal leached from treated waste as a percentage of total leachable metal in the untreated waste. The values for this ratio are small; 8.2% and 7.4% for lead and cadmium, respectively. Small magnitudes for this parameter have also been observed in previous studies (Taylor and Fuessle, 1994). The TCLP concentrations used for averaging in row 4 are significant due to stringent TCLP standards. Therefore, treatment effectiveness defined by TCLP standards is determined by the fate of the last few percent of leachable metal; stabilization success and failure is determined in the 90-100 % treatment range.

Table 5.1 Time-averaged TCLP Concentrations as a Fraction of Leaching Potential for Selected Metals in Stabilized K061 Waste: Natural Cure

Row	Measure (Method) [units]	Cadmium	Lead	Calcium[2]	Chromium[2]
1	Total Metal Available (AA on Nitric Digestates of untreated waste) [g/kg waste][1]	0.42	16.4	75.3	1.35
2	Total Leachable Metal (TCLP on Untreated Waste) [g/kg waste]	0.20	0.42	26	3.8×10^{-4}
3	Leaching Potential (Row 2 divided by row 1)	48%	2.6%	35%	0.028%
4	Average TCLP Concentrations (average of data from samples cured 2-370 days) [g/kg]	0.0163	0.0309	20.3	0.0137
5	Leachate results as percent of Leaching Potential(Row 4 divided by row 2) [%]	8.2	7.4		

1. grams of metal/kg of waste.
2. The principle sources of calcium and chromium are the binders.

Although it is possible to represent results for each individual test as fractions of total leachable metal as shown in Table 5.1, the number of tests required becomes prohibitive. To improve the validity of comparisons, samples to be cured individually for different testing procedures were mixed at one time in the mixer-bowl. Waste variability has been accounted for by reporting concentrations as a percent ratio, C/C_o, where: C_o is the amount of metal available as measured by atomic absorption spectrophotometry(AA) on nitric acid digestates of untreated waste; and C is the metal concentration in TCLP extracts. Both C and C_o have units of grams of metal/gram of waste. A single determination of C_o was made for each bowl mix prepared.

5.3 Time Profile of Leaching with Cure Age

Results of TCLP analyses for lead and cadmium are shown in Figures 5.1 and 5.2, respectively. The amount of lead leached as a fraction of the total lead is quite small

ranging from 0.1 to 0.7 percent of the total lead available. The results are quite variable among different mix designs for short, mid, and long-term curing. However, the time profile for leaching of lead has the same general shape for all five mix designs up to about 100 days. These trends shown in Figure 5.1 are considered valid because they are similar for all mix designs that were prepared and tested independently. Initially after two days of curing, TCLP lead results are relatively high for all mix designs. During the first 30 days of cure, all mix designs provide improvement in TCLP results. After 30 days of cure, all mix designs yield a higher TCLP lead concentration that may be somewhat lower or higher than the initial 2-day results. After 60-120 days of curing, the results of different mix designs start to diverge significantly. At the extremes, [8:20] shows deterioration while [26:30] shows improvement.

As shown in Figure 5.2, the general shape of the cadmium leaching profile with cure age is similar for all mix designs but is different from that for lead. Initially, all mix designs yield relatively low cadmium concentrations in TCLP extracts. With curing, the leaching profile begins to rise over time for all five mixes. Mix designs deficient in binder (e.g. [8:20]) yield cadmium TCLP concentrations that rise more quickly with sample cure age compared to designs with more adequate binder.

Simple regression can be used to compare the treatment performance of two mix designs with time. The controlled independent variable X is the sample cure age. The dependent variable Y will be defined as the difference in TCLP concentrations of extracts from the two mix designs being compared. If difference Y increases with sample age, then the treatment effectiveness of the first mix design is deteriorating significantly with respect to the treatment effectiveness of the second design. Regression permits a determination of the significance of the divergence in performance among different mix designs in a pair-wise manner. Assumptions for simple regression include: X, sample cure age, is an independent variable that has little error, and the dependent variable Y, TCLP metal concentration difference, is mutually independent with constant variance over X. Linear regression is used because these conditions are satisfied reasonably well in this case. The Y variable has some uncontrollable random variations due to variations in waste composition, binders, mixing, TCLP, and indeterminate errors associated with chemical analyses. These measured Y values are independent because samples for each cure age were prepared and tested independently. In agreement with conclusions from section 4.5, a visual examination of data scatter plots shows that the linear assumption for Y with X is reasonable.

Results of TCLP tests on mixes [8:20] and [26:30] described in Table 4.1 are compared in Figures 5.3 and 5.4. Sample cure age at the time of TCLP testing is shown on the horizontal axis. The vertical axis is TCLP for [8:20] – TCLP for [26:30] at each cure age. The positive slope in each figure indicates that mix design [8:20] is significantly deteriorating with respect to [26:30]. The correlation coefficient r^2 indicates a measure of data fit. A 95% confidence interval is also indicated for the slope.

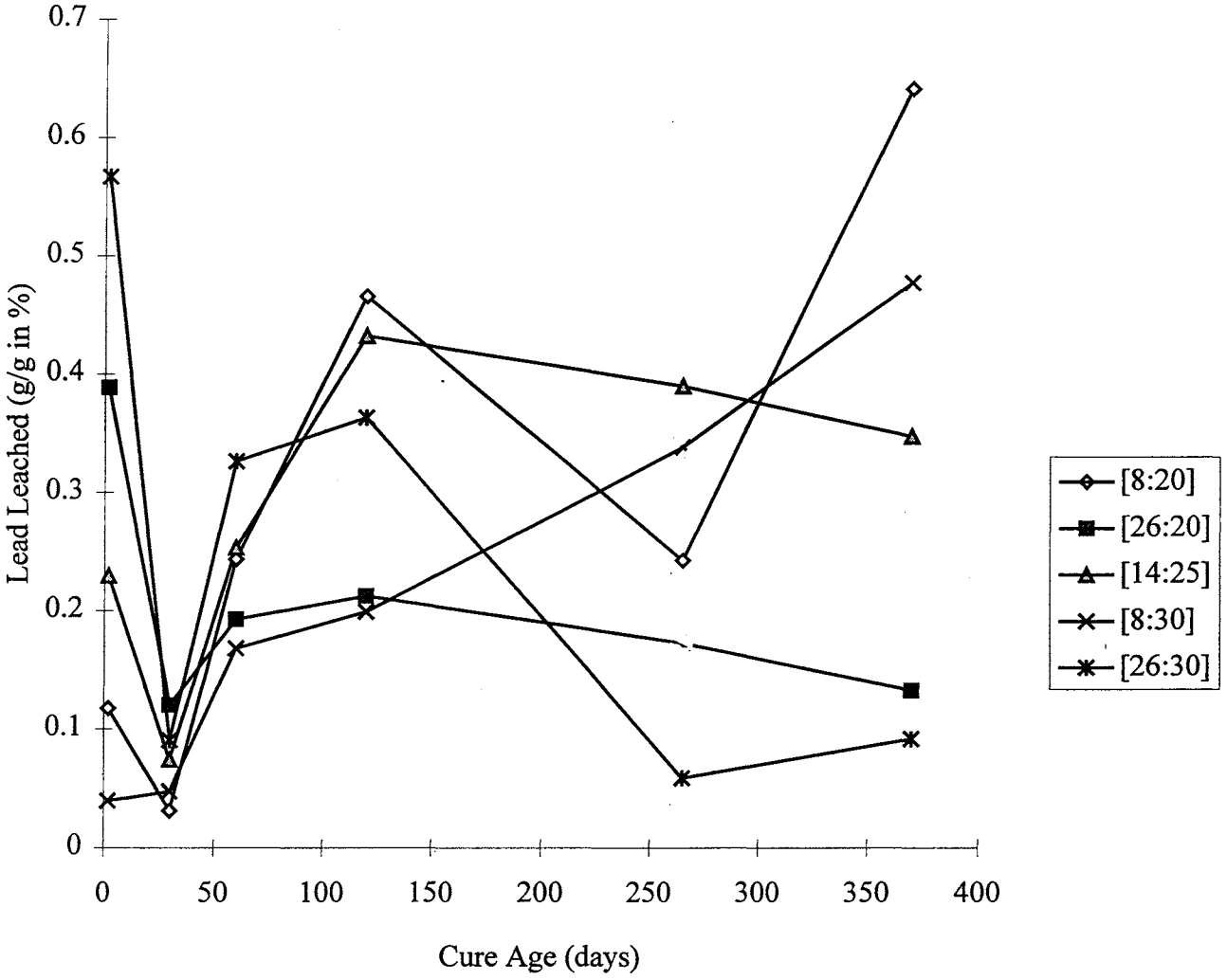

Figure 5.1 Lead TCLP Concentrations versus Natural Cure Age

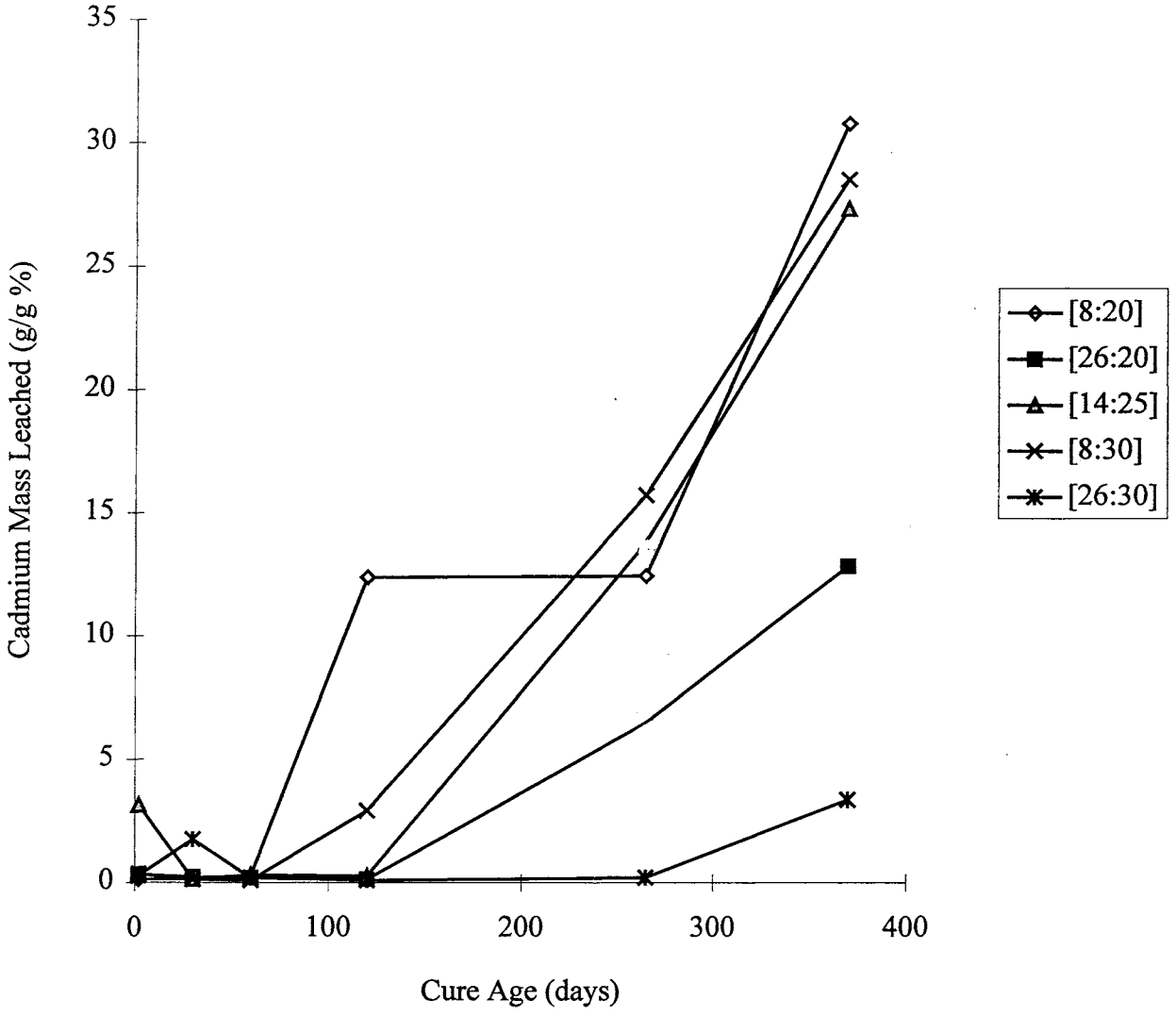

Figure 5.2 Cadmium TCLP Concentrations versus Natural Cure Age

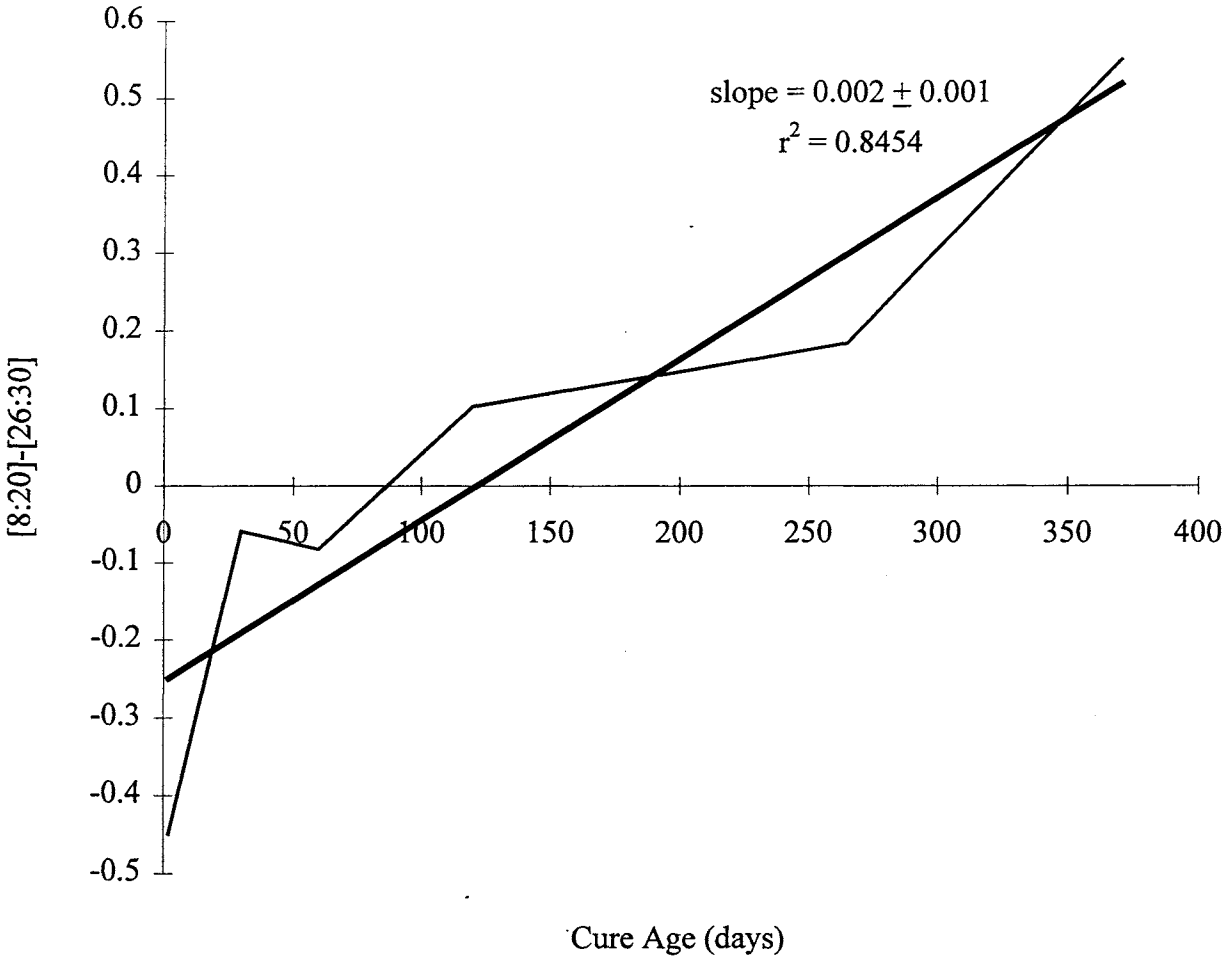

Figure 5.3 Divergence Between [8:20] and [26:30] with Cure Age: Lead

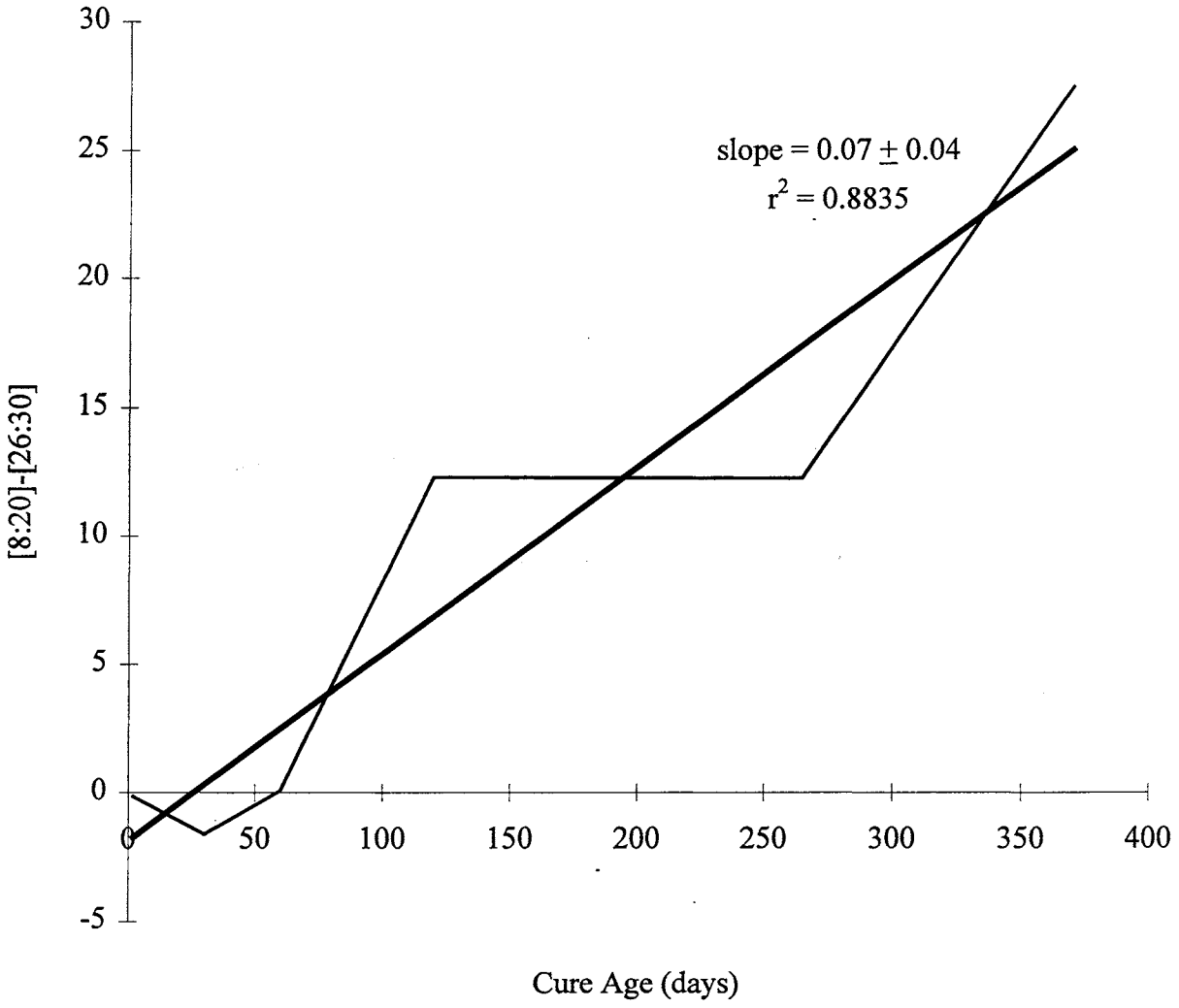

Figure 5.4 Divergence Between [8:20] and [26:30] with Natural Cure Age: Cadmium

Figures 5.3 and 5.4 indicate the long-term deterioration in treatment effectiveness of [8:20] compared to [26:30]. However, these figures also indicate a negative difference for samples of young age; this implies that [8:20] has better TCLP results than [26:30] for young samples. The short-term TCLP test does not predict long-term performance.

Continuing in a similar manner, regression analyses were performed between pairs of corner mix designs described in Table 4.1. Figure 5.5 provides an overview of results. The four corner mix designs are designated by their bracket notation defined earlier and enclosed in bold boxes. Moving horizontally, the mix design becomes more binder rich as indicated by an arrow at the top of Figure 5.5. With vertical movement downward, the mix design includes more water. Figure 5.5 also consists of arrows directed from one mix design to another. The direction of the arrow points toward a net improvement in TCLP concentrations over the long-term, although in some cases

improvement is minimal. Arrows of the form, [I] [J], are directed from inferior

mix [I] to better mix [J]; where r^2 = correlation coefficient for the regression of divergence versus cure age where divergence is defined as {TCLP metal concentration in mix [I] – TCLP metal concentration in mix [J]}. For example, the divergence in performance between mix designs [8:20] and [26:30] is defined as the difference: TCLP metal from [8:20] – TCLP metal from [26:30] as indicated by the arrow from [8:20] to [26:30]. The correlation coefficients for the lead and cadmium regressions are 0.91 and 0.83, respectively.

Moving on either diagonal toward more binder results in significant improvement over time for both metals. For example, the long-term improvement of [26:30] with respect to [8:20] as indicated in Figures 5.3 and 5.4 is also indicated in Figure 5.5 by an arrow from [8:20] to [26:30]. A horizontal comparison of mix designs shows that more binder aids the treatment of cadmium, but lead treatment shows no benefit. A vertical comparison of mix designs shows the effect of adding more water. Little or no improvement is indicated with a low ratio of binder/waste of 0.08. However, with a more adequate binder/waste ratio of 0.26, additional water for that binder improves the capture of cadmium as indicated by a correlation coefficient of 0.92.

Mixes [8:20] and [26:30] were selected to be used in the development of a short-term test that indicates long-term treatment effectiveness. Using only tests carried out on samples cured for a short time, the objective is to predict the difference in treatment effectiveness for these two mix designs after long-term curing. These mixes were selected because the treatment divergence is concealed in the short-term; in fact, [8:20] performs better than [26:30] in the short-term (the divergence is negative). For example, consider the regressions shown in Figures 5.3 and 5.4 for lead and cadmium, respectively. In each case, the negative divergence with only 2 days of curing indicates that [8:20] yields better TCLP results than [26:30] at that time. However, with cure age, the positive difference indicated by the positive slope shows that [26:30] outperforms [8:20] in the long-term. Figures 5.3 and 5.4 show correlation coefficients of 0.91 and 0.83 respectively for lead and cadmium. Furthermore, the treatment divergence with time is significant for these two mixes as indicated by the 95% confidence interval for the regression slopes

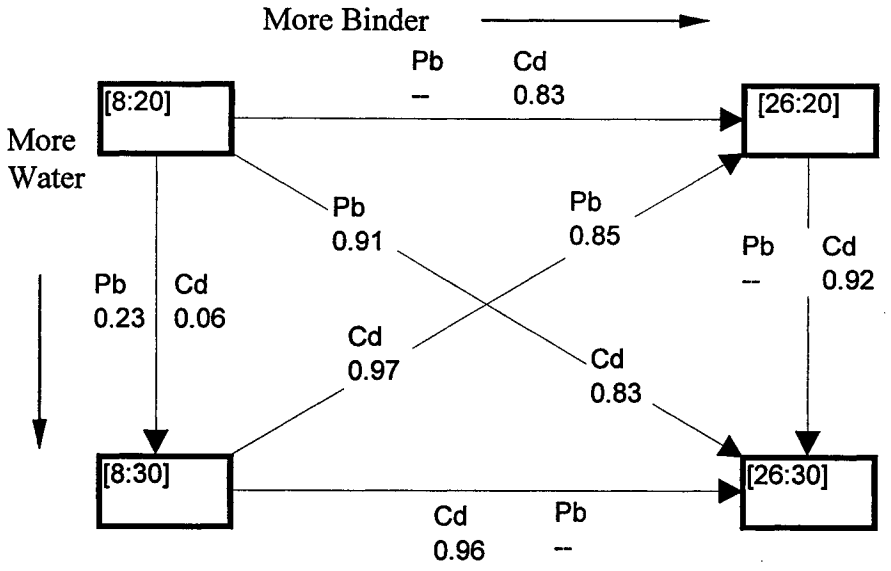

Figure 5.5 Overview of Regression Results

for lead and cadmium. The null hypothesis that the slope of the regression line is equal to zero means that the observed improvement of [26:30] over [8:20] may not be real- only a result of randomness. This null hypothesis can be rejected at the 95 percent level of significance for lead and cadmium respectively. Therefore, these two mixes were selected to undergo accelerated testing to see if the long-term treatment divergence could be detected with a short-term test.

5.4 Discussion of the Observed Leaching Profile with Cure Age

5.4.1 Mechanism of Metal Immobilization

Recent researchers have used a wide variety of highly sophisticated techniques (e.g. ^{29}Si NMR, XRD, XPS, EDS, FTIR, SEM, EDX) to investigate the mechanism of immobilizing metals in the S/S process. Results of these investigations are helpful but there remains considerable uncertainty among researchers about mechanisms for metal immobilization. At one extreme, the heavy metals are merely physically captured within the cement matrix, and at the other extreme, metals are chemically bound to cement constituents. The chemi-adsorption of metals may be within the cement matrix or may only be at surfaces. In either case, the binding energy, metal speciation, and nature of the surface compounds are uncertain. Further complications occur because cement chemistry

changes significantly during the first year, so binding mechanisms may be a function of cure time and mix design.

Many researchers have studied cement S/S of heavy metals by doping cement with low concentrations of metal nitrate solutions. The nitrate anion has been suspected of causing potassium to show up on cement surfaces contaminated by heavy metals. Although the use of metal nitrate solutions to contaminate a cement sample has advantages, Roy, et. al., (1992) point out that the chemistry may be significantly different for a treated metal sludge that has been precipitated and dewatered. They explain that metals may be present in the sludge as non-crystalline hydroxide gels, non-stoichiometric salts with more than one metal, or as complex salts with more than one anion. These complications make chemical analyses and physiochemical characterizations very difficult.

An actual complex waste is used in this study. The investigators assume that several binding mechanisms are possible for a metal. Furthermore, the proportion of metal bound by any one mechanism may vary with cure age. Finally, as shown in Table 5.1, more than 97% of the TCLP-leachable lead and cadmium is effectively bound at all cure ages (up to 635 days in this study). Small fractions of the total leachable metal will determine the long-term success or failure of stabilization treatment.

5.4.2 Effect of pH on Metal Immobilization

The deceptive behavior of [8:20] and the improvement of [26:30] can be explained in part by cement science and the relation between metal solubility and pH. Figures 5.6 and 5.7 show TCLP results for various mix designs as a function of the extract's pH for lead and cadmium, respectively. The plot of empirical data is similar in shape and magnitude to the corresponding metal hydroxide solubility curves calculated by chemical equilibrium considerations.

The comparison between empirical and calculated solubility curves is similar to that reported by other researchers. Using synthetic wastes, Cote (1986) demonstrated the differences between calculated hydroxide solubility curves and those determined empirically. The calculated hydroxide curves showed a much greater dependence on pH than empirical data. The calculated minimum solubility was also lower by a factor of 5 to 10 than the minimum solubility obtained by experiment. Andres and Irabien (1994) and Rajan, et. al., (1995) also concluded that leachate metal concentrations follow the behavior of the corresponding hydroxides with pH. Thus the lowest metal concentration in the leachate is obtained in the range of pH values in which metal hydroxides also have minimum solubility. The minimum metal solubility occurs at different pH values depending on the metal. Since the alkalinity of a cement-based stabilized waste is strongly related to the binder/waste ratio, pH control during extraction has been a major objective of successful treatment.

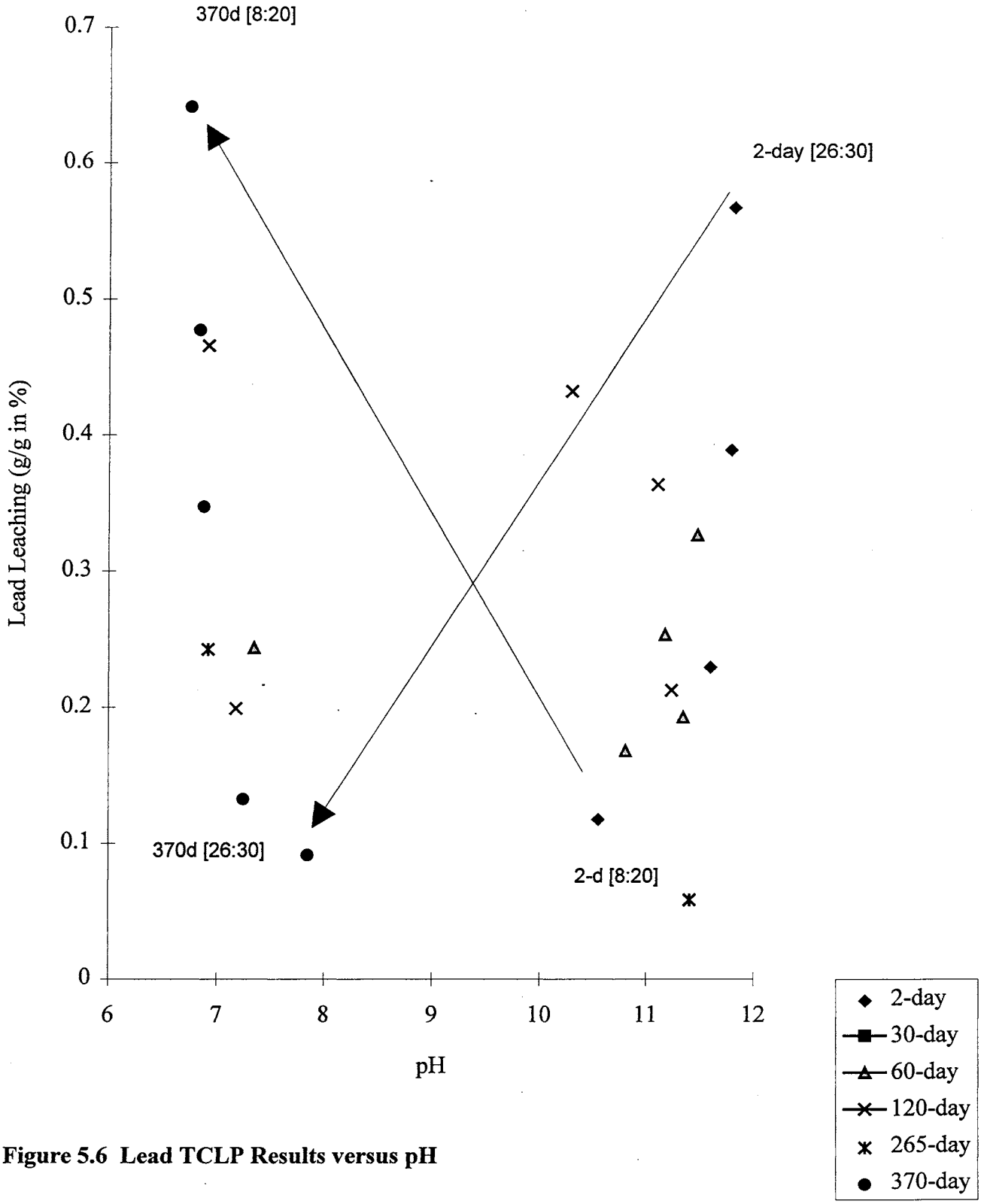

Figure 5.6 Lead TCLP Results versus pH

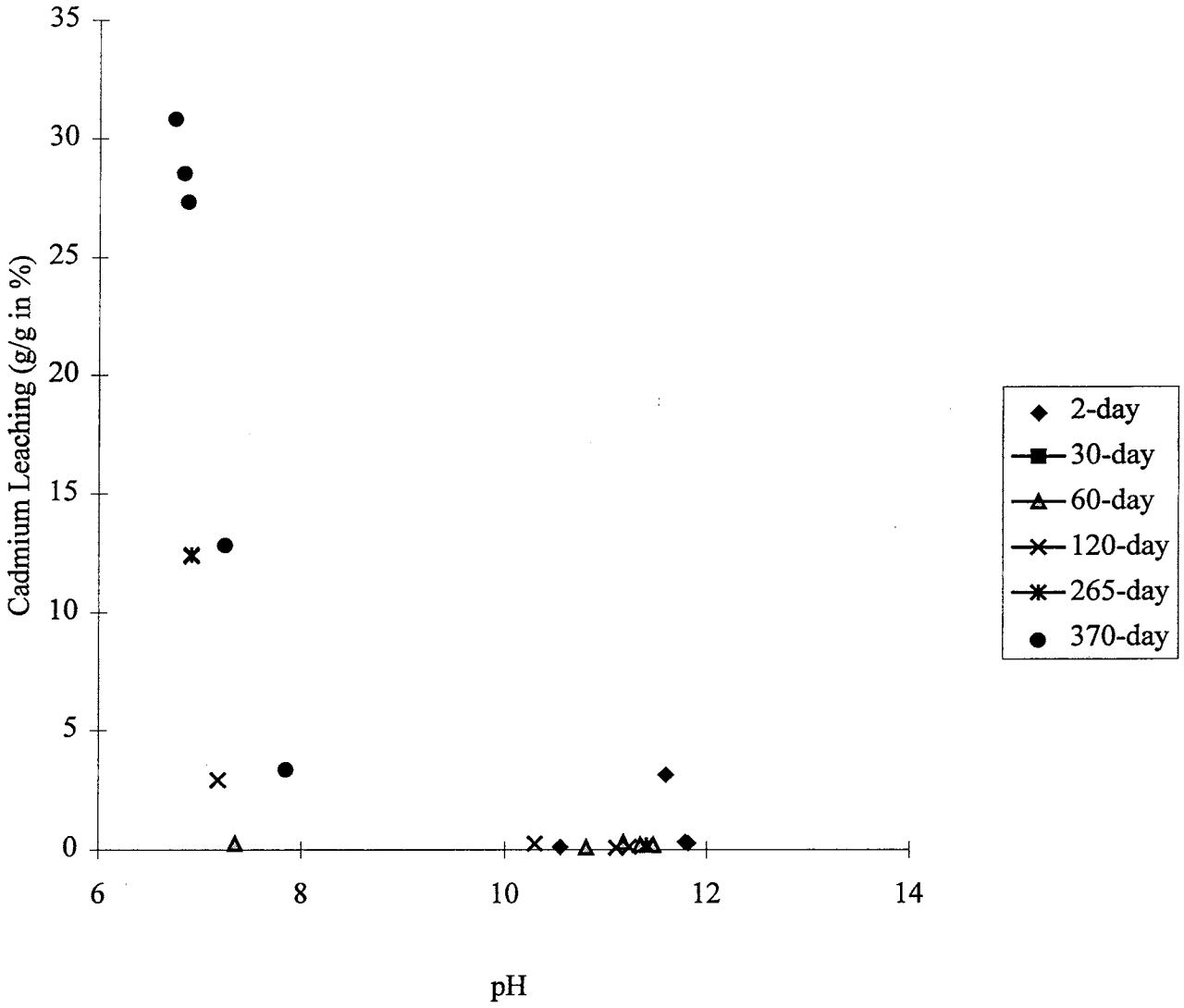

Figure 5.7 Cadmium TCLP Results versus pH

For the same stabilization mix designs, the expected extract pH will vary depending on the age of the sample undergoing TCLP. If pozzolans are present, curing yields an increase of C-S-H while the CH phase decreases as shown in Figure 2.2. This growth of C-S-H and decay of CH also results in a drop in acid neutralization capacity because calcium silicates have less acid neutralization capacity (ANC) than calcium hydroxides. This expected drop in ANC may cause a change in extract pH with a corresponding change in metal solubility. With cure age, the decrease in extract pH moves the expected TCLP concentration from the right side of the curve toward the left side.

For example, consider the lead TCLP concentrations shown in Figure 5.6. The U-shaped pattern of data reflects the amphoteric nature of lead. Mix [8:20] with only two days curing yields an extract pH of 10.55, while mix [26:30] with more binder has a corresponding higher pH of 11.82 at the same cure age. Both of these data points are indicated on the right leg of the U-shaped pattern of data. The lower pH of [8:20] yields a TCLP lead concentration on the solubility curve closer to the minimum. With long-term curing of 370 days, arrows on the graph show the decrease in extract pH and the resulting change in TCLP lead concentration. As explained in the previous paragraph, the TCLP extract pH is expected to decrease with curing age. At 370 days, mix [26:30] is closer to minimum lead solubility with a pH = 7.85, while mix [8:20] yielded a lower extract pH of 6.75. The pH values and corresponding TCLP lead concentrations follow the amphoteric pattern of the lead-hydroxide solubility curve.

The environment of lead in S/S processes is unknown. Cocke, et. al., (1989) state that Pb^{2+} locates at the surface of clinker components. These insoluble salts with low surface binding energies coat the clinker grains with a passivating layer that retards hydration. This hypothesis concurs with a model study conducted by Thomas (1981). Upon titration in the presence of mixed salts of lead, Thomas (1981) noted an ill-defined endpoint in the pH range of 8.5-10.0. Dissolution and reprecipitation of first formed solids was given as an explanation. Although lead retards cement hydration, Ortego, et. al., (1991) state this effect is overcome in about 4 weeks and that silicate condensation is enhanced by lead. They model the effect of enhanced Si polymerization by lead as follows:

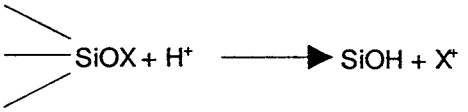

where X^+ may be Na^+, Cd^{2+}, or Pb^{2+}. A lower binder/waste in [8:20] implies a higher ratio of acid to siliceous binder during the TCLP. The proportionally larger extent of silicate polymerization for low binder mixes [8:20] may explain the larger leachate concentration observed at longer cure ages.

Figure 5.7 shows TCLP cadmium concentrations with respect to extract pH for various mix designs. The extract pH decreases with cure age as observed with lead. The leaching profile of cadmium and lead are different. One significant difference is that cadmium leaching at 2-days curing is minimal no matter what mix design is used. This may be explained by the fact that cadmium is not nearly as amphoteric in behavior as

lead. Cadmium does not show an increase in solubility up to a pH of 12. $Cd(OH)_5^{3-}$ will occur in measurable amounts only above pH=13. Cartledge, et. al., (1990) hypothesize that $Cd(OH)_2$ precipitates to form nucleation sites for the development of C-S-H or $Ca(OH)_2$. Cadmium might also replace calcium during the cement hydration and a slight increase in cement hydration has been observed.

It is widely acknowledged that cement-based S/S relies heavily on pH control for metal containment. Some believe it may be the only important factor. However, there is evidence of other factors important for S/S. Bishop (1988) demonstrated that even after the alkalinity was leached out of the cement-based waste form, lead and chromium leaching was much lower than would be predicted by metal hydroxide solubility.

5.5 Column Leaching

5.5.1 Motivation and Hypothesis

One research objective is to predict the long-term treatment effectiveness of a mix design from a short-term test. A stabilization treatment is effective in the long-term if a sample undergoes TCLP after curing for the long-term and if the extract metal concentrations satisfy TCLP standards. Different types of leaching tests, longer leaching periods, and more severe leaching conditions have been investigated to estimate long-term treatment as discussed in Chapter 2. This project differs by utilizing accelerated curing of stabilized wastes and a leach test that is comparable in severity to the TCLP. In this section, results of dynamic column leaching are discussed. The column leaching procedure has been described in Chapter 3. The pH of the leachant and total leachant/solid ratio were maintained to be comparable to the TCLP. Curing methods for the stabilized wastes included: 4-day and 20-day natural cure, 4-day heating at 40°C, 3-hour 40°C heat followed by 10-hour natural cure, and 4-day cure with chemical accelerators. Details of the experimental design are provided in chapter 4.

Dynamic leaching provides the time rate of metal release from the stabilized waste. The hypothesis is that the rate of metal leaching from young samples is correlated with the long-term treatment effectiveness of the stabilization. This hypothesis is reasonable if we assume that long-term effectiveness may depend on what proportion of metal is most accessible to the leachant, i.e. what proportion is available on exposed external surfaces versus on internal surfaces. The metal release from exposed external surfaces is characterized by a wash-off mechanism where metal retention relies on the relatively weak binding energies of these metals. On the other hand, metal that is on internal surfaces is physically encapsulated, and a slower diffusive process is frequently used to explain leaching of this metal. Metals on internal surfaces leach less readily. With early cure, the proportion of metal on internal versus external surfaces and rate of metal release may be an indicator of the quality of long-term treatment.

5.5.2 Four-day Natural Cure

Results for lead and cadmium are presented in Figures 5.8 and 5.9, respectively. The cumulative metal release in grams of metal extracted per gram metal in waste (%) is plotted against leaching time. The slope of this graph equals the rate of metal leaching. According to Figure 5.5, treatment was satisfactory for naturally-cured samples of [8:20] with young sample age, but yielded high TCLP results on aged samples. Conversely, naturally-cured samples of [26:30] yielded relatively poor results with early cure, but TCLP results improved with increasing cure age. This trend clearly correlates with the rate of metal release (the slope) on both Figures 5.8 and 5.9 for lead and cadmium, respectively. After a cumulative leachant volume of 0.4L, the lower rate of lead release for [26:30] clearly indicates its superior long-term effectiveness compared to that for [8:20]. In Figure 5.9, the rate of cadmium release from [8:20] exceeds that from [26:30] even more significantly than the corresponding difference for lead. In both figures, regression lines are drawn after the data diverge. The slopes and corresponding 99% confidence limits are also indicated.

In Figures 5.8 and 5.9, significance of the different rates of metal release can be quantified by regressing the quantity $\{[8:20]_{metal} - [26:30]_{metal}\}$ versus time of leaching. The slope B_1 of this linear regression is a measure of the divergence of eluant metal concentration between [8:20] and [26:30] throughout the duration of the column leaching. A positive B_1 indicates that the eluant concentrations from [8:20] are increasing at a higher rate than the eluant concentrations from [26:30]. If B_1 were to equal zero, then the metal release rates of [8:20] and [26:30] are equal. The confidence that the metal leaching rate from [8:20] exceeds that from [26:30] equals the confidence that $B_1 > 0$. The right-tailed hypothesis test can be stated as: H_o: $\beta_1 = 0$ or H_1: $\beta_1 > 0$. The null hypothesis: $\beta_1 = 0$ (no real slope difference, or the true metal leaching rates of [8:20] and [26:30] are actually equal) may be rejected with $(1-\alpha)\times 100\%$ confidence for large positive values of the test statistic defined as follows:

$$\text{Statistic:} \quad T_{n-2} = \frac{(B_1 - \beta_1)}{S / \sqrt{S_{xx}}}$$

where:

$$\alpha = P(T_{n-2} \le t_{n-2})$$

$$S_{xx} = \sum_{i=1}^{n} (x_i - \bar{x})^2$$

$$S^2 = \frac{SSE}{(n-2)}$$

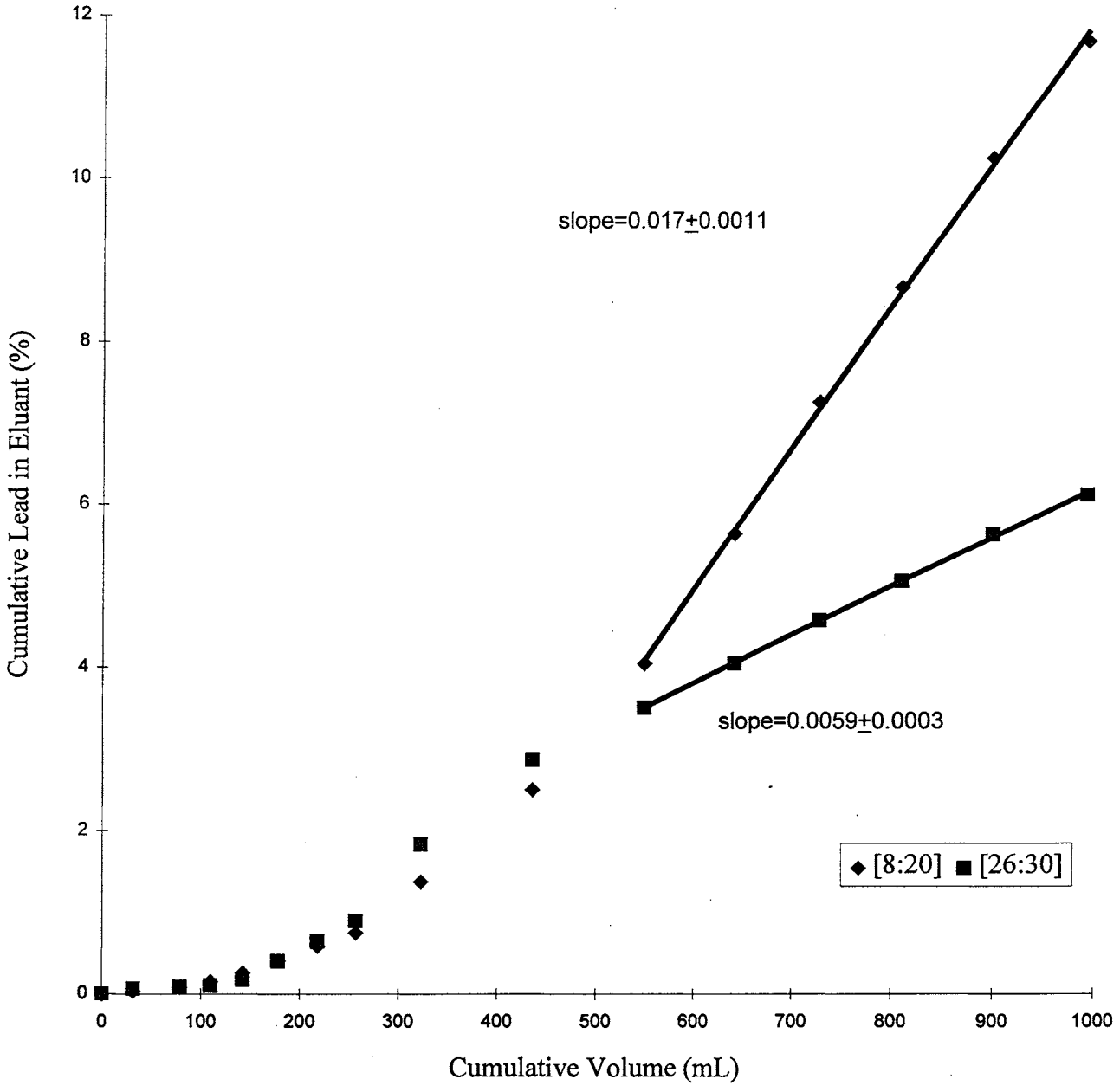

Figure 5.8 Column Leaching of 4-Day Old Samples: Lead

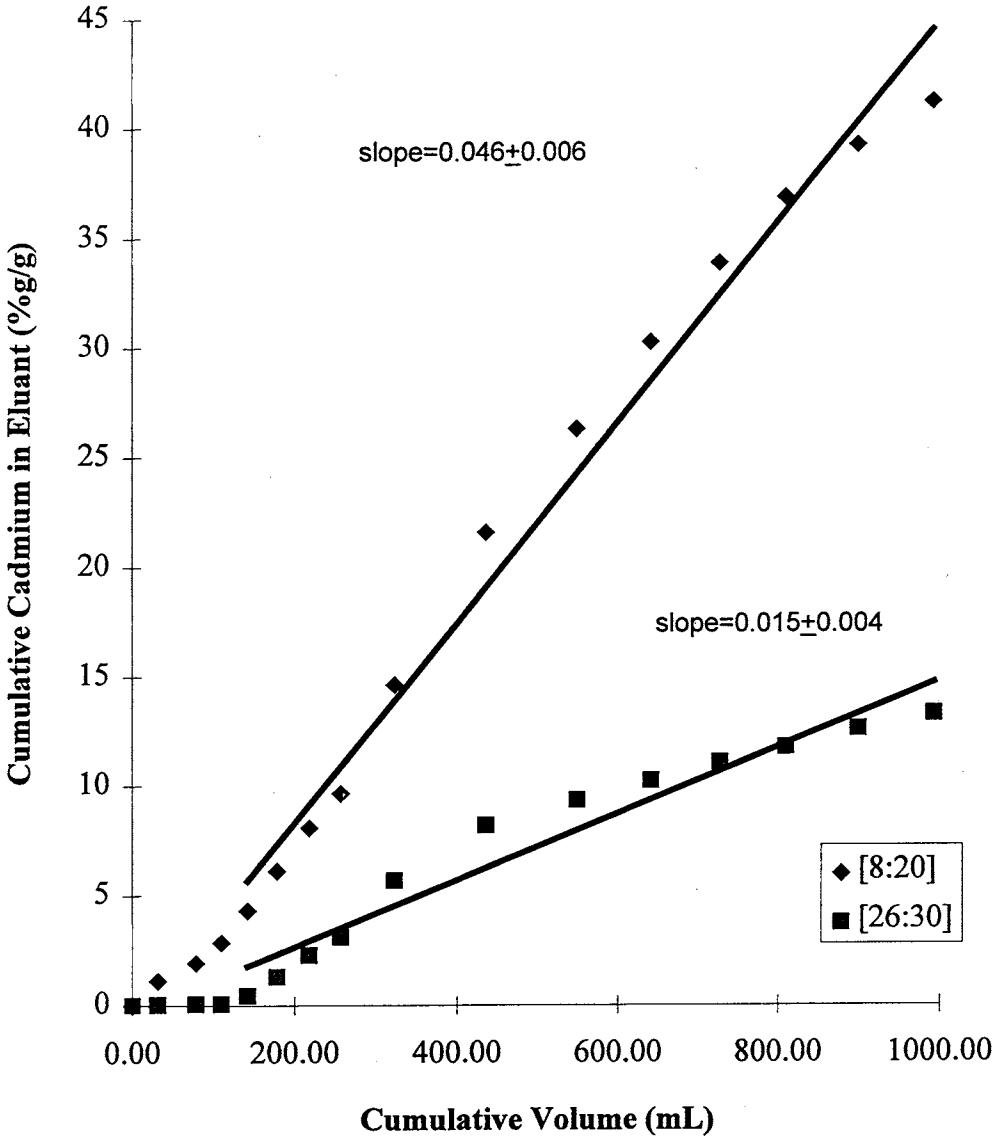

Figure 5.9 Column Leaching on 4-Day Old Samples: Cadmium

SSE = sum of squares of residuals;

$$SSE = \sum_{i=1}^{n} (y_i - B_o - B_1 x_i)^2$$

B_o = intercept of linear regression line through observed data;

B_1 = slope of linear regression line through observed data;

β_1 = slope of the true linear regression line;

t_{n-2} = t - statistic with n - 2 degrees of freedom;

n = number of sample points.

Table 5.2 summarizes statistical results for metal release rate differences in this chapter.

Table 5.2 Summary of Statistical Regression Data for Column Leaching

Figure No.	Number of data points	Absolute slope Difference, B_1	T–Statistic from data	Test T-Statistic for Confidence	Confidence Level
5.8	6	0.0114	48.99	4.60	>99%
5.9	12	0.0305	16.16	3.17	>99%
5.12	8	0.000281	1.419	1.419	79%
5.13	6	0.00281	4.61	4.61	99%
5.15	6	0.00671	103.03	4.60	>99%
5.16	6	0.0113	57.63	4.6	>99%
5.17	8	0.00065	1.23	1.23	74%
5.18	4	0.0173	23.48	9.92	>99%
5.19	5	0.00197	10.4	5.84	>99%
5.20	15	0.00511	34.33	3.01	>99%
5.22	6	0.0137	8.06	4.60	>99%
5.23	7	0.00962	7.66	4.03	>99%

The dramatic difference in metal release rates between samples [8:20] and [26:30] cannot be explained by just an effect of pH. Figure 5.10 shows the pH of samples from these column extractions. Compared with [8:20], the additional acid neutralization capacity of [26:30] is quickly exhausted early in the run (about 50 minutes). The sudden decrease of acid neutralization in [26:30] may be explained by unhydrated binder that provides a high amount of alkalinity but is quickly washed out in the eluant. After fifty minutes, the pH of extracts from the [26:30] column are actually lower than those from [8:20]. With lower pH measurements from [26:30], higher metal concentrations are

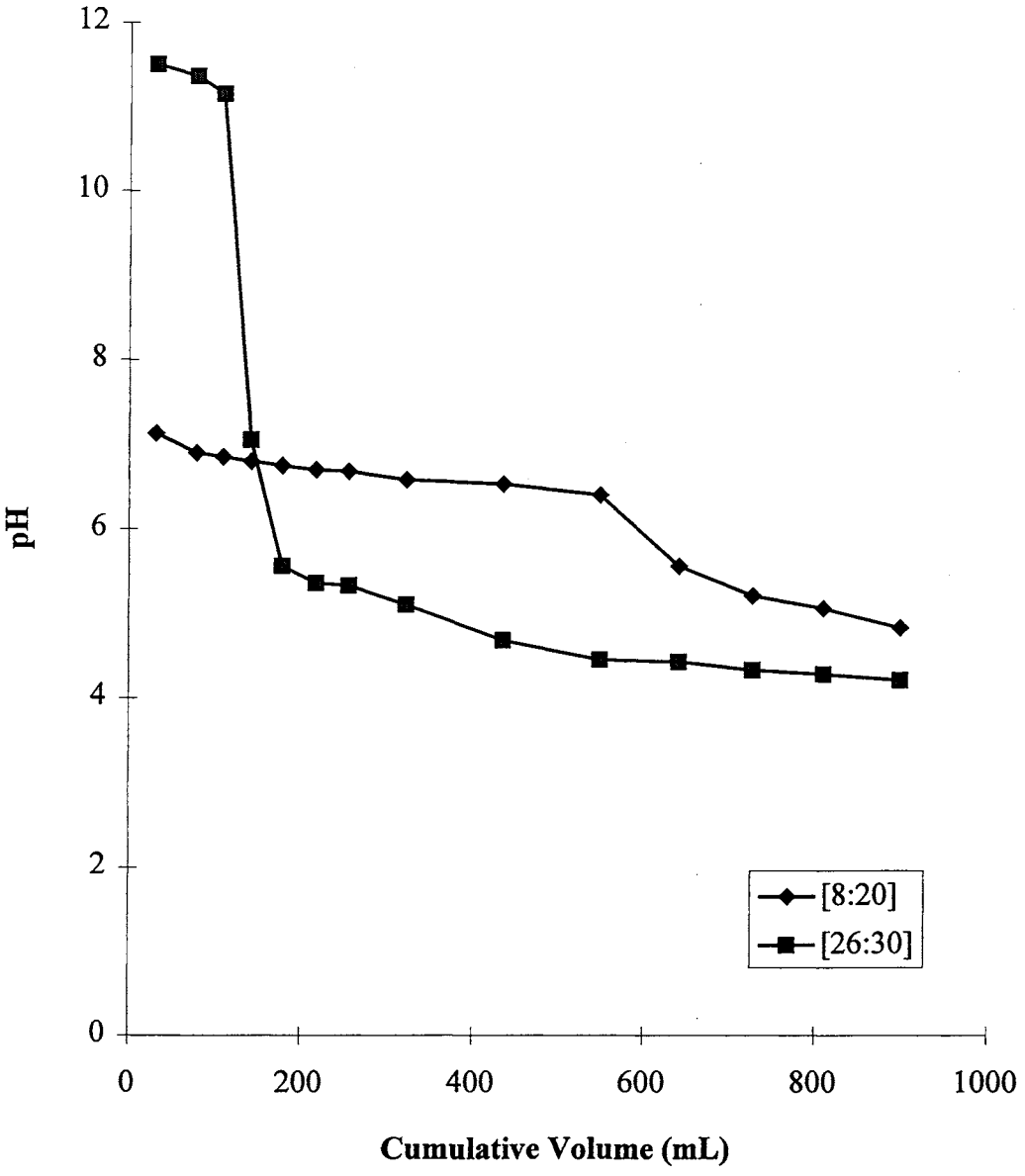

Figure 5.10 pH of Column Extracts from 4-Day Old Samples

expected according to metal-hydroxide solubility, but the opposite was observed. Furthermore, the extract pH values from both mixes begin to converge as time progresses. The more acidic nature of extracts from [26:30] and the convergence pH values with leaching time cannot explain the larger metal release of [8:20] in both amount and rate. These trends are observed in other column experiments described below. Therefore, the metal release rate cannot be explained by solubility considerations of metal hydroxides and pH.

Although pH has been considered a major control variable for successful stabilization, other researchers have observed that pH considerations do not always fully explain leaching results. Bishop (1988) demonstrated that even after the alkali had been leached from cement-based forms, lead and chromium leaching were much lower than would be expected from metal hydroxide solubility. Conner (1990) concluded that the metals were physically bound into the matrix. Roy, et. al., (1992) concluded that physical encapsulation on the microscopic scale was the principal mechanism of metal immobilization. Webster and Loehr (1996) performed two sequences of TCLP-like extractions, one using TCLP fluid and another using sea water. They observed that while the higher leachate pH values occurred during sea water sequential extractions, the higher pH does not account for the difference in leaching behavior compared to the more acidic extractions using TCLP fluid. They concluded that the microstructural integrity of the matrix was also important for successful stabilization. Gress and Korchi (1993) propose that the release of heavy metals is more dependent on the precipitation/desorption characteristics of the metal and not on the porosity of the stabilized waste. These observations indicate that leachate-solid surface processes are also important.

Both pH considerations and cement microstructural integrity are important for S/S. pH is a master variable that influences many chemical processes important in S/S. Microstructural integrity is important for physical processes such as diffusion, surface area, and porosity. The microstructure of cement is largely described by C-S-H development and calcium hydroxide. Several theories attempt to explain various observations of the mechanism of cement hydration. Although these theories may appear to be separate, there are many common features (Ramachandran (1984), Pratt and Jennings (1981)). Knowledge of these common features and pH considerations can be used to suggest a reasonable hypothesis that explains why metal release rates from short-term column leaching tests may predict long-term TCLP results.

During the initial hydration of cement grains, calcium and hydroxide ions dissolve from the cement into the pore water elevating its pH up to about 11-12. Calcium hydroxide supersaturation is thought to be related to the development of a C-S-H rind around each cement grain. As shown in Figure 2.2, this rind grows and changes in character with curing. Diamond (1976) has proposed one classification system of four types of C-S-H. Type I C-S-H shown in Figure 2.2b occurs in early hydration and is characterized by elongated or fibrous particles or spines that are a few micrometers long. These spines grow and interlace somewhat, but little strength is attributed to this network. Type II C-S-H forms in conjunction with Type I and is described as reticular or honey-combed structures. Continuing C-S-H development comes from a rind of inner C-S-H growing around each clinker grain as shown in Figure 2.2c. In older cement, Type III

C-S-H morphology is characterized by flattened particles. At late hydration, Type IV is compact and dimpled-shaped as the spines of Type I disappear into a denser matrix. According to Ramachandran (1984), Types I and II form after 3 days while Type III appears after 28 days.

Table 5.3 presents a qualitative overview of data trends in TCLP and column testing. The first two rows summarize TCLP data on samples cured naturally in the short and long-term. The extent of bars indicate the relative magnitude of the data. A possible explanation for this TCLP data has been presented in section 5.3.2. The TCLP data follow the U-shaped pattern expected for metal solubilities in relation to pH. In the TCLP, pH appears to be a controlling factor which is expected considering the nature of the TCLP test. One hundred grams of stabilized waste are ground and agitated in 2 liters of acidic fluid for 18 hours, a time interval long enough to nearly attain equilibrium. Except at the microscale, physical factors affecting metal stabilization are masked by the TCLP. However, physiochemical factors such as microstructural developments are important in the cement matrix between short and longer term. These factors are precisely why TCLP results change with curing. These microstructural developments include C-S-H growth.

Using samples with short-term curing, the column test provides an indication of how stabilization may develop over time. Figure 5.11 shows a schematic illustration of [8:20] and [26:30] during early hydration. Although [8:20] has enough binder in reality to coat each waste particle a thousand times over, the relatively small amount of binder in [8:20] is illustrated in Figure 5.11 by one layer of cement particles. The thin layer of binder in [8:20] permits more diffusive exchange of water and metal to and from the K061 waste particle. Furthermore, the mix [8:20] is on the "dry side" of our experimental matrix of designs compared to [26:30]. Less water in [8:20] results in less calcium hydroxide and stunted growth of C-S-H. The lesser amounts of calcium hydroxide in [8:20] are indicated by the extent and size of amorphous crystals that grow between spaces of C-S-H. The stunted growth of C-S-H in [8:20] is indicated by a thinner rind and fewer number of fibrils (Types I and II C-S-H).

The lesser amount of calcium hydroxide in [8:20] correlates with the lower pH of TCLP extracts compared to those of [26:30]. The lower extract pH of [8:20] places its TCLP metal concentrations closer to minimum metal solubility; thus, 2-day TCLP results

Table 5.3 Qualitative View of Trends in Column and TCLP Data

Test	Sample Age	Measure	[8:20]	[26:30]
TCLP	2-days	extract metal concentration		
TCLP	370-days	extract metal concentration		
Column	4-days	rate of metal release		

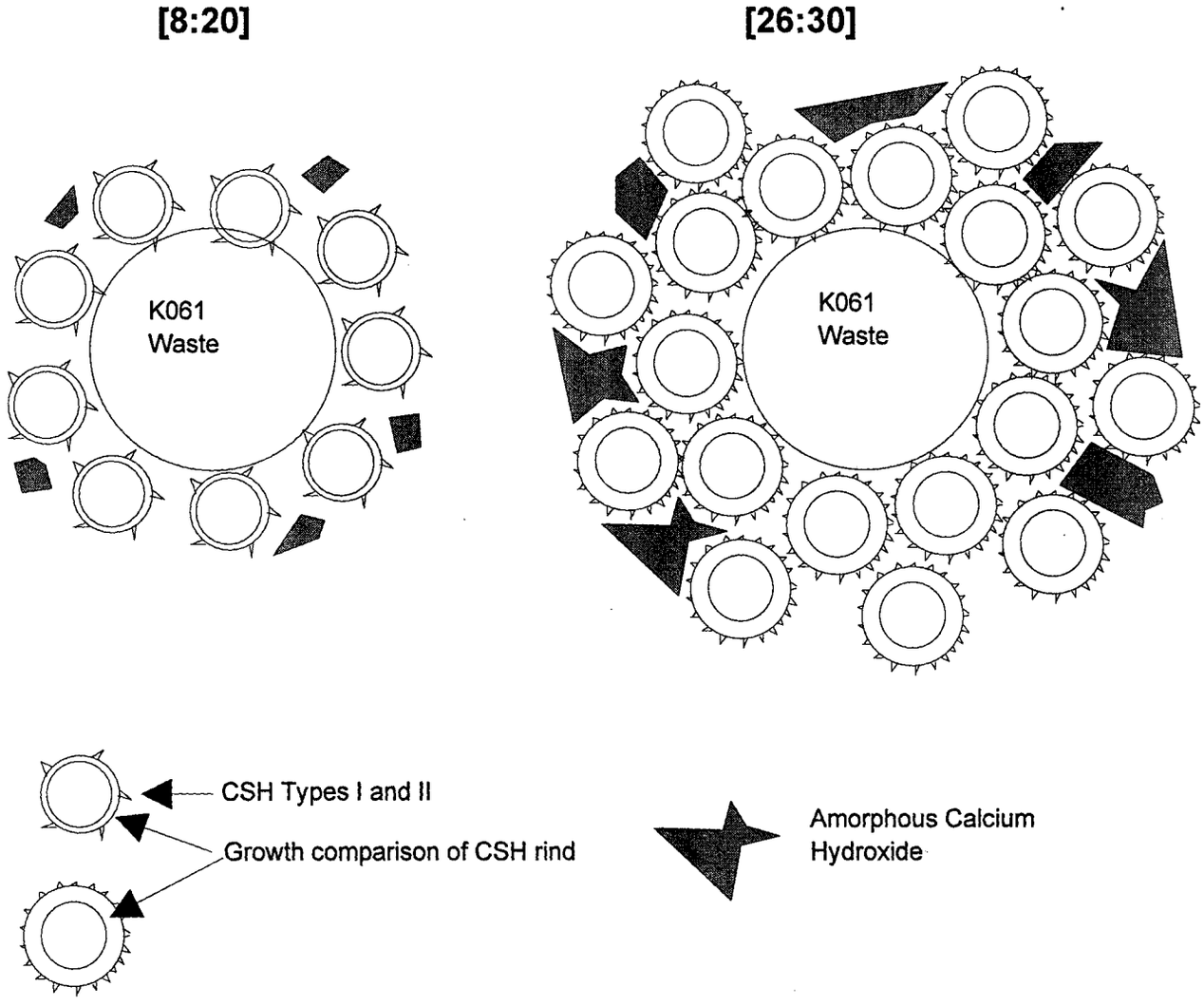

Figure 5.11 Schematic Illustration of [8:20] and [26:30]

from [8:20] are less than that of [26:30]. In a column leaching environment, the rate of metal release from [26:30] should be more limited than from [8:20] because of its superior network of Type I and type II C-S-H. This network is not as dense as more mature C-S-H. Strength development is not attributed to Types I and II C-S-H. However, this quality of early C-S-H forecasts the quality of more mature C-S-H, the growing rind around each clinker grain. Directly related to the rate of metal release, the quality of the early C-S-H network also forecasts long-term treatment effectiveness because C-S-H is important for long-term physical encapsulation. Therefore, the rate of metal release from a young sample undergoing column leaching may forecast its TCLP performance in the long-term.

A schematic diagram of the other corner mix designs is shown in Figure 5.12. Like [8:20] in Figure 5.11, [8:30] in Figure 5.12 has limited binder as indicated by one layer of cement particles around the waste. Unlike [8:20], [8:30] has sufficient water to hydrate the binder, so a thicker rind of C-S-H is shown in the cement surrounding the waste for [8:30]. Like [26:30] in Figure 5.11, [26:20] in Figure 5.12 has abundant binder as indicated by multiple layers of binder. Unlike [26:30], [26:20] has less water which is indicated in Figure 5.12 by some unhydrated clinker. For curing during the first year, there are unhydrated products in all mix designs that slowly react (Mindess and Young (1981)). Unhydrated products are included only in [26:20] to illustrate it has more unhydrated products resulting from more binder and less water compared to all other mix designs included in this study. Insufficient water for all the binder in [26:20] may result in stunted C-S-H growth as indicated by the thinner rind. However, with sufficient time and air moisture, C-S-H may improve in [26:20]. According to Figure 5.1 and 5.2, TCLP results for [8:30] and [26:20] are indistinguishable for up to at least 120 days. At 360 days, the stabilization of [26:20] yields superior TCLP results compared to those from [8:30].

5.5.3 Twenty-day Natural Curing

The column leaching tests discussed in section 5.5.2 were performed after 4 days of natural curing. Samples were also cured for 20 days of natural curing before undergoing column leaching. Results are shown in Figures 5.13 and 5.14. The column test for [26:30] was repeated and the results compare closely. Using the data from 200 minutes on, the slopes of the data begin to show a trend that is expected in the future: [8:20] deteriorates while [26:30] improves. Compared with data from 4-day column leaching, the difference in metal release rates between [8:20] and [26:30] is less dramatic. Furthermore, the difference in the quantity of metal released from 20-day column leaching is significantly less that that from 4-day column leaching for these two mixes. Interestingly, this result also mimics TCLP performance with cure age. According to Figure 5.1, lead concentrations from TCLP extracts improved for all mix designs that were cured for 30 days.

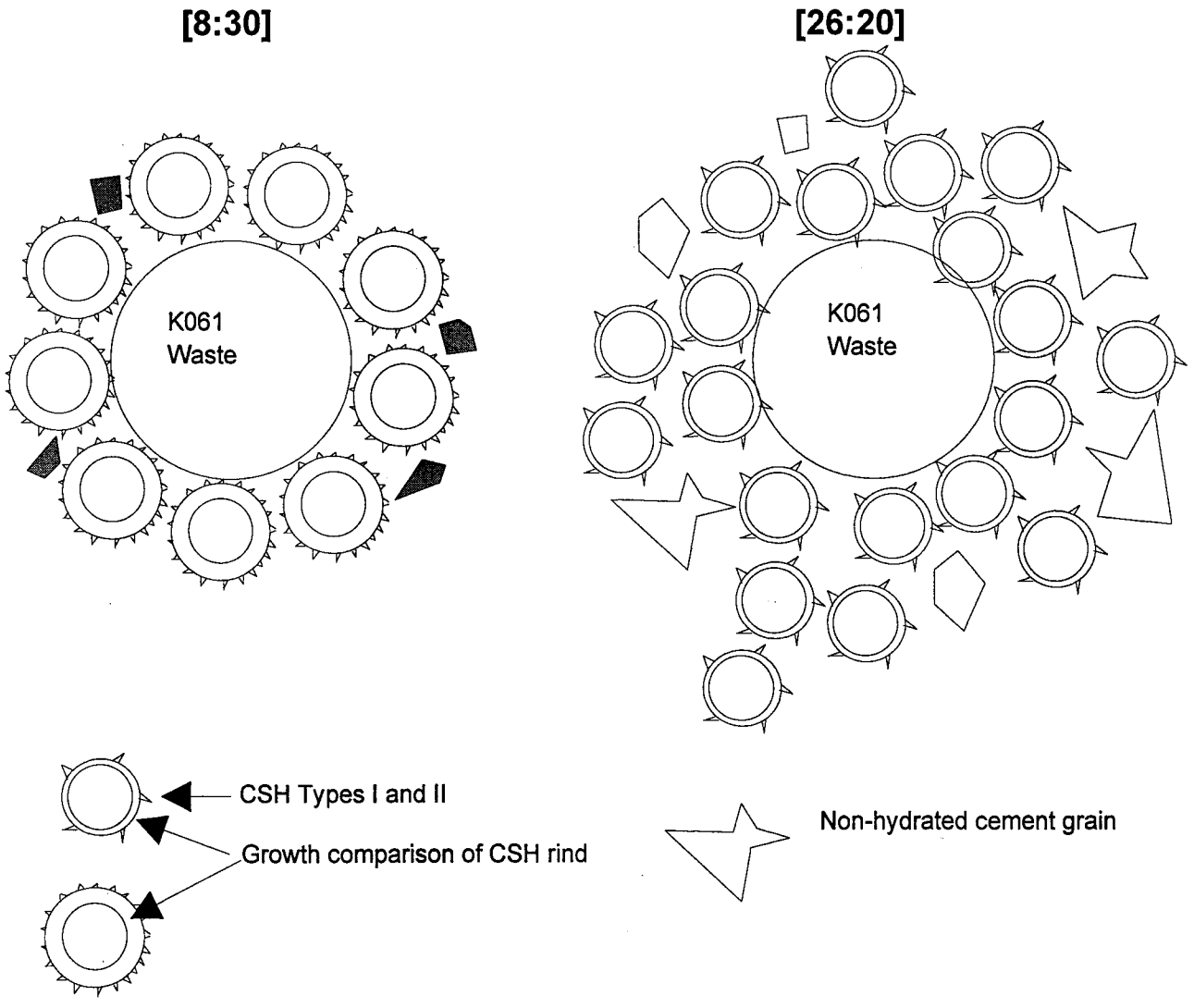

Figure 5.12 Schematic Illustration of [8:30] and [26:20]

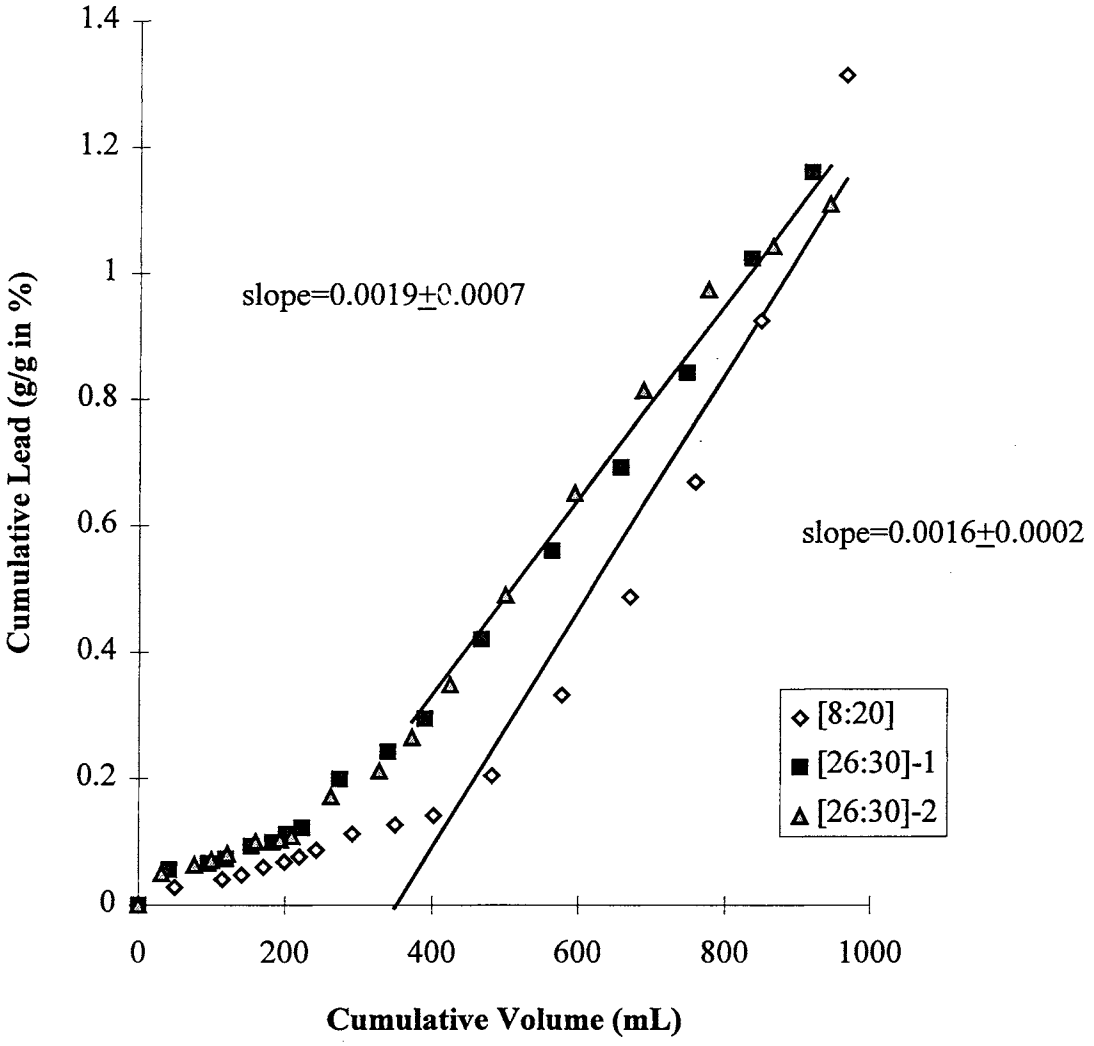

Figure 5.13 Column Leaching of 20 Day-Old Samples: Lead

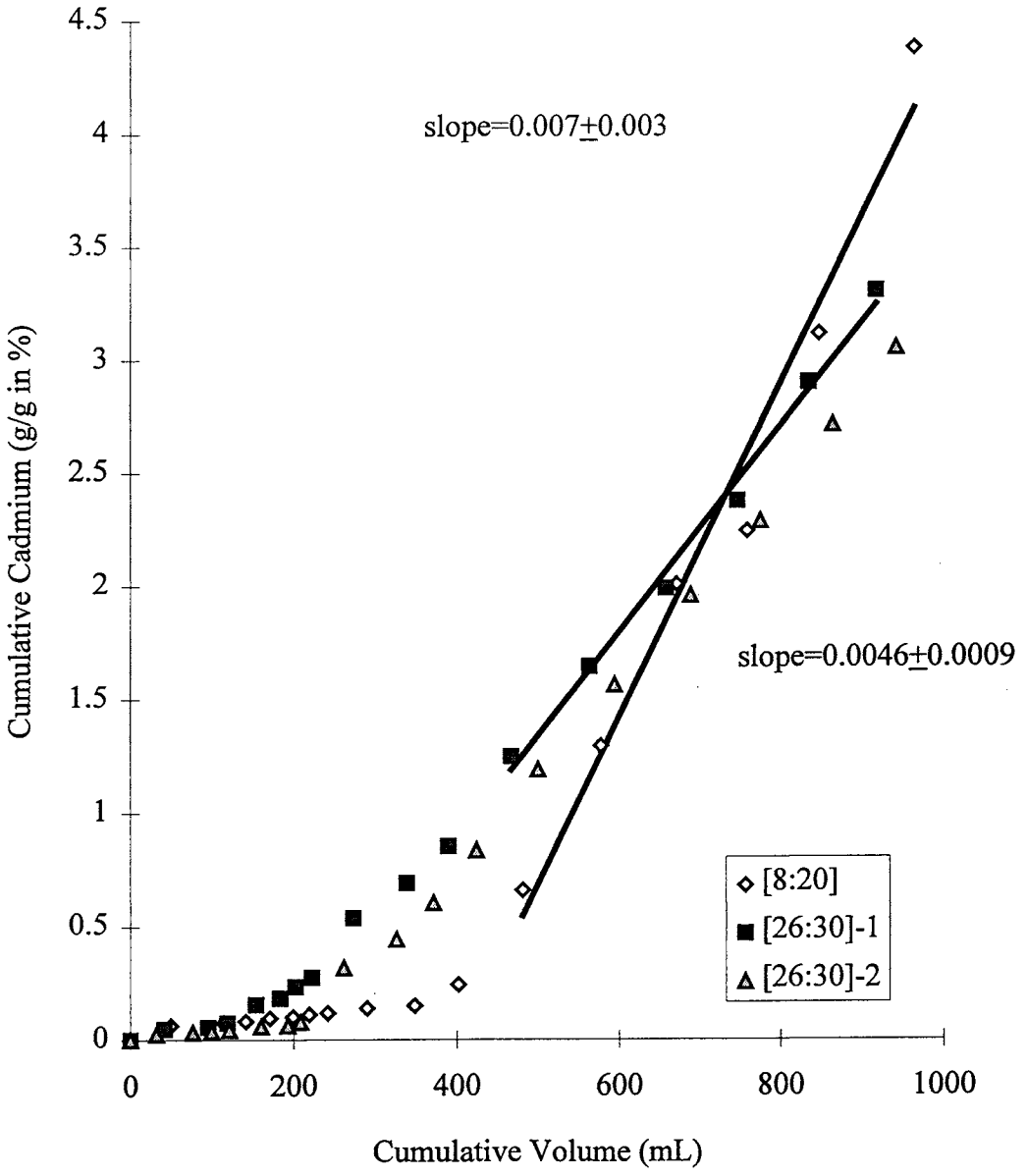

Figure 5.14 Column Leaching on 20-Day Old Samples: Cadmium

Figure 5.15 shows that the observed rates of metal release cannot be explained completely by pH. Mix [26:30] with lower metal release rates has lower extract pH similar to data for 4-day column leaching. This is not the expected result based on metal solubility and pH considerations. These column tests were not repeated because a 20-day test does not fulfill the research objective of a short-term test to predict long-term trends. In keeping with a short-term test objective, column test duration was limited so as to have the same final leachant/solid ratio as that in the TCLP.

5.5.4 Column Results for [8:30] and [26:20]

Column leaching was also conducted on 4-day samples of [8:30] and [26:20]. As shown in Figures 5.16 and 5.17, the metal release rates (slopes) do not follow exactly the same trends identified in the comparison of [8:20] and [26:30] in section 5.5.2. There is one difference and one similarity. For the difference, the metal release rate of [26:20] exceeds that of [8:30], but the long-term TCLP of [26:20] is lower that that of [8:30] according to Figures 5.1 and 5.2. Therefore, for the comparison of [8:30] and [26:20], metal release rates do not predict long-term treatment performance.

The similarity in all the column leaching data lies with the extract pH. The lower extract pH is associated with the mix design exhibiting a lower release rate. As discussed previously for Figure 5.10, the extract pH of the binder-rich [26:30] lies below that of [8:20]. The metal release rate from [26:30] is lower than that from [8:20]. In contrast, Figure 5.18 shows that the extract pH of [8:30] lies below that of the binder rich [26:20], but in the same way mix [8:30] with the lower extract pH has the lower metal leaching rate from the column. As in indicated in Figure 5.12, the unhydrated products of [26:30] are probably causing the increase in pH.

5.6 Column Results of Samples Cured with Heat

Why wait four days before performing the column test? According to Ramachandran (1984), early C-S-H development in normal cements may require 2-3 days. Furthermore, the pore structure of normal cements changes rapidly during the first few days of hydration (Mindess and Young (1981)). Many researchers have observed that a waste frequently retards cement hydration, so four days of natural curing is reasonable. In an effort to develop a quicker test, heat and chemical accelerators were also used.

Accelerated curing with heat was investigated to see if trends established in section 5.4.2 might be amplified further. Furthermore, heat might permit a test that can be completed in less than 4 days. Two sets of heat-cured samples were prepared. The

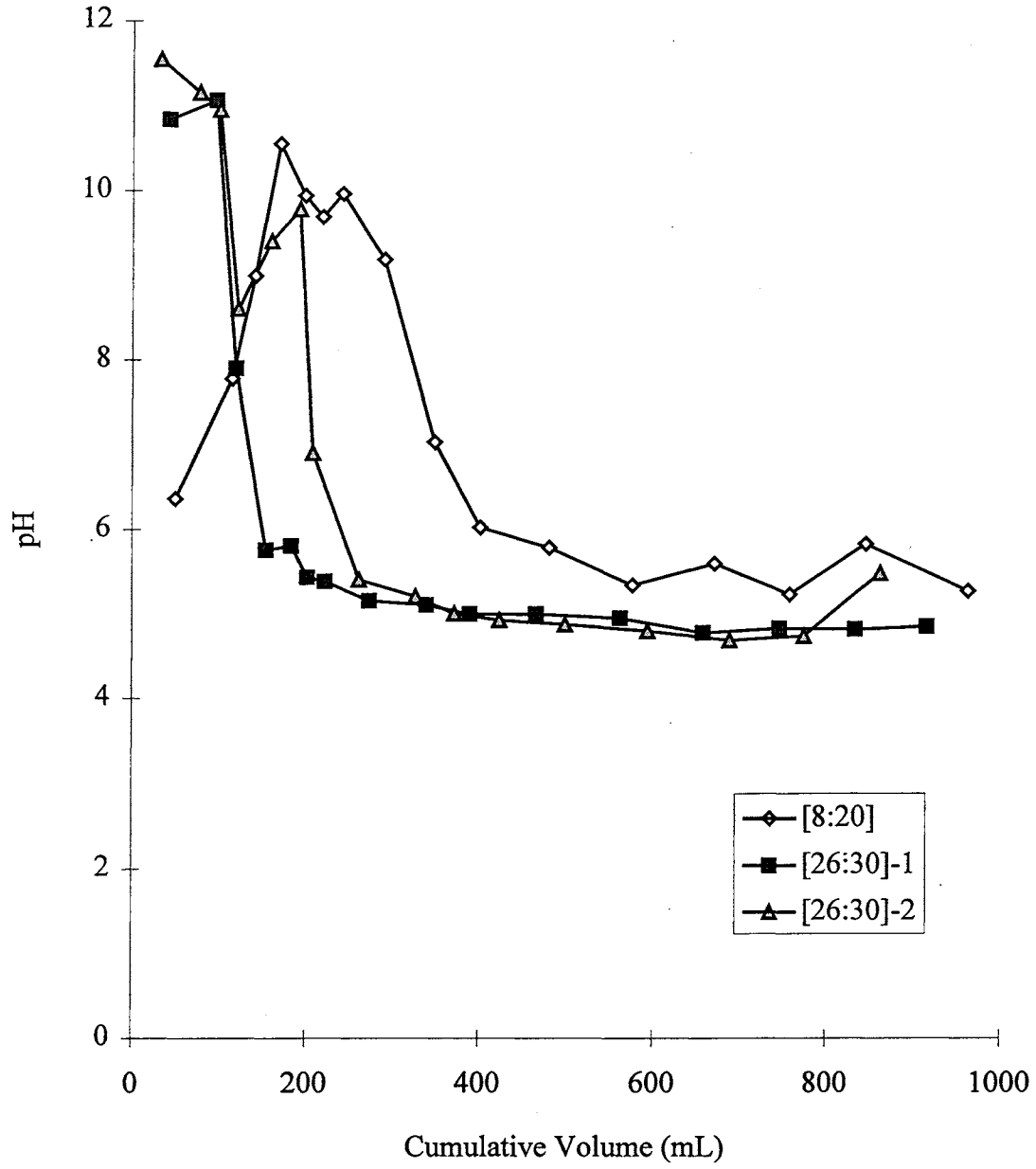

Figure 5.15 pH of Column Extracts from 20-Day Old Samples

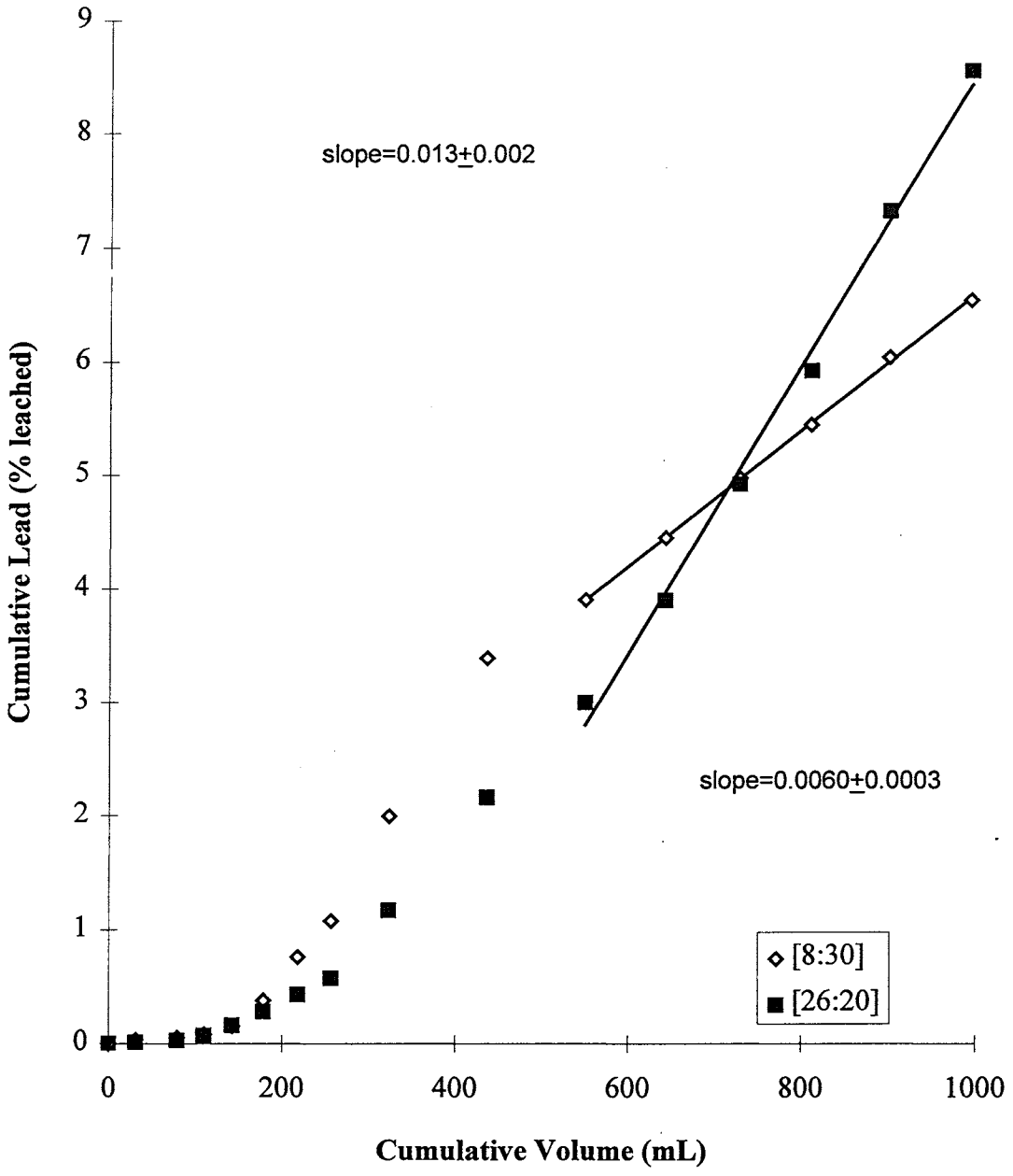

Figure 5.16 Column Leaching of 4-Day Old Samples: Lead

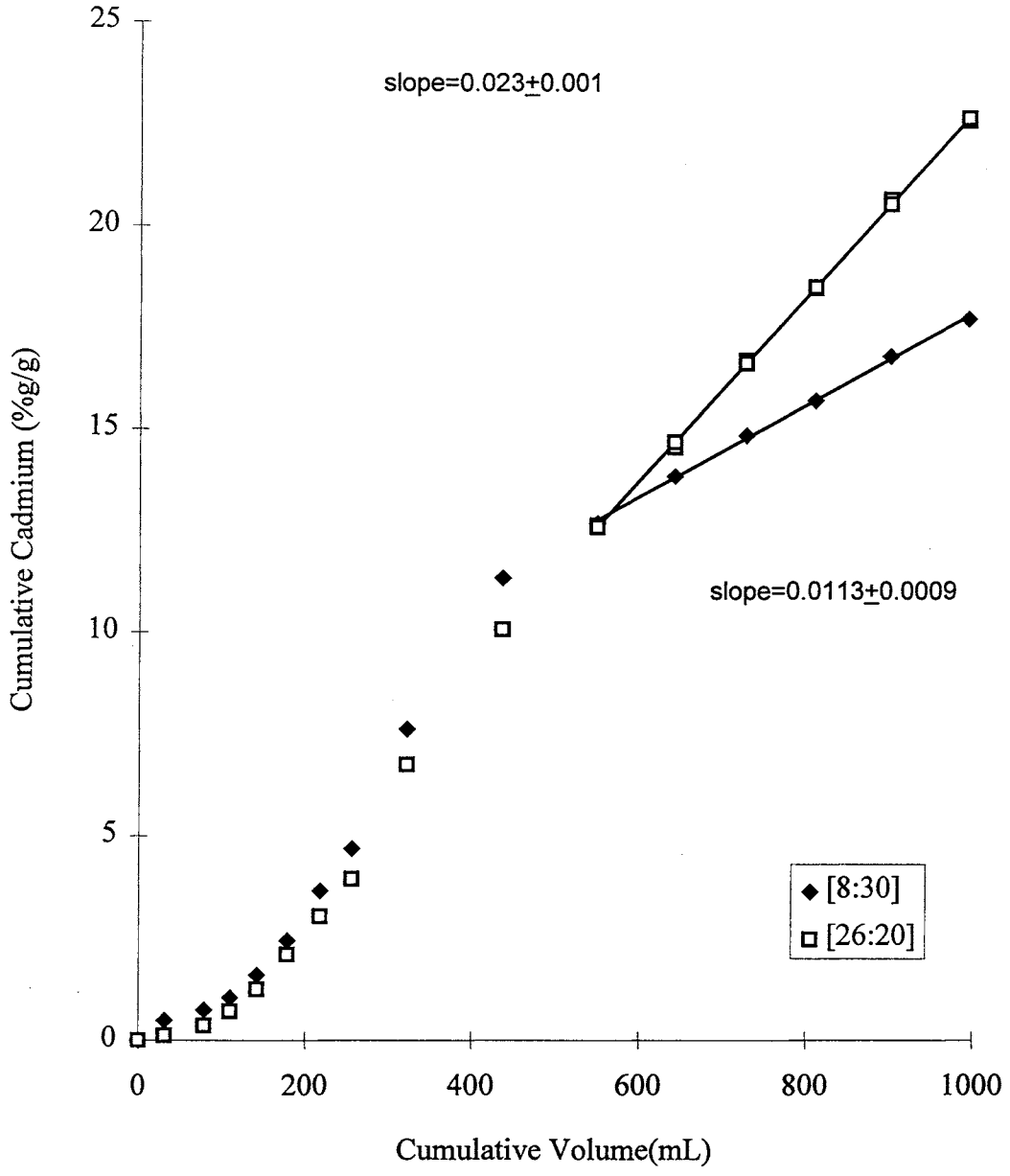

Figure 5.17 Column Leaching on 4-Day Old Samples: Cadmium

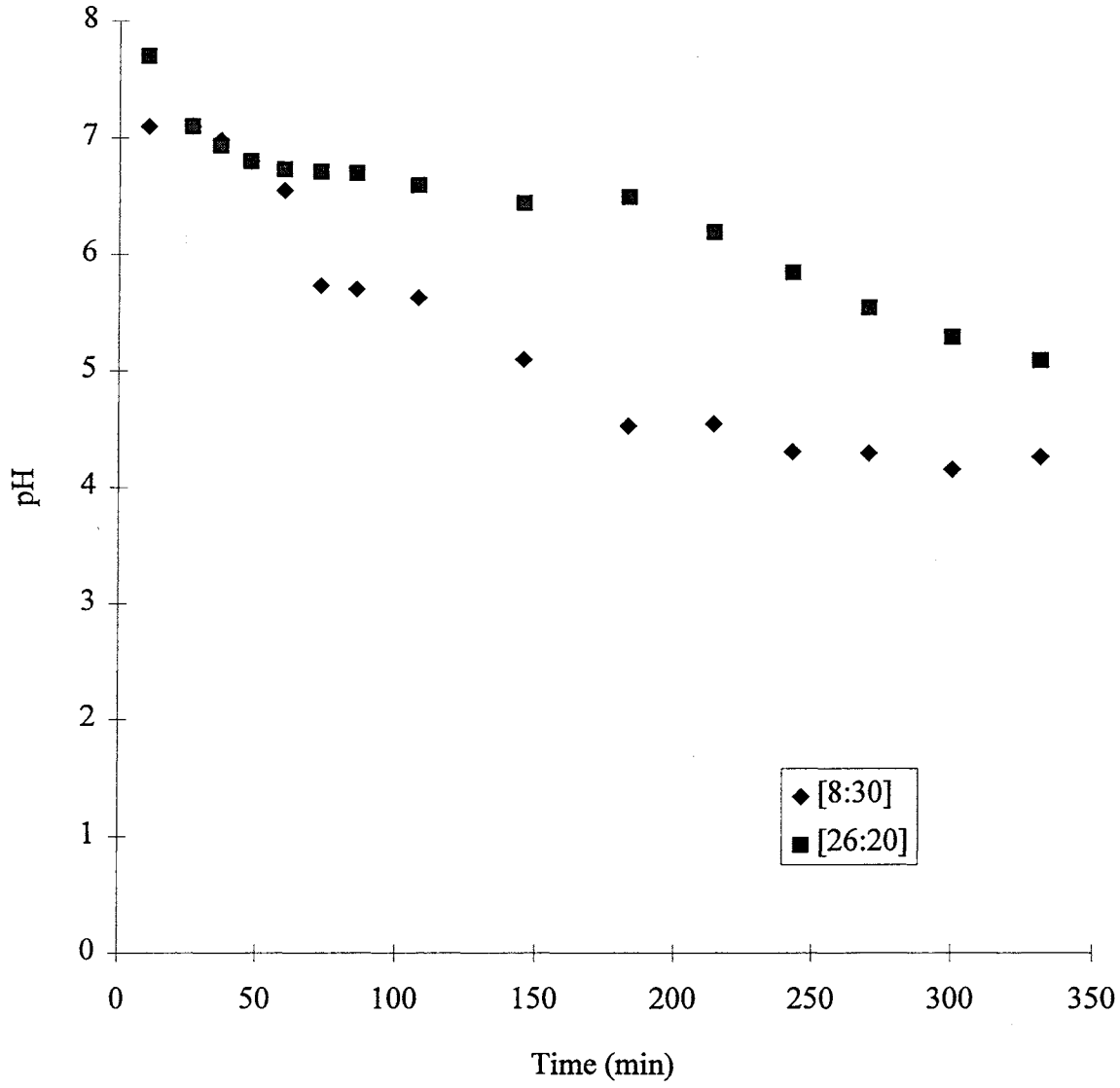

Figure 5.18 pH of Column Extracts from 4-Day Old Samples

first set underwent 40° C heat at 100% relative humidity for 4 days. Figure 5.19 and 5.20 present results for lead and cadmium respectively. The rate of lead release is essentially the same for mixes [8:20] and [26:30]. The absolute amounts of lead leached are opposite of expectations: lead from [26:30] consistently leaches more than from [8:20]. For cadmium data shown in Figure 5.20, there is a slope difference between [8:20] and [26:30] near the end of the run. Evidently, 4 days of 40°C heat is detrimental to the cement matrix especially with respect to lead.

The second set of samples underwent 3-hours of 40° C heat at 100% relative humidity followed by 10 hours of natural cure. Results are shown in Figures 5.21 through 5.23. Lead concentrations diverge toward the end of the run, while cadmium concentrations are significantly different for the two mixes. The pH data do not explain the difference in metal release rates between [8:20] and [26:30], because the lesser pH values associated with [26:30] imply higher metal release rates based on pH and metal solubility. However, smaller metal leaching rates from the column do predict long-term treatment effectiveness.

According to Chapter 2, excessive amounts and durations of heat have significant physiochemical and morphological effects on cement. The long-term cement reactions important in stabilization are not very sensitive to acceleration by temperature due to their low activation energies. Higher temperatures and durations sufficient to accelerate these reactions cause morphological changes and prevent accurate prediction of long-term stabilization effectiveness. The use of lower temperatures does not provide enough acceleration to be useful for prediction.

5.7 Column Results of Samples Cured with Accelerators

Another method of accelerated curing is the use of chemical accelerators. Chemical accelerators A and B were selected because of their commercial availability and different chemical composition. Accelerator A is a calcium chloride solution, and accelerator B is a solution of calcium nitrite. The dosages used fall in the manufacturer's recommended range for practice. Mix designs [8:20] and [26:30] with chemical accelerators were cured 4 days naturally.

Column tests were performed for all the mix designs indicated in Table 4.3. The results from the column tests follow the same trends identified above. Leaching rates do correlate with trends in long-term treatment effectiveness. Figures 5.24 and 5.25 show typical results for samples cured with 1% and 2% additions of accelerator B.

5.8 Silica Chain Length Analysis

Using the laboratory procedure outlined in Chapter 4, experiments were carried out to analyze the silica chain length in several samples. The time dependence of the absorbance was modeled by noting that only monomeric silica can form the absorbing blue molybdate complex. The conditions of the experiment are such that hydrolysis of

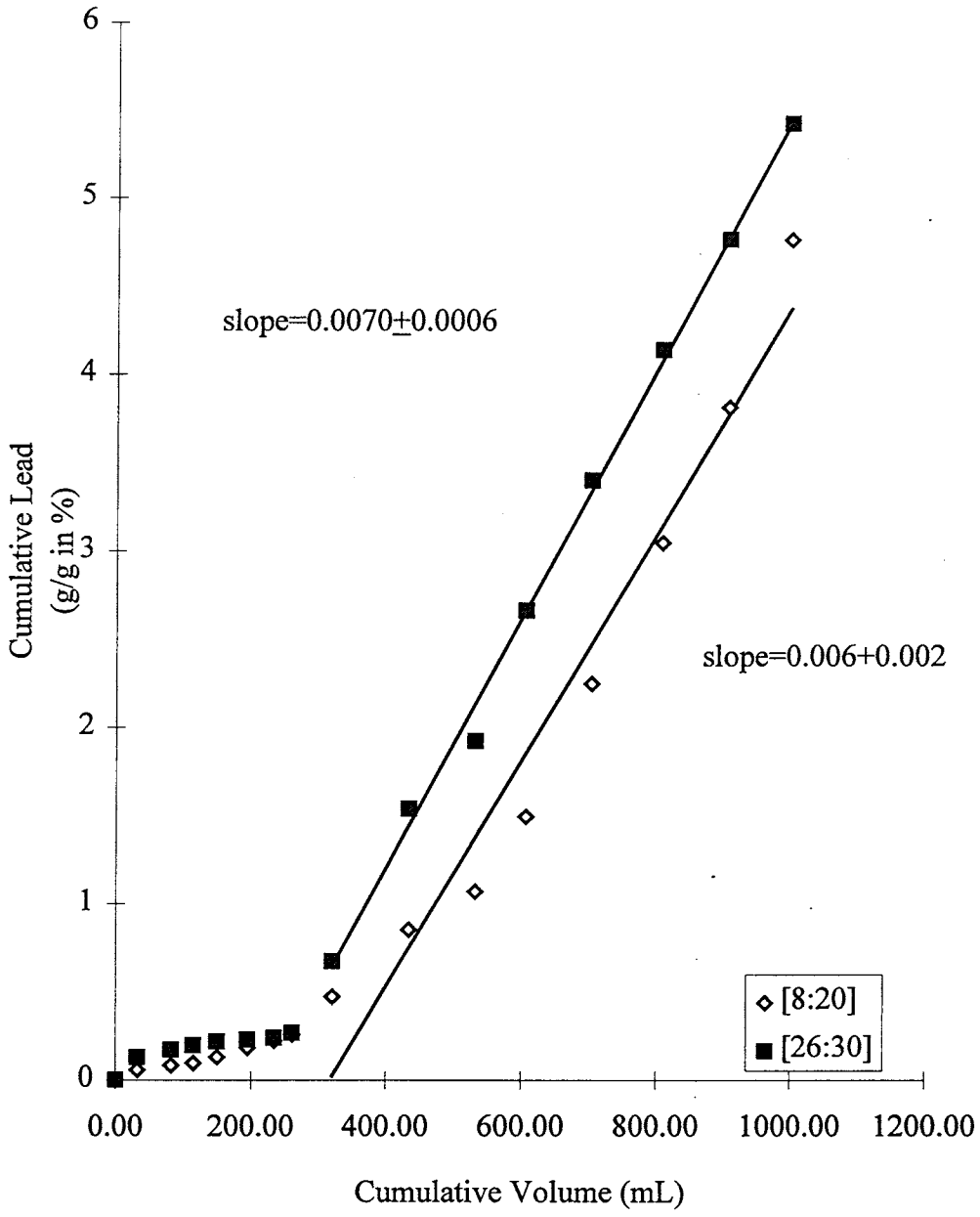

Figure 5.19 Column Leaching of 4-Day Heat-Cured Samples: Lead

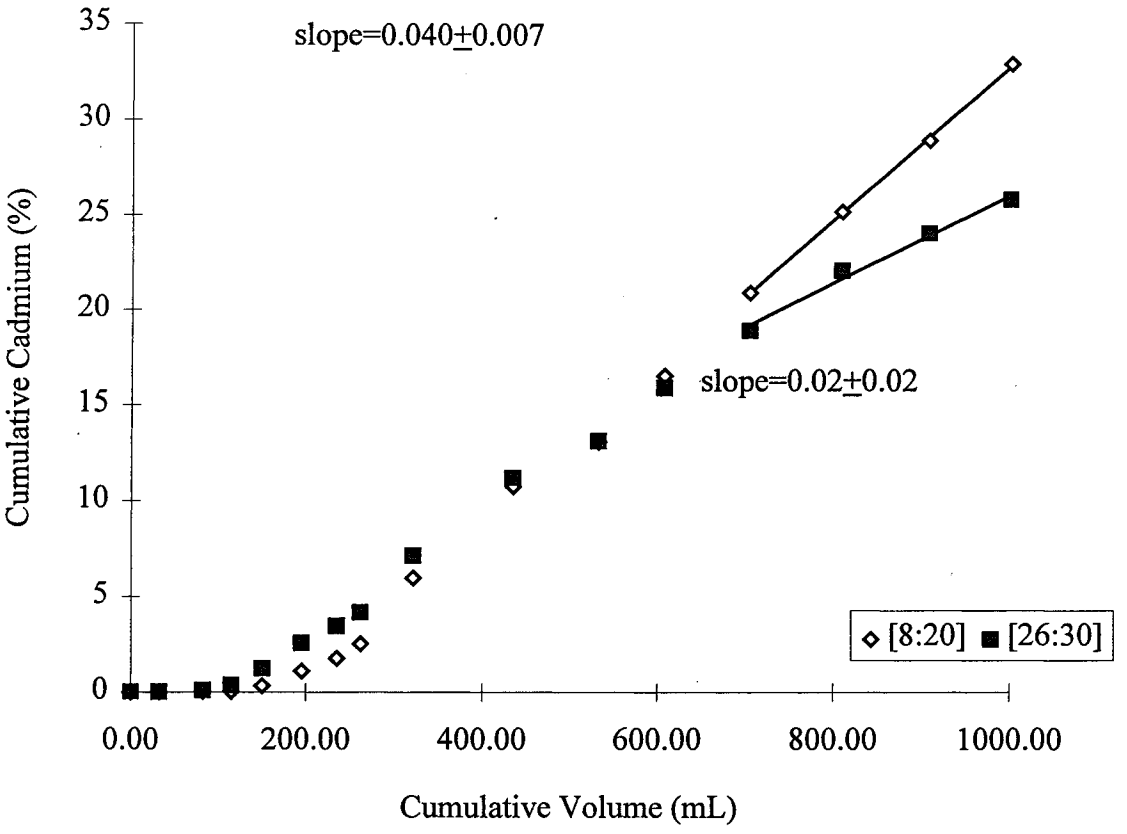

Figure 5.20 Column Leaching of 4-Day Heat-Cured Samples: Cadmium

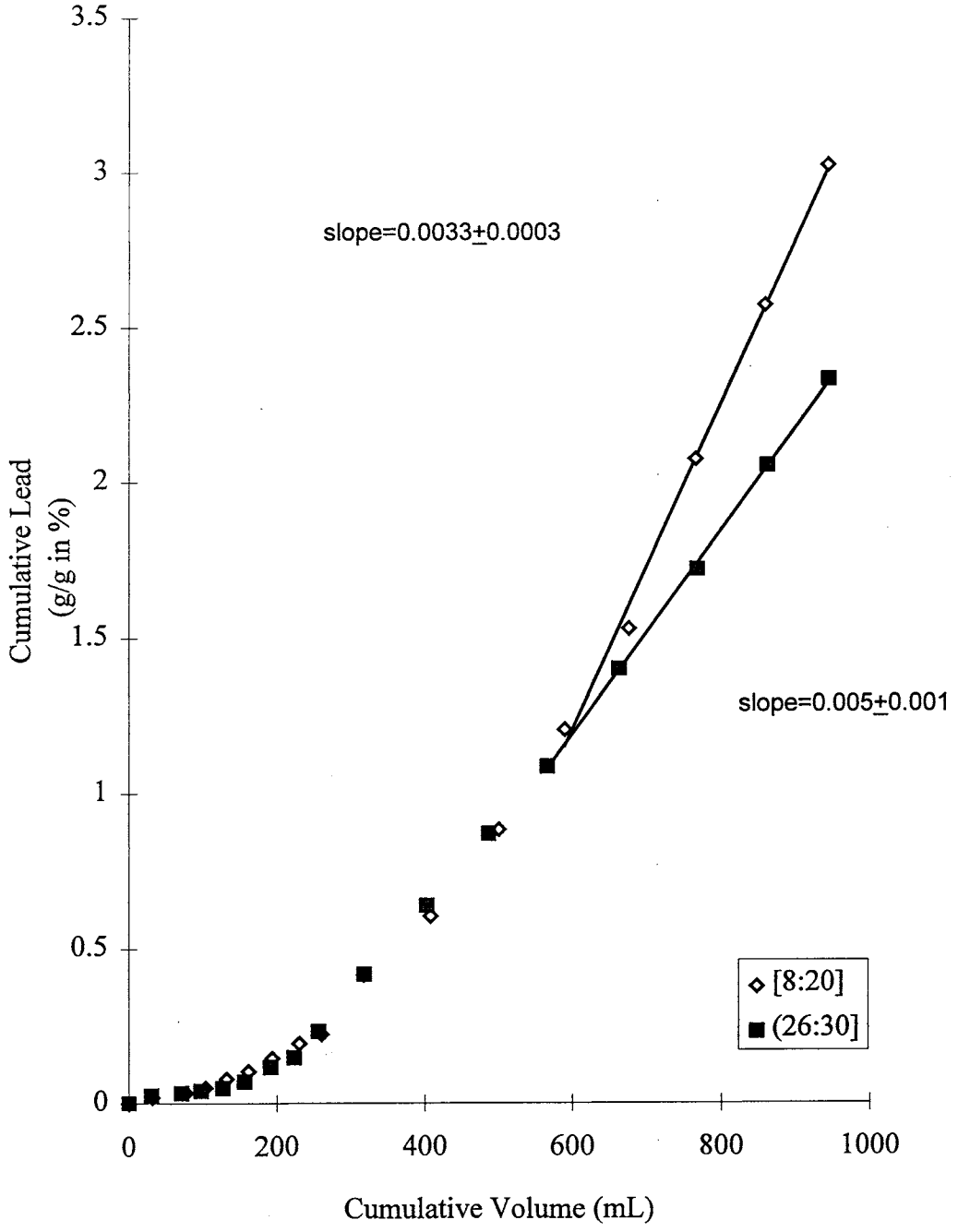

Figure 5.21 Column Leaching of 3-Hour Heat-Cured Samples: Lead

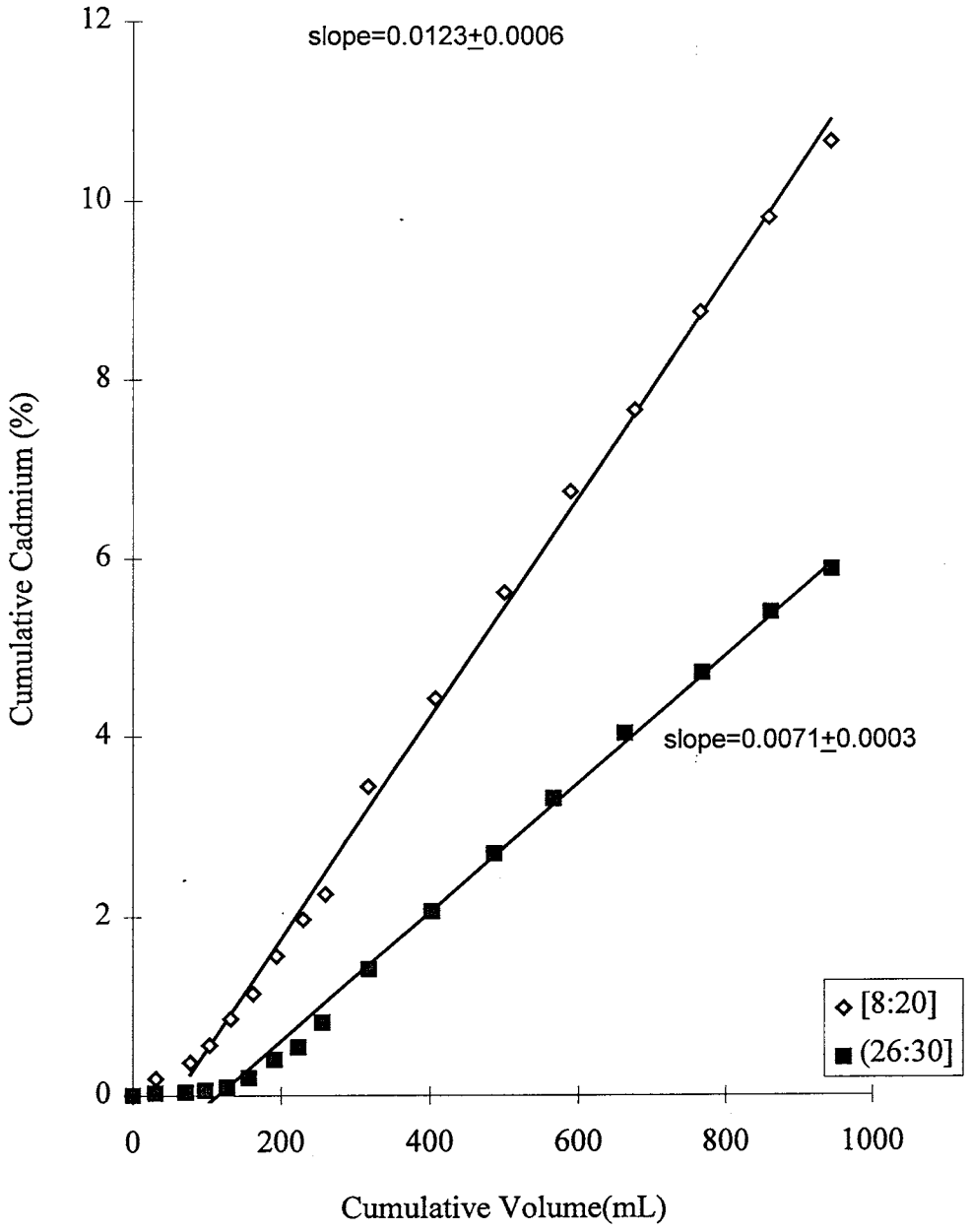

Figure 5.22 Column Leaching of 3-Hour Heat-Cured Samples: Cadmium

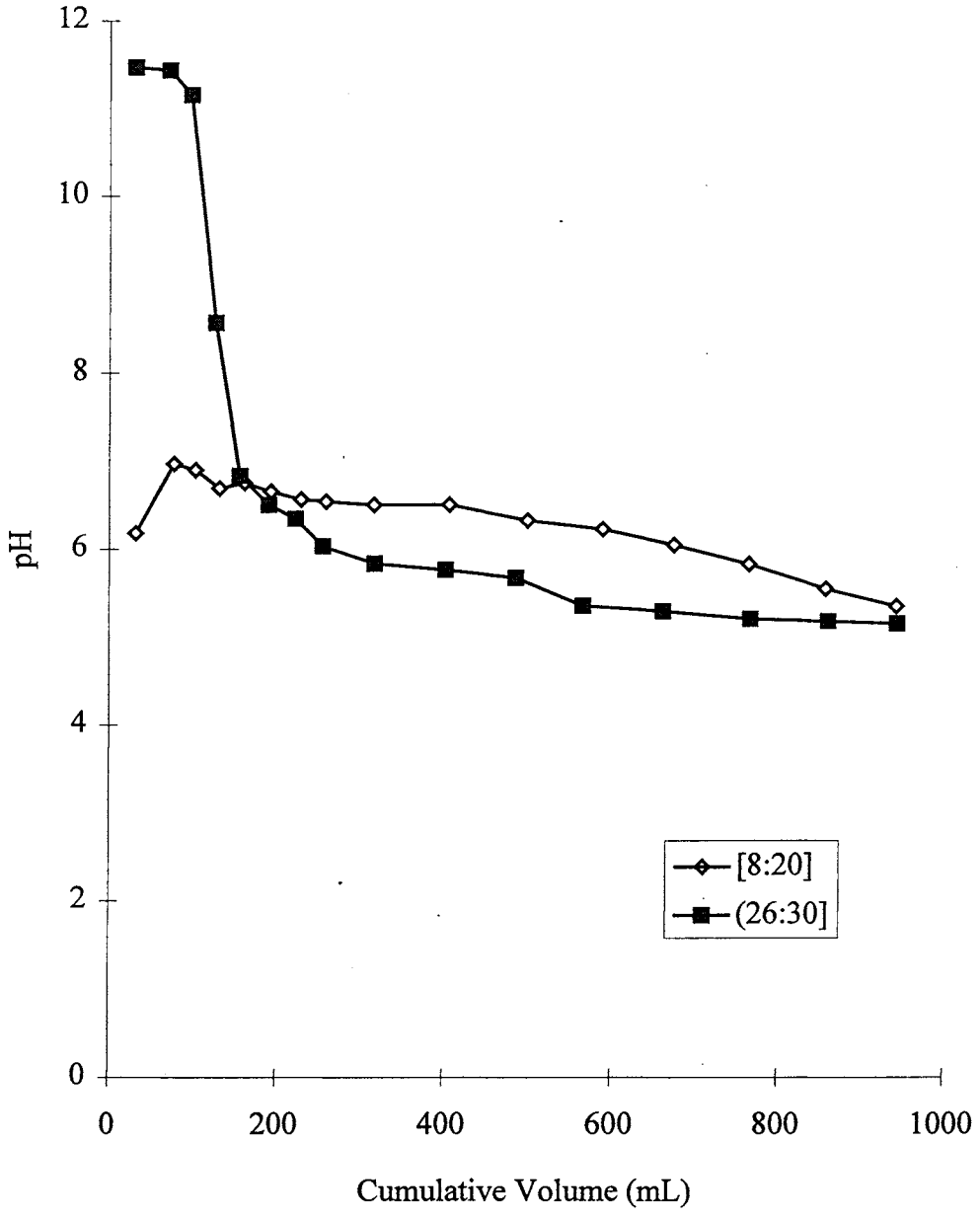

Figure 5.23 pH of Column Extracts for 3-Hour Heat-Cured Samples

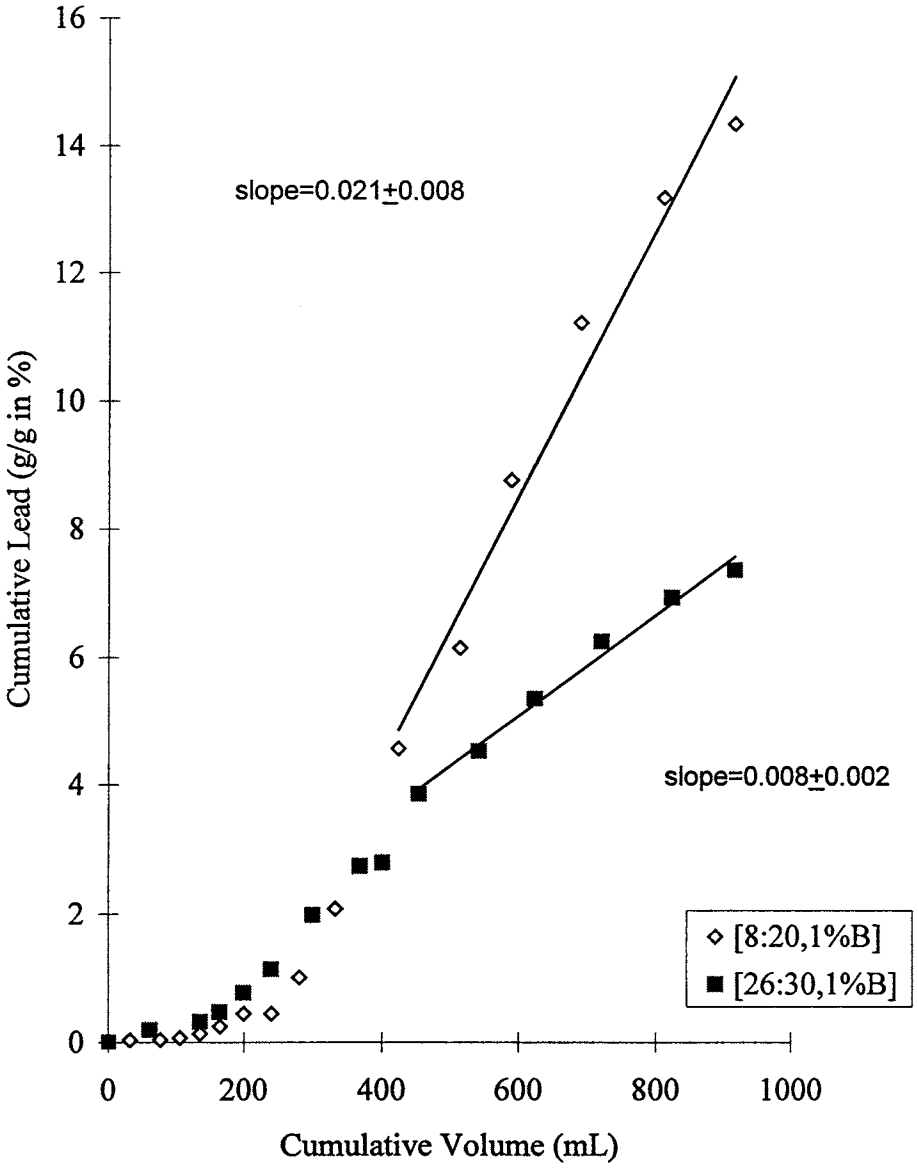

Figure 5.24 Column Leaching of 1% Accelerator B Samples: Lead

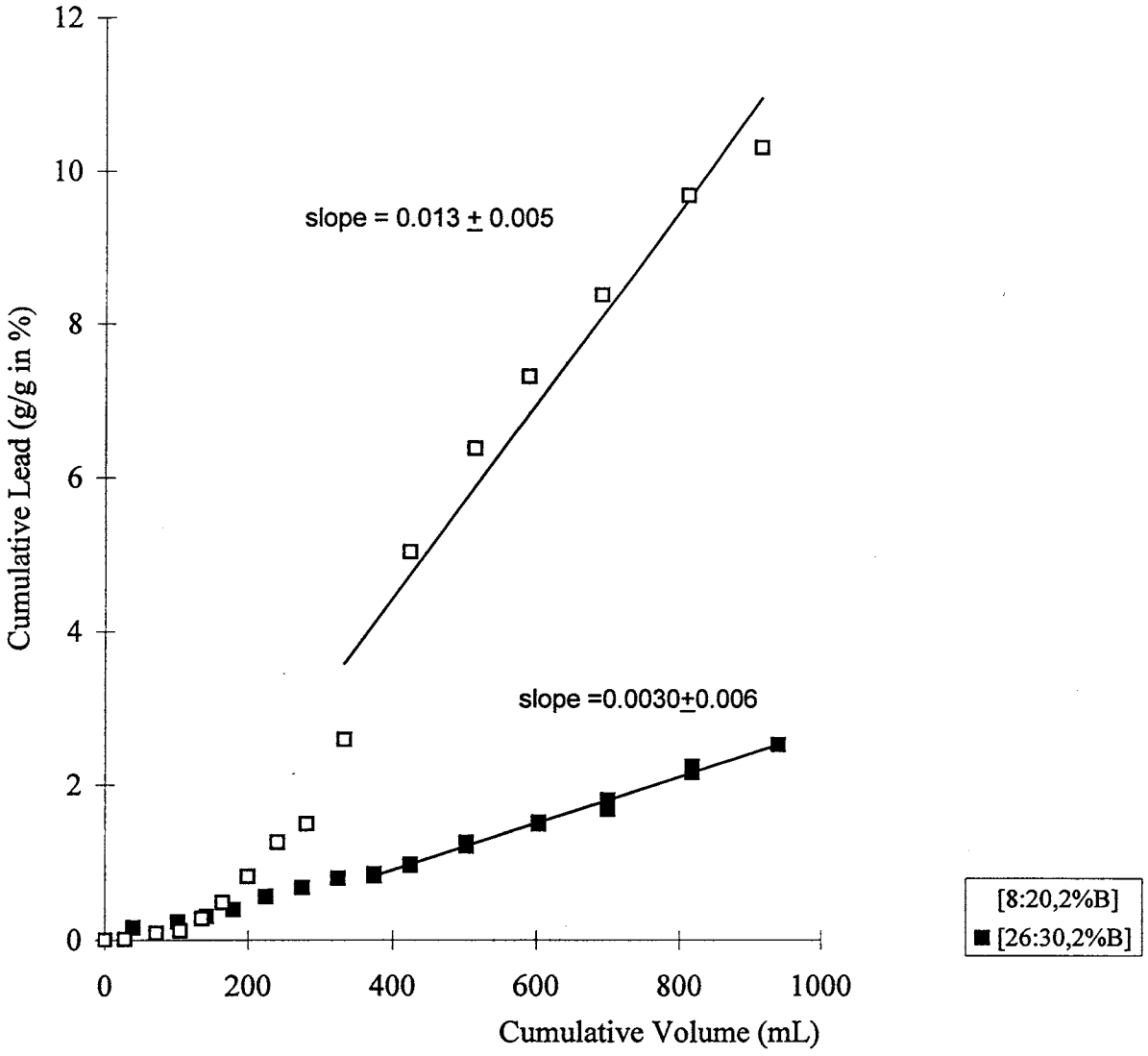

Figure 5.25 Column Leaching of 2% Accelerator B Samples: Lead

larger silica aggregates takes place. We take the population of silica to be adequately represented by monomeric, dimeric and polymeric species. The rate of hydrolysis is taken to depend on the aggregate size, with smaller aggregates hydrolyzing more rapidly than larger ones. The chemical mechanism is modeled as:

monomer + reagent → molybdate blue	rate = b_1	(very fast)
dimer → monomer	rate = b_2	Delay time = t_2
polymer → monomer + polymer.$_1$	rate = b_3	Delay time = t_3

This mechanism leads to the mathematical model for the total absorbance of the solution:

$$A_{total} = a_{monomer} + a_{dimer} X + a_{polymer} Y \quad (1)$$

where a_i = absorbance due to species;
$X = 1 - \exp[b_2(t - t_2)]$;
$Y = 1 - \exp[b_3(t - t_3)]$.

The a_i values are determined by fitting the time-dependent absorbance, A_{total}, of the silica extract from a sample to equation (1). Values for the b_i and t_i parameters are taken from Parrott and Taylor (1979) and are found in Table 5.4.

Table 5.4 Silica Chain Hydrolysis Parameters

Silica Chain Length	b_i	t_i
Dimer	0.0152	5.5
Polymer	0.00189	12

Multilinear least-squares techniques were used to estimate the a_i values. Because the actual amount of silica polymer in a physical sample could not be controlled during the sampling process, the individual a_i values are expressed as a percent of the total.

When analyzing stabilized waste samples, some experiments produced absorbance vs. time graphs whose shape did not conform to that expected theoretically. The cause for this behavior is not known at this time, although it is expected that the waste contains components which would interfere with the stability of the molybdosilicate blue complex.

The absorbance versus time graphs for a cement paste mix with 2 grams cement mixed with 1 gram water taken at several cure times are shown in Figure 5.26. The symbols represent laboratory data points and the lines represent the data fitted to Equation 1.

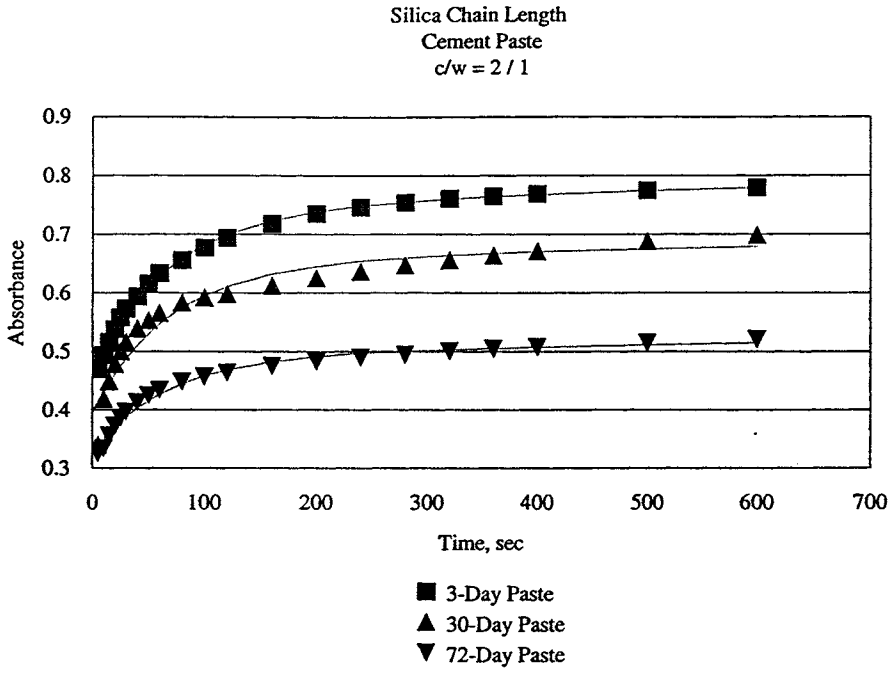

Figure 5.26. Cement Paste Silica Chain Length Data

The values of a_i parameters determined for the cement paste are shown in Table 5.5 along with one standard deviation statistical uncertainties. The percent ratio of polymer/monomer appears to decrease linearly with cure age, as does the percent ratio, dimer/monomer.

Raw absorbance versus time are plotted as points in Figure 5.25 for stabilized waste of composition [8:20]. The lines represent equation 1 fitted to the data. The curve for [8:20:2D] is an example of a curve shape which does not agree with theory. Representative data are summarized in Table 5.6. Chemical accelerator B produces a larger change in dimer/monomer ratio for the improving mix design, [26: 30],

Table 5.5: Silica Chain Length Results for Cement Paste

Cure Age	% Monomer	% Dimer	% Polymer	Poly/Mono	Di/Mono
3 Days	60.3 ± 0.7	31.1± 0.9	9.6 ± 1.5	0.16 ± 0.03	0.52 ± 0.02
30 Days	59.6 ± 3.6	31.9 ± 4.4	8.5 ± 7.5	0.14 ± 0.14	0.54 ± 0.11
72 Days	64.4 ± 1.5	27.8 ± 1.9	7.8 ± 3.2	0.12 ± 0.05	0.43 ± 0.04

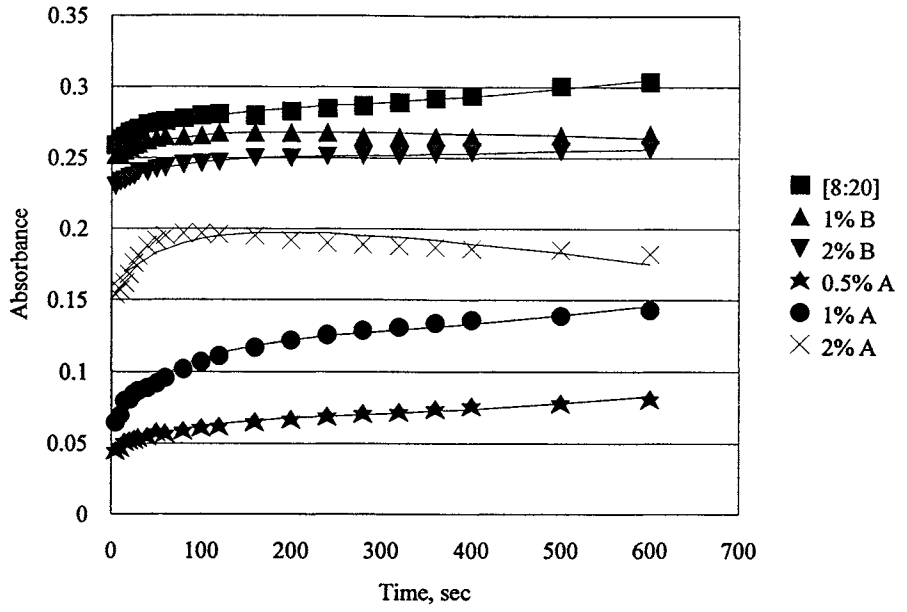

Figure 5.27 Stabilized Waste Silica Chain Length Data, 2-Day Cure

than for the deceptive mix design, [8:20]. On the other hand, the addition of accelerator A seems to produce a significant effect on the [8:20] mix, and a very small effect on the [26:30] mix. The results are not very conclusive or precise for this experiment because the procedure uses a very small sample amount which is of the same physical size as the larger particles in the waste. As a result, sampling errors should be quite large considering the non-homogeneity of the waste. The use of larger samples is not practical in this experimental procedure. In order to be able to draw definitive conclusions from this technique, we also need results for more samples at a larger variety of cure times and conditions.

5.9 Summary

As the cement-based stabilization matrix cures, physiochemical and morphological changes occur rapidly at first and continue more slowly for years. These changes affect the treatment performance of the stabilization as defined by the TCLP. A profile of treatment performance with sample age must follow one of four prospects: 1) a good stabilization design yields satisfactory TCLP results for all time; 2) an unacceptable design yields unsatisfactory TCLP results at any time; 3) deceptive designs yield satisfactory TCLP results with early curing but would exceed TCLP standards at

Table 5.6 Silica Chain Length Results for Stabilized Waste, 2 Day Cure Times

Mix	% Monomer	% Dimer	% Polymer	Poly/Mono	Di/Mono
[8:20]	97.8 ± 0.7	6.5 ± 6.3	-4.3 ± 4.1	-0.04 ± 0.04	0.07 ± .06
[8:20:1B]	93.0 ± 0.7	5.9 ± 0.6	1.1 ± 0.4	0.012 ± 0.04	0.063 ± 0.007
[8:20:2B]	94.3 ± 0.3	6.7 ± 0.3	-1.0 ± 0.2	-0.11 ± 0.02	0.071 ± 0.003
[8:20:0.5A]	74.0 ± 2.0	27.4 ± 1.7	-1.4 ± 1.1	-0.019 ± 0.002	0.37 ± 0.03
[26:30]	68.4 ± 2.7	26.3 ±2.5	5.4 ± 1.6	0.079 ± 0.027	0.38 ± 0.13
[26:30:1B]	85.1 ± 0.7	16.6 ± 0.6	-1.2 ± 0.4	-0.014 ± 0.005	0.20 ± 0.009
[26:30:0.5A]	71.2 ± 3.8	21.3 ± 3.4	7.4 ± 2.2	0.10 ± 0.04	0.30 ± 0.06
[26:30:1A]	69.2 ± 3.1	29.1 ± 2.7	1.7 ± 1.7	0.024 ± 0.025	0.42 ± 0.14

later sample ages; 4) improving designs exceed TCLP standards when immature but satisfy standards when allowed to cure longer. A procedure is needed to identify which prospect a given stabilization design will follow. For practical reasons, the identification procedure should be a short-term test.

Various research efforts have been made in an attempt to fulfill this need. Severe leaching tests have been proposed. The severity of the leaching could be attributed to either leachant, duration of the test, or both. If the duration of the test is lengthy, it defeats the practical need of a landfill operator for a quick test that identifies the long-term treatment effectiveness of a design. If the leachant is exceedingly severe, the stabilized matrix will deteriorate, but the long-term treatment effectiveness of the stabilization has not been assessed. This project focused on using other curing methods while using leaching test comparable in severity to the TCLP. Heat and chemical accelerators were used. Tests included TCLP, column leaching, FTIR, calorimetry, silicate polymerization chain length.

Stabilization designs for K061 waste exist that exemplify each of the prospects above. The research team has characterized a range of mix designs and their long-term treatment effectiveness. The range of mix designs selected for research falls between the extremes of stabilizations that are effectiveness for all time (prospect 1) and totally inadequate S/S that exceeds TCLP standards at any age (prospect 2). The selected range of mix designs exemplify deceptive and improving mix designs, prospects 3 and 4 respectively. Figure 5-28 provides a description of treatment effectiveness and physical character.

Mix designs that fail at any cure age have lower ratios of binder to waste and of water to binder. Mix designs that satisfy TCLP for all cure ages have a binder to waste ratio of about 0.4. In addition to the issues of volume inefficiency and dilution versus treatment, binder to waste ratios in the range of 0.4 are not as economical.

The binder/waste parameter is most critical for a mix design. For long-term stabilization of lead, the amount of water is relatively insensitive, but for cadmium stabilization, the amount of water is a sensitive parameter. This difference in the

behavior of lead and cadmium reflects the different stabilization mechanisms at work for these metals.

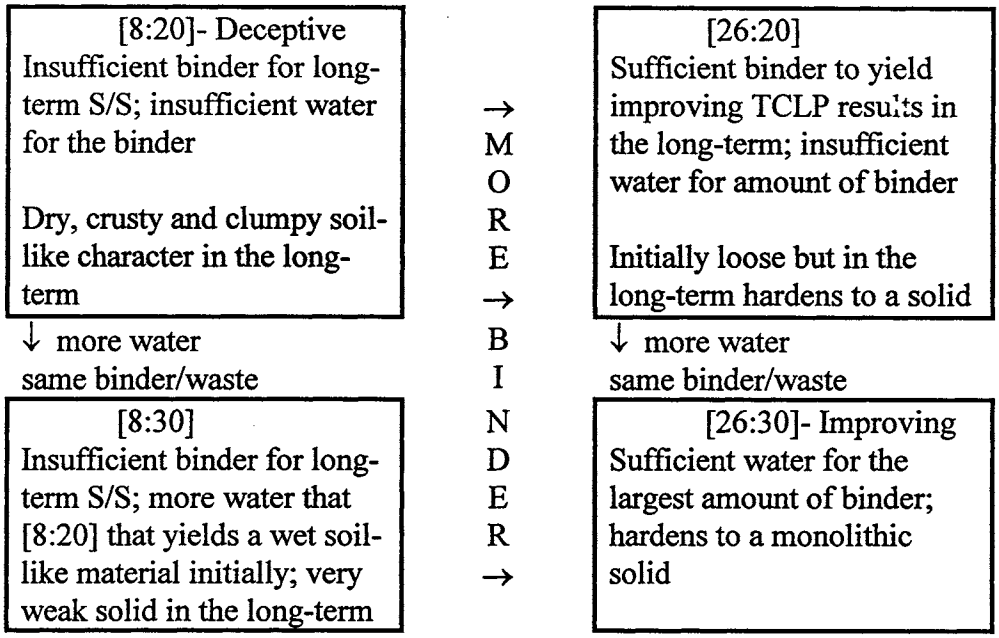

Figure 5.28 Mix Description and Physical Parameters

The TCLP extract pH may affect metal leaching after short-term as well as long-term curing, especially for lead. Mix designs with sufficient binder like [26:20] and [26:30] had extract pH values that remained in the 11-12 range for up to 265 days of curing. With about a year of curing, extract pH dropped to 7.5-8.0 range indicating a decrease in the CH phase and increasing growth of C-S-H. The sufficiency of binder indicates that C-S-H growth was adequate to stabilize the waste. Compared to pure cement hydration, the development of C-S-H microstructure is retarded in this cement-waste mix.

On the other hand, mix designs with insufficient binder like [8:20] and [8:30] yielded extract pH values that dropped to 7-7.5 in about 60 to 120 days. Insufficient CH yields less acid neutralization capacity, and long-term microstructure is also insufficient to provide long-term effective stabilization.

Accelerated curing of S/S samples were performed for five mix designs with emphasis on [8:20] and [26:30]. Accelerated curing at temperatures ranging from 40°C to 120°C with 100% relative humidity were conducted for various periods of time. Comparisons of TCLP of short-term heat-accelerated samples with naturally cured samples over the long-term did not yield consistent results. Heat curing by itself will not provide a cure method that yields results predicting future treatment performance.

A different leaching method was used for short-term samples to see if results indicated long-term treatment effectiveness. The rate of metal release during column leaching of young samples was hypothesized to indicate the prospective pattern of TCLP results on aging samples of corresponding mix design. A summary of metal leaching rates for lead and cadmium are supplied by Figure 5.29. The arrows point in the direction of improving long-term treatment effectiveness as measured by the TCLP on aged samples. The first and second numbers in the corner boxes indicate the lead and cadmium leaching rates from 4-day old samples in the column. In many of the cases, the comparison of metal release rates for two mix designs provides a qualitative indicator of which stabilization will perform better at later ages. One notable exception is the comparison of [8:30] and [26:20]. If a quantifiable correlation is possible between short-term results and long-term-treatment effectiveness, much more work with sophisticated instrumentation will be required.

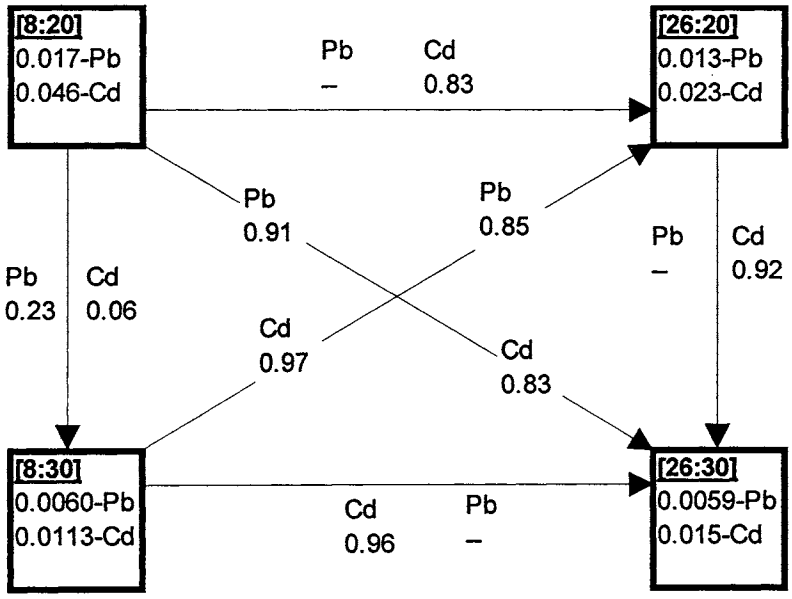

Figure 5.29 Summary of Metal Leaching Rates and Long-Term Treatment Effectiveness

REFERENCES

Adaska, Wayne, S., Stewart W. Tresouthick, and Presbury B. West, 1991. Solidification and Stabilization of Wastes Using Portland Cement. Portland Cement Association, Skokie, IL.

Andres, A. and J.A. Irabien. 1994. "Solidification/Stabilization Process for Steel Foundry Dust Using Cement Based Binders: Influence of Processing Variables," Waste Management and Research, 12(5):405–415.

Andrade, C. 1993. "Calculation of Chloride Diffusion Coefficients in Concrete from Ionic Migration Measrements," Cement and Concrete Research, 23: 724–742.

Atkins, M., F.P. Glasser, and L.P. Moroni, 1991. "The Long-Term Propoerties of Cement and Concretes," Mat. Res. Soc. Symp. Proc., Vol. 212.

Aye, Aye Kyi and Bill Batchelor, 1994. "An Electrical Conductivity Method for Measuring the Effects of Additives on Effective Diffusivities in Portland Cement Pastes," Cement and Concrete Research, 24(4):752-764.

Barnes, J.R., A.D.H. Clague, N.J. Clayden, C.M. Dobson, C.J. Hayes, G.W. Groves, S.A. Rodger, 1985. "Hydration of Portland Cement Followed by ^{29}Si Solid State NMR Spectroscopy," Journal of Materials Science Letters, pp. 1293-1295.

Batchelor, Bill. 1990. "Leach Models: Theory and Application," Journal of Hazardous Materials, 24: 255-266.

Bayasi, Z., R. Fuessle, M. Taylor. 1992. "Improvements in the Solidification of Hazardous Inorganic Wastes by Silica Fume Concrete." Final Report submitted to the Hazardous Waste and Research Information Center, Champaign, Il.

Bishop, P.L. 1988. "Leaching of Inorganic Hazardous Constituents from Stabilized/Solidified Hazardous Wastes." Hazardous Wastes and Hazardous Materials, 5(2):129-143.

Buenfeld, N.R. and J.B. Newman. 1987. "Examination of Three Methods for Studying Ion Diffusion in Cement Pastes, Mortars and Concrete," Material and Structures/Materiaux et Construction, 20(115):3-10.

Butler, L.G., F.K. Cartledge, H.C. Eaton, and M.E. Tittlebaum, 1993. "Microscopic and NMR Spectroscopic Characterization of Cement-Solidified Hazardous Wastes," in Spence, Roger D. (ed.), Chemistry and Microstructure of Solidified Waste Forms, Lewis Publishers, pp 151-167.

Candlot, E. 1886. "Cement with Quick Setting Time," Mon. Ind. Belge, 13:182.

Cao, Y. and R.J. Detwiler, 1995. "Backscattered Electron Imaging of Cement Pastes Cured at Elevated Temperatures," Cem. and Concr. Res., 25(3):627-638.

Cartledge, F.K. and M.E. Tittlebaum, 1993. "Solidification of Salts of As, Cr and Pb Using Cement and Various Additives," Gulf Coast Hazardous Substances Research Center, Annual Report of Project 101LSU4015.

Chatterji, S. 1994. "Transportation of Ions through Cement Based Materials. Part 1. Fundamental Equations and Basic Measurement Techniques," Cement and Concrete Research, 24(5):907-912.

Chatterji, S. 1994. "Transportation of Ions through Cement Based Materials. Part 2. Adaptation of the Fundamental Equations and Relevant Comments.," Cement and Concrete Research, 24(6):1010-1014.

Clayden, N.J., C.M. Dobson, G.W. Groves, S.A.Rodger, 1984. "Solid State NMR Studies of Cement Hydration," British Ceramic Proceedings, 35: 55-63.

Clifton, J.R. and L.I. Knab, "Service Life of Concrete," NUREG/CR-5466, NISTIR 89-4086, 1980.

Code of Federal Regulations. 1987. Vol. 40, Part 268, App. I, July, pp. 692-707.

Collepardi, M., and Marchese, B., 1972. "Morphology and Surface Properties of Hydrated Tricalcium Silicate Pastes," Cem. Concr. Res. 2:57-65.

Collepardi, M., L. Massida, and G. Usai. 1972. "Sull'idratazione Del β-Silicatao Bi-Calcico-Nota I. Idratazione in Pasta." Annal. di Chimica 62:321-328.

Collepardi, M., L. Massida, and E.G. Merlo. 1972. "Sull'idratazione Del β-Silicatao Bi-Calcico-Nota II-Idratazione in Sospensione." Anal. di Chimica 62:329-336.

Collepardi, M., A. Marcialis, and E.L. Massida. 1972. "Sull'idratazione Del β-Silicatao Bi-Calcico-Nota III-Idratazione in Mulino a Sfere." Annal. Di Chimica 62:337-344.

Cong, Xiandong and R. James Kirkpatrick, 1995. "Effects of the Termpature and Relative Humidity on the Structure of C-S-H Gel," Cement and Concrete Research, 25(6):1237-1245.

Conner, J.C., 1990. Chemical Fixation & Solidification of Hazardous Wastes, New York: Van Nostrand Reinhold, Inc.

Cote, P. 1986. Contaminant Leaching from Cement-Based Waste Forms Under Acidic Conditions. PhD Thesis, McMaster University, Hamilton, Ont., Canada.

Cote, Pierre L., Thomas W. Constable, and Alan Moreira. 1987. "An Evaluation of Cement-Based Waste Forms Using the Results of Approximately Two Years of Dynamic Leaching," Nuclear and Chemical Waste Management. 7: 129-139.

Diamond, S., 1976. "Cement paste microstructure - An overview at several levels in hydraulic cement pastes - Their structure and properties," Conference, University of Sheffield, April, pp. 334.

Fuhrmann, M., J.H. Heiser, R.F. Pietrzak, E.M. Franz, and P. Colombo, 1990. "Method for Accelerated Leaching of Solidified Waste," BNL-52268, Brookhaven National Laboratory, Upton, NY, October.

Fuhrmann, M., J.H. Heiser, R.F. Pietrzak, E.M. Franz, and P. Colombo, 1990. "Accelerated Leach Test Development Program," BNL-52270, Brookhaven National Laboratory, Upton, NY, October.

Gress, D.L. and T. El-Korchi, 1993. "Microstructural Characterization of Cement-Solidified Heavy Metal Wastes," in Spence, Roger D. (ed.), Chemistry and Microstructure of Solidified Waste Forms, Lewis Publishers, pp 169-185.

Groot, G.J. de and H.A. Sloot. 1992. "Determination of Leaching Characteristics of Waste Materials Leading to Environmental Product Cerification," Stabilization and Solidification of Hazardous, Radioactive, and Mixed Wastes, 2nd Volume, ASTM STP 1123, T.M. Gillaim and C.C. Wiles, Eds., American Society for Testing and Materials, Philadelphia, pp. 149-170.

Haegermann, G. and L. Forsen 1938. "The Chemistry of Retarders and Accelerators," Symp. Chem. Cements, Stockholm, pp. 298-363.

Hannawayya, Francisa, 1984. "Microstructural Study of Accelerated Vacuum Curing of Cement Mortar with Carbon Dioxide - Part 1," World Cement, pp. 326 - 334. Nov., 1984. and World Cement, Dec. pp. 378 - 384.

Heimann, R.B., D. Conrad, L.Z. Florence, M. Neuwirth, D.G. Ivey, R.J. Mikula, and W.W. Lam. 1992. Journal of Hazardous Materials, 31(1): 39-57.

Hirljac, J., Z.–Q. Wu, and J.F. Young. 1983. "Silicate Polymerization During the Hydration of Alite," Cement and Concrete Research. 13:877-886.

Hung, Cheng Y. 1982. "Prediction of Long-Term Leachability of a Solidified Radioactive Waste from a Short-Term Leachability Test by a Similitude Law for Leaching Systems," Nuclear and Chemical Waste Management, 3(4): 235-243.

IEPA, 1990. LPC/90-104, January.

Kasai, Y. 1990. "Testing Methods of Cement and Water Content in Fresh Concretes and Estimation of 28-Day Strength at Early Stages – State of the Art in Japan," in Testing During Concrete Construction, Proceedings of International Rilem Workshop, Mainz, Germany, Chapman & Hall Publishers.

Kawada, A. and A. Nemoto, 1967. "Calcium Silicates in the Early Stage of Hydration," Zement Kalk Gips. 20:65-71.

Kurczyk, H.G. and H.G. Schwiete. 1960. "Electron Microscopic and Thermochemical Investigations on the Hydration of the Calcium Silicates $3CaO \cdot SiO_2$ and β-$2CaO \cdot SiO_2$ and the Effects of Calcium Chloride and Gypsum on the Process of Hydration. Tonind. Ztg. 84:585-598.

Lange, Lisete C., Colin D. Hills, and Alan B. Poole, 1996. "Preliminary Investigation into the Effects of Carbonation on Cement-Solidified Hazardous Wastes," Env. Sci. & Tech., 30(1):25-30.

Lenz, C.W., 1966. "The Silicate Structure Analysis of Hydrated Portland Cement Paste," Symp. Structure of Portland Cement Paste and Concrete, Highway Research Board Special Report 90, Washington DC, pp. 269-283.

Leung, C.K.Y. and T. Pheeraphan, 1995. "Very High Early Strength of Microwave Cured Concrete." Cem. and Concr. Res., 25(1):136-146.

Masse, S., H. Zanni, J. Lecourtier, J.C. Roussel, A. Rivereau, 1993. "^{29}Si Solid State NMR Study of Tricalcium Silicate and Cement Hydration at High Temperature," Cement and Concrete Research, 23(5):1169-1177.

Medici, F., C. Merli, G. Scoccia, and R. Vope. 1992. "Release of Toxic Elements from Solidified Waste: A Mathematical Model," Stabilization and Solidification of Hazardous, Radioactive, and Mixed Wastes, 2nd Volume, ASTM STP 1123, T.M. Gillaim and C.C. Wiles, Eds., American Society for Testing and Materials, Philadelphia, pp. 171-181.

Milton, J.S. and Jesse C. Arnold. 1990. Introduction to Probability and Statistics: Principles and Applications for Engineering and the Computing Sciences, McGraw-Hill.

Mindess, S. and J.F. Young, Concrete, New Jersey: Prentice-Hall, Inc., 1981.

Mohan, K. and H.F.W. Taylor. 1982. "A Trimethylsilylation Study of Tricalcium Silicate Pastes," Cement and Concrete Research, 12:25-31.

Mollah, M.Y.A., U. Tsai, R.T. Hess, and D. L. Cocke. 1992. Journal of Hazardous Materials, 30:273-283.

Murakami, K. and H. Tanaka. 1968. "Contribution of Calcium Thiosulfate to the Acceleration of the Hydration of Portland Cement and Comparison with Other Soluble Inorganic Salts" Supp. paper II-2, V International Symp. Chem. Cements. pp 422-436.

Odler, I. and J. Skalny. 1971. "Influence of Calcium Chlordie on Paste Hydration of Tricalcium Silicate." J. Am. Ceram. Soc. 54:362-363.

Ortego, J. Dale, Yudith Barroeta, Frank K. Cartledge, and Humayoun Akhter, 1991. "Leaching Effects on Silicate Polymerization. An FTIR and ^{29}Si NMR Study of Lead and Zinc in Portland Cement." Environmental Science and Technology, 25(6):1171-1174.

Parrott, L.J. and M.G. Taylor. 1979. "A Development of the Molybdate Complexing Method for the Analysis of Silicate Mixtures," Cement and Concrete Research, 9:483-488.

Parrott, L.J. 1981. "An Examination of the Silicate Structure of Tricalcium Silicate Hydrated at Elevated Temperature," Cement and Concrete Research, 11:415-420.

Parrott, Leslie J, Mette Geiker, Walter A Gutteridge, and David Killoh. 1990. "Monitoring Portland Cement Hydration: Comparison of Methods," Cement and Concrete Research, 20(6): 919-926.

Patel, H.H., Bland, C.H., and Poole, A.B., 1995. "The Microstructure of Concrete Cured at Elevated Temperatures," Cement and Concrete Research, 25(3):485-490.

Perry, K.J., N.E. Prange, and W.F. Garvey. 1992. "Long-Term Leaching Performance for Commercially Stabilized Wastes," Stabilization and Solidification of Hazardous, Radioactive, and Mixed Wastes, 2nd Volume, ASTM STP 1123, T.M. Gillaim and C.C. Wiles, Eds., American Society for Testing and Materials, Philadelphia, pp. 242-251.

Pratt, P.L. and H.M. Jennings, 1981. "The Microchemistry and Microstructure of Portland Cement," Annual Review of Materials Science, 11:123-149.

Ramachandran, V.S., 1981. Calcium Chloride in Concrete – Science and Technology, London; Applied Science Publishers

Ramachandran, V.S., 1984. Concrete Admixtures Handbook, Noyes Publications: Park Ridge, New Jersey.

Rio, A., A. Celani, and A. Saini, 1970. "New Investigations on the Action Mechanism of Gypsum and Calcium Chloride and Their Influence on the Structural and Mechanical Characteristics of the Hydrosilicates Produced by the Hydration of C_3S," Il Cemento, 67: 17-26.

Sabir, B.B., 1995. "High Strength Condensed Silica Fume Concrete," Magazine of Concrete Res., 47(172):219-226.

Shackelford, Charles D. 1991. "Laboratory Diffusion Testing for Waste Disposal - A Review," Journal of Contaminant Hydrology, 7:177-217.

Shi, Caijun, and Robert L. Day. 1993. "Acceleration of Strength Gain of Lime-Pozzolan Cements by Thermal Activation," Cement and Concrete Research, 23: 824-832.

Shively, W., T. Brown, P. Bishop, and D. Gress. 1984. Proceedings of the Industrial Wastes Symposia, 57th Annual WPCF Conference, New Orleans, LA, Sept. 30-Oct 4.

Skalny, J., and J.N. Maycock, 1974. "Mechanism of Acceleration by Calcium Chloride-A Review," 77th Annual Meeting ASTM, Washington, June, 1974.

Skalny, J. and I. Odler, 1967. "The Effect of Chlorides Upon the Hydration of Portland Cement and Upon Some Clinker Minerals," Mag. Concr. Res., 19:203-210.

Sloane, R.C., W.J. McCaughey, W.D. Foster, and C. Shreve, 1931. "Effect of Calcium Chloride as an Admixture in Portland Cement Paste," Eng. Expt. Station, Ohio State Bull. 61:81.

Spence, Roger D. (ed.), 1992. Chemistry and Microstructure of Solidified Waste Forms, Lewis Publishers.

Stanton, T.E. 1940. Proceedings ASCE 66:1781-1811.

Taffinder, Glen Gregory and Bill Batchelor. 1993. "Measurement of Effective Diffusivities in Solidified Wastes," ASCE, Jour. of Env. Eng., 119(1): 17-33.

Tamas, F.D., A.K. Sarkar, D.M. Roy, 1976. "Effect of Variables Upon the Silylation Products of Hydrated Cements," Proc. Conf. Hydraulic Cement Pastes-Their Structure and Properties, Cem. Conr. Assoc., pp. 55-72. Univ. Sheffield.

Taylor, D.R., 1986. "Single Laboratory Testing of the Toxicity Characteristic Leaching Procedure (TCLP) Using Conventaionl Apparatus," Tasks 4,9, and 14, Contract 68-03-1958, Environmental Protection Agency, Washington DC, February.

Taylor, M.A. and R.W. Fuessle, 1994. "Stabilization of Arsenic Wastes." Final Report submitted to the Illinois Department of Energy and Natural Resources, Hazardous Waste Research and Information Center, HWR 92095.

Teoreanu, I. and M. Muntean. 1974. Calcium Silicates-Water-Electrolyte System." Supp. paper, Section II, VI International Cong. Chem. Cem. pp.16. Moscow, Sept.

Thomas, N.L., D.A. Jameson, and D.D. Double. 1981. "The Effect of Lead Nitrate on the Early Hydration of Portland Cement," Cement and Concrete Research, 11(5):143-153.

Traetteberg, A., and V S. Ramachandran, 1974. "The Microstructural and Hardening Behvaior of Tricalcium Silicate Pastes in Presence of $CaCl_2$," J. App. Chem. Biotech., 24:157-170.

Tsivilis, S., G. Kakali, and G. Parissakis. 1995. "Mathematical Model for the Control of Cement Setting Using Calcium Chloride as Accelerator." Cement and Conr. Res. 25(5):948-954.

USEPA, 1989. Superfund Innovative Technology Evaluation Program. EPA/540/A5-89/001 and EPA/540/A5-89/004.

USEPA, 1987. Test Methods for Evaluating Solid Waste, Physical/Chemical Methods, SW 846, 3 volumes, Sept. 1986 and 1 revision, Dec. 1987.

USEPA, 1982. Federal Register. 47(225), 52687. Nov. 22

Wilk, Charles M. and Raghu Arora, 1995. "Cement-Based Solidification/Stabilization of Lead-Contaminated Soil at a Utah Highway Construction Site." Remediation, the Journal of Environmental Cleanup Cost, Technologies & Techniques, Portland Cement Association, Skokie, IL.

Williams, L.R., Francis, C.W., Maskarinec, M.P., Taylor, D.R., and N. Rothman. 1986. "Single-Laboratory Evaluation of Mobility Procedure for Solid Waste," Environmental Monitroing System Laboratory, Office of Reserch and Development, Environmental Protection Agency, Las Vegas, NV.

Young, J.F. 1974. "Capillary Porosity in Hardened Tricalcium Silicate Paste." Powder Technology. 9:173-179.

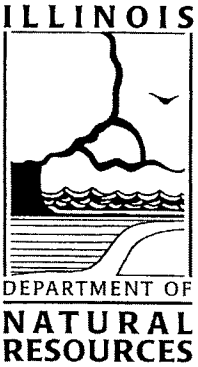
ILLINOIS
DEPARTMENT OF
NATURAL
RESOURCES